NASA CR-137937

Final Report

ENERGY CONSUMPTION CHARACTERISTICS OF TRANSPORTS USING THE PROP-FAN CONCEPT

OCTOBER, 1976

BOEING COMMERCIAL AIRPLANE COMPANY
PRELIMINARY DESIGN

P.O. BOX 3707 SEATTLE, WASHINGTON 98124

Prepared under Contract No. NAS2-9104 for

AMES RESEARCH CENTER
NATIONAL AERONAUTICS AND SPACE ADMINISTRATION
MOFFETT FIELD, CALIFORNIA

1. Report No.	2. Government Accession No.	3. Recipient's Catalog No.
CR-137937		

4. Title and Subtitle	5. Report Date
Energy Consumption Characteristics of Transports Using the Prop-Fan Concept	October 1976
	6. Performing Organization Code
7. Author(s)	8. Performing Organization Report No.
BCAC Preliminary Design Department	D6-75780
	10. Work Unit No.
9. Performing Organization Name and Address	11. Contract or Grant No.
Boeing Commercial Airplane Co. (BCAC) P.O. Box 3707 Seattle, Washington 98124	NAS2-9104
	13. Type of Report and Period Covered
12. Sponsoring Agency Name and Address	Contractor Report-Final
Ames Research Center National Aeronautics and Space Administration Moffett Field, California	14. Sponsoring Agency Code

15. Supplementary Notes

16. Abstract

The fuel saving and economic potentials of the prop-fan high-speed propeller concept were evaluated for twin-engine commercial transport airplanes designed for 3333.6 km (1800 nmi) range, 180 passengers, and Mach 0.8 cruise. A fuel saving of 9.7% at the design range was estimated for a prop-fan airplane having wing-mounted engines, while a 5.8% saving was estimated for a design having the engines mounted on the aft body. The fuel savings and cost were found to be sensitive to the propeller noise level and to aerodynamic drag effects due to wing-slipstream interaction. Uncertainties in these effects could change the fuel savings as much as $\pm$50%. A modest improvement in direct operating cost (DOC) was estimated for the wing-mounted prop-fan at current fuel prices. This improvement could become substantial in the event of further relative increases in the price of oil. The improvement in DOC requires the achievement of the nominal fuel saving and reductions in propeller and gearbox maintenance costs relative to current experience.

17. Key Words (Suggested by Author(s))	18. Distribution Statement
Propellers Prop-fan Fuel conservation	

19. Security Classif. (of this report)	20. Security Classif. (of this page)	21. No. of Pages	22. Price*
Unclassified	Unclassified	146	

*For sale by the National Technical Information Service, Springfield, Virginia 22151

CONTENTS

CONTENTS-Continued

CONTENTS-Concluded

FIGURES

FIGURES - Continued

FIGURES — Concluded

TABLES

TABLES - Concluded

1.0 SUMMARY

1.1 GENERAL

The fuel saving and economic potentials of the prop-fan, a high-speed advanced technology propeller proposed by Hamilton Standard, have been evaluated for application to twin-engine Mach 0.8 commercial transport airplanes designed for 3333.6 km (1800 nmi) range with 180 passengers. Three designs were analyzed:

1. A turbofan powered airplane to serve as a basis for comparison
2. A prop-fan airplane with engines mounted on the wings
3. A prop-fan airplane with engines mounted on struts extending from the aft body

Figure 1 shows the three airplanes and lists their major characteristics. Current airframe technology and core engines based on the technology corresponding to certification in the 1980-1985 time period were assumed. Hamilton Standard's estimated propulsive efficiency, propeller and gearbox weights, and prices were used for all analyses.

The prop-fan engine is of interest because of its high inherent propulsive efficiency. In this study, at Mach 0.8 cruise, the installed thrust specific fuel consumption (TSFC) of the prop-fan (including allowances for reduction gearing) is 0.546 lb of fuel per hr per lb of thrust (0.0155 kg/kN-sec), versus 0.666 for the turbofan. In the absence of compensating penalties, this 18% advantage in cruise TSFC would result in a net fuel saving approaching 25%, through reduction of the airplane size needed to do the mission. However, both the weight and the drag of the prop-fan airplanes are inferior to those of the turbofan and the resulting fuel savings are reduced to 9.7% for the wing-mounted prop-fan airplane and 5.8% for aft-mounted prop-fan.

	Model 767-761 Reference Turbofan	Model 767-762 Wing-Mounted Prop-Fan	Model 767-764 Aft-Mounted Prop-Fan
	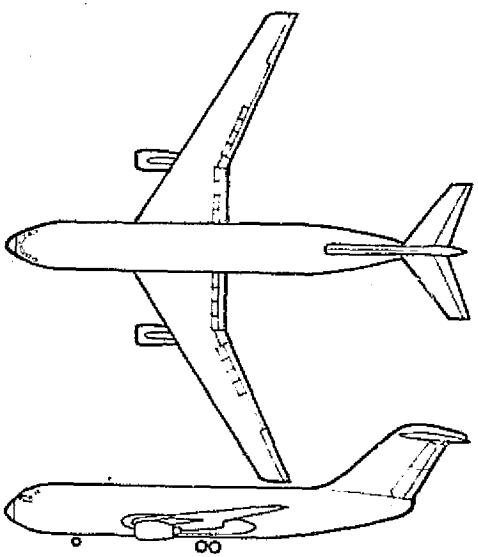	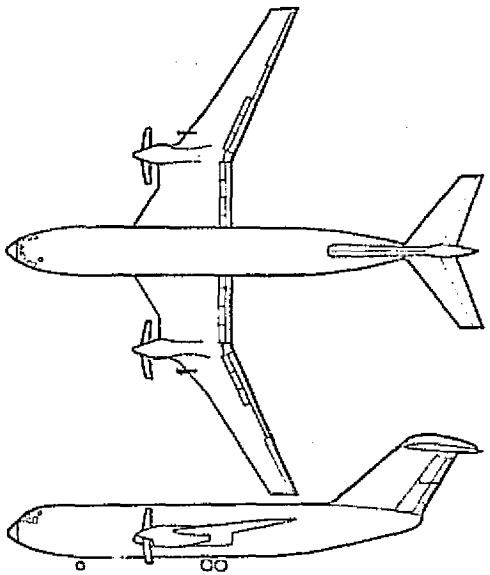	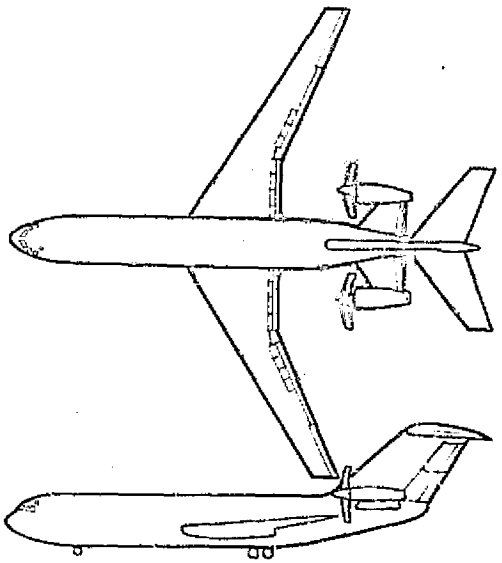
Takeoff Weight (max)	115 350 kg (254 300 lb)	122 000 kg (269 100 lb)	123 900 kg (273 300 lb)
Operating Empty Weight	75 100 kg (165 500 lb)	83 700 kg (184 500 lb)	84 700 kg (186 700 lb)
Wing Area	243.2 m^2 (2618 ft^2)	260.8 m^2 (2807 ft^2)	242.8 m^2 (2613 ft^2)
Propulsion System	(2) 16 960 kg (37 400 lb) SLST BPR 6 turbofans	(2) 22 722 kw (30 470 hp) Engines * driving 5.98 m (19.6 ft) dia prop-fans	(2) 23 110 kw (30 990 hp) Engines * driving 6.03 m (19.8 ft) dia prop-fans

* Scaled STS 476 turboshafts

Figure 1 Airplane Comparison

1.2 WEIGHT

The operating empty weights of the prop-fans are about 8640 and 9630 kg (19 100 and 21 200 lb) higher than the reference turbofan. More than half of the added weight is simply the difference between the "propulsors," i.e., between a fan and a propeller-gearbox combination. The remainder of the added weight is due to a variety of causes. One problem peculiar to the prop-fan deserves special emphasis: In cruising flight, the helical tip Mach number of its blade is 1.13, so a very high noise level may be expected with much of the energy in a narrow band around the blade passing frequency. An added fuselage weight of 2670 kg (5880 lb) is required for the wing-mounted prop-fan to reduce the cabin noise to the level attained by the turbofan. The arrangement having aft-mounted propellers was designed to reduce that penalty. However, additional structure is required to support the engine struts, very heavy skin gauges must be employed to prevent acoustic fatigue damage, and balance problems resulting from the heavy stern necessitates a bigger empennage.

1.3 DRAG

Both prop-fans have higher parasite drag than the turbofan. The wing-mounted prop-fan requires added wing area to meet the approach speed requirement with a $C_{L_{MAX}}$ penalty caused by the placement of the nacelles on the wing leading edge. The aft-mounted prop-fan has large nacelle struts and a longer body. Both (especially the aft mount) have larger tail surfaces. A 0.012 M penalty in drag-rise Mach number was charged to the wing-mounted prop-fan because of the slipstream, which adds an average of 0.04 M to the flow velocity over 30% of the exposed wing area.

1.4 FUEL ECONOMY

The block fuel of the prop-fan airplanes is shown in figure 2 as a fraction of the reference turbofan's. The net result of the combined effects of TSFC, weight, and drag is a fuel saving of 9.7% for the wing-mounted prop-fan and 5.8% for the aft-mounted prop-fan at the design range of 3333.6 km (1800 nmi). Most trips flown by airplanes of this design range are at stage lengths between 926 and 1852 km (500 to 1000 nmi). The prop-fans save somewhat more at such ranges because a greater proportion of the flight is spent in climb and maneuver, where the speed is lower than Mach 0.8 and the prop-fan's efficiency advantage is even greater.

1.5 DIRECT OPERATING COST (DOC)

Figure 3 shows the relative direct operating cost of the wing-mounted prop-fan and the turbofan at Air Transport Association (ATA) ranges of 966 and 1850 km (600 and 1150 statute miles) for fuel prices from 3.96¢ to 15.85¢ per liter (15¢ to 60¢ per gal.) in 1973 money. Hamilton Standard's estimate of propeller and gearbox maintenance costs was used to compute the DOC data shown. Those maintenance costs take credit for advanced design features providing better modularity and increased mean time between failures of components, and are only about 15% of the current experience maintenance costs on the propellers and gear boxes of airplanes like the Lockheed Electra.

The prop-fan fuel economy is offset by higher first cost and maintenance to the degree that little net advantage results at the 3.96¢ per liter (15¢/gal.) level prevalent before the 1973 oil embargo. At today's prices it offers a modest gain in DOC, and if world conditions should cause another jump in fuel costs, the gain could be greater.

Figure 4 shows the effect of applying current turboprop maintenance cost experience to the prop-fan for the 1850 km (1150 statute mile) ATA trip. The DOC breakeven fuel price is increased to more than 7.93¢ per liter (30¢/gal.) and the economic benefit due to fuel saving is wiped out. Measures planned to reduce prop-fan maintenance costs are therefore of central importance to the concept.

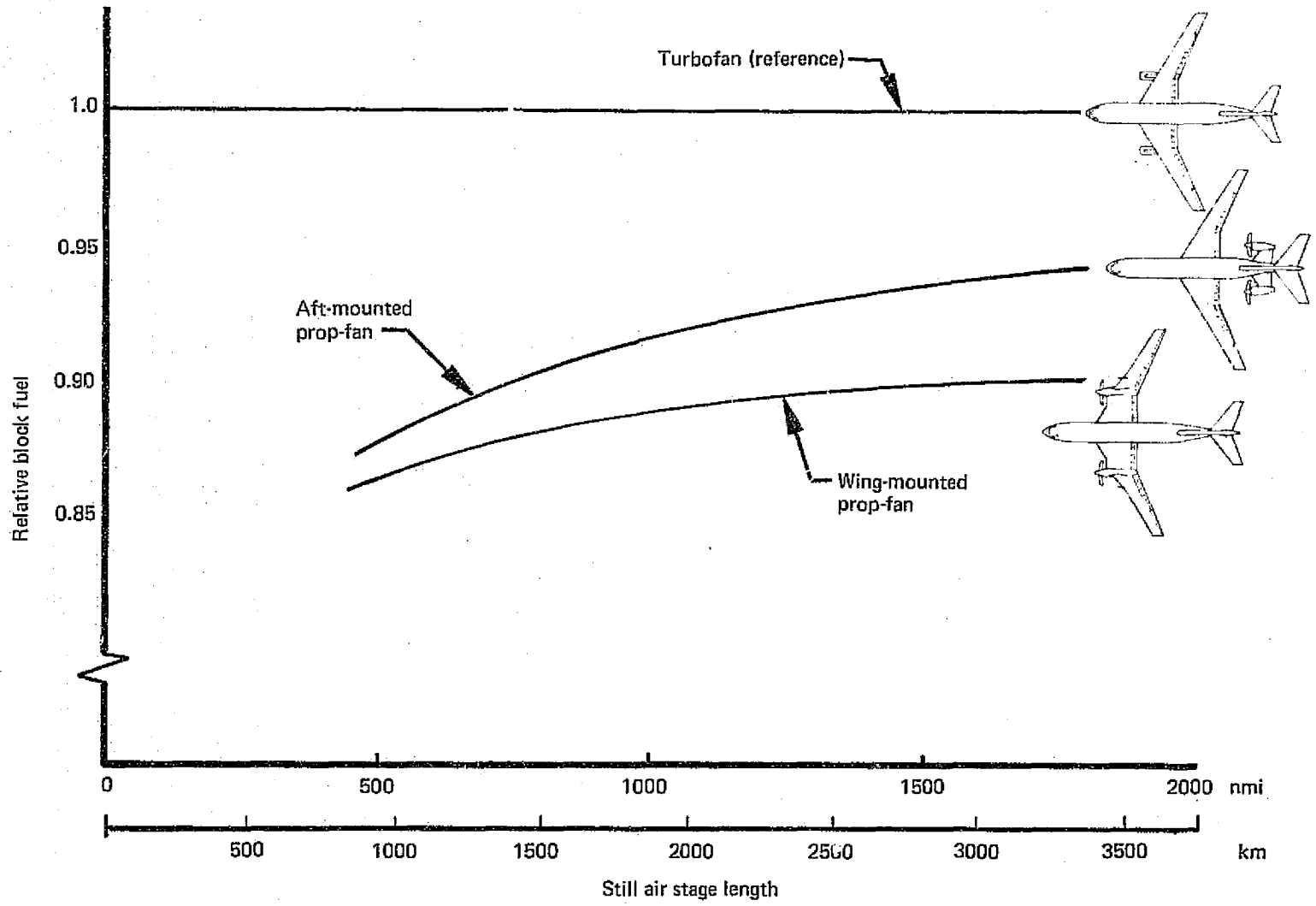

Figure 2 Block Fuel Comparison; Mach 0.8 Cruise, 180 Passengers

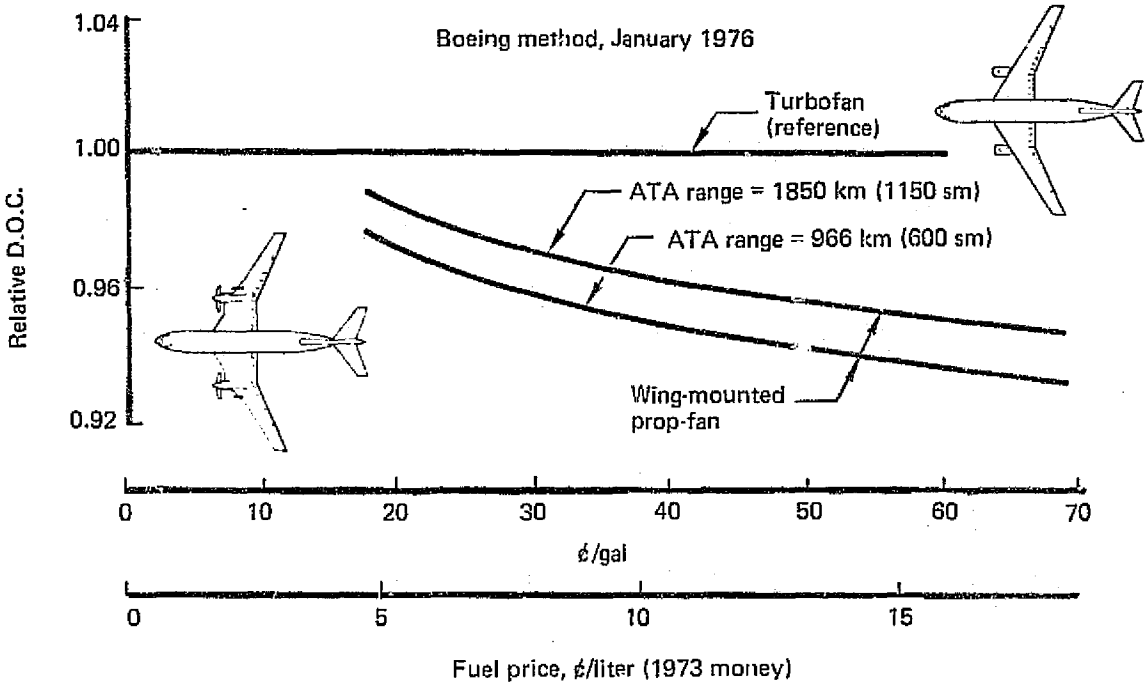

Figure 3 Direct Operating Cost Comparison, Wing-Mounted Prop-Fan and Turbofan

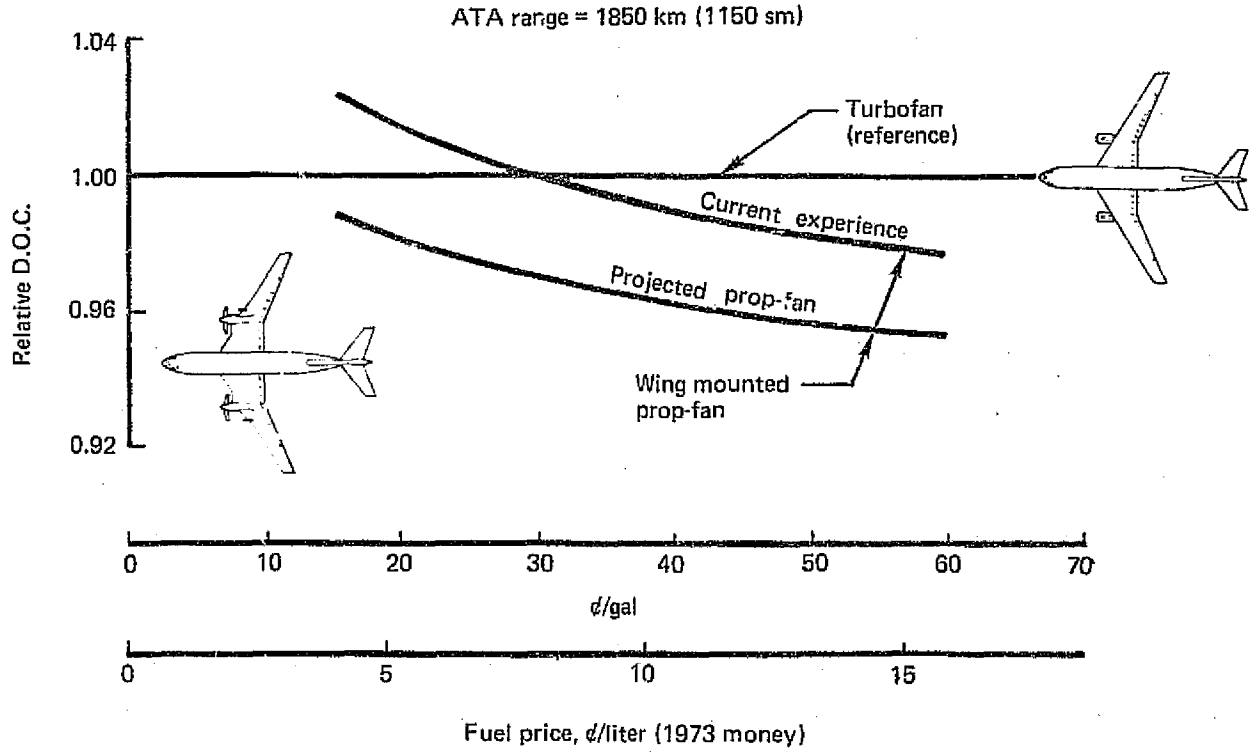

Figure 4 Effect of Propeller and Gearbox Maintenance Cost on Direct Operating Cost

1.6 UNCERTAINTIES

1.6.1 DRAG

The interference drag penalty to be expected as a result of interaction between the slipstream of a heavily loaded propeller (such as the prop-fan) and a sweptback wing at a high subsonic Mach number is not well understood. The propeller adds up to 0.06 M locally to the Mach number across the wing. Because of its high torque, the propeller also induces swirl, changing local angle of attack from zero to +6° to -6° and back to zero over a short span. These influences probably will substantially increase wing section drag, even if an effort is made to tailor the wing shape to minimize the penalty. On the other hand, the wing can be expected to develop a thrust force because of slipstream derotation. Swirl accounts for a loss of about 8% in propulsive efficiency for a prop-fan of the power loading studied here. Potential flow calculations indicate that as much as one half of this decrement may be recovered.

The issue cannot be resolved by available test data. The data are scant, hard to interpret, and subject to doubts regarding the level of propeller thrust and with respect to the effects of shock-boundary layer interaction, because modern transition stimulation practices were not followed.

In the present study, the drag-rise Mach number (M_{DR}) of the wing-mounted prop-fan was determined by an area-weighted average of the M_{DR}'s of the immersed and unimmersed portions of the wing. This approach is convenient and gives a plausible result, but on the basis of present knowledge the correction so calculated could easily be in error by 100% in either direction.

1.6.2 BODY WEIGHT

According to Hamilton Standard the 30° sweepback of the prop-fan blade tip, together with its 2% thick supercritical airfoil section, will result in a

noise level 10 dB lower than the value used in this study. An independent calculation treating the noise radiated by the supersonic tip as a series of little sonic booms, using an approximation found satisfactory in Boeing supersonic transport studies, give a level near the higher value. The issue must be resolved by future tests.

The weight of body structural changes designed to attenuate propeller noise is also uncertain. The blade-passing frequency, around 100 Hz, is too low for effective absorption by conventional fiberglass insulation, and reliance on mass effects (heavy walls) alone would be prohibitively heavy. The approach assumed here is the use of tuned-panel structure with integral damping.

Accurate weight determination using this new method would require more effort than could be spent here. Also, the relation between weight and noise attenuation for this scheme is not linear, and a noise level on the high side would result in a rapidly steepening penalty. The 2670-kg (5880-lb) allowance for noise reduction is therefore subject to a double uncertainty. If the weight estimating method is correct, but the actual noise level is the lower value, the allowance would be reduced to 900 kg (1984 lb).

1.6.3 FUEL SAVING

The 0.012 M_{DR} penalty charged to wing-slipstream interference on the wing-mounted prop-fan is worth 2.7% in block fuel at the design range, while the 2670 Kg (5800 lb) for fuselage noise reduction costs another 3.6%. Together, these effects imply an uncertainty equal to about half the estimated fuel saving, in either direction.

1.6.4 DIRECT OPERATING COST

The effect of the drag and weight uncertainties on the estimated DOC is substantial, equaling plus or minus one-half of the estimated 3% reduction at 30¢/gal. for an 1850 km (1150 statute mile) trip.

1.7 CONCLUSIONS

The results of this study indicate the following:

- The twin prop-fan airplane offers a fuel saving of about 10% over the twin turbofan airplane for the study mission.

- Mounting prop-fans on the aft body of the airplane causes balance problems that more than offset the expected savings resulting from cabin noise reduction.

- Uncertainties regarding slipstream drag effects at high Mach number, the noise radiated by the propeller, and the weight of the consequent noise reduction features could increase or decrease the fuel saving by as much as 50%.

- The prop-fan offers a modest direct operating cost reduction at today's fuel prices, and a substantial one in the event of further major increases in the relative cost of petroleum.

- The drag and weight uncertainties are great enough to have a decisive influence on the prop-fan's economic potential.

1.8 RECOMMENDATIONS

A convincing evaluation of the prop-fan's economic and energy saving potentials requires further research and technology effort. In particular, the following tests should be made:

- Wing/nacelle/propeller combinations should be wind tunnel tested to establish the drag penalty and swirl recovery due to wing/slipstream interaction at high subsonic Mach numbers. Tests involving a simulated slipstream, emitted from a blowing device upstream of the wing, could be very useful because of the degree of control over slipstream velocity and swirl.

- Careful attention to tailoring the wing for local variations in angle of attack due to the slipstream may be essential to the full realization of the prop-fan's potential.

- Noise characteristics of thin, swept-tip propellers operating at supersonic tip Mach number and high advance ratio must be measured. This could be done in a wind tunnel if a facility combining the necessary speed capability and acoustic characteristics can be found or developed. Alternately, a scale model might be flight-tested on a business jet class airplane.

In support of these test programs, theoretical methods should be developed in both aerodynamics and acoustics for the analysis and design of high-speed propellers and wings in their mutual presence.

2.0 INTRODUCTION

2.1 BACKGROUND

Elementary considerations of momentum and energy lead to the conclusion that, in the absence of compensating losses, propulsive efficiency is always improved by accelerating more fluid by a smaller velocity increment. Introduction of the high bypass ratio turbofan engine stimulated a new generation of transport aircraft by using that principle to reduce fuel consumption without substantially sacrificing the simplicity, reliability, and low maintenance costs that have come to be expected by the airlines since reciprocating engines were replaced by turbojets.

The dramatic increase in the relative cost of fuel following the 1973 Arab oil embargo, along with national concern over the long-term prospect of fossil fuel depletion, have prompted government and industry to examine possibilities for further reducing aircraft fuel consumption.

A recent NASA-sponsored study (ref. 1) concluded that modest gains in efficiency could be achieved by pushing the turbofan technology further. Geared fans, very high overall pressure ratios, and even more elevated turbine inlet temperatures would be required, and engine price and maintenance costs would be expected to rise. The same study also noted that the propeller offered much more dramatic gains than advanced turbofans if it could be adapted to the Mach 0.75+ cruise speed favored by airframe technology and expected by the traveling public.

The high propulsive efficiency of propellers is hard to maintain at cruise speeds above Mach 0.7 because either

- The helical tip Mach number becomes supersonic, and the outer section of the blade incurs drag and noise penalties, or

- The rotational speed must be reduced to the point where excessive slipstream swirl necessitates the added weight and complexity of dual rotation.

In 1975, the Hamilton Standard Division of United Technologies Corporation proposed the prop-fan concept, in which a supersonic tip Mach number is accepted, but very thin, swept-back blade tips are used to alleviate drag and noise. To keep the diameter reasonable while absorbing the very high power required for a high-speed transport airplane, eight broad blades are used. Figure 5 shows the appearance of this "advanced technology unducted propulsor."

Hamilton Standard estimated that an installed propulsive efficiency of 79.5% at Mach 0.8 cruise could be achieved. A net reduction of 18% in TSFC over a bypass ratio 6 turbofan would then be expected. At the time of this writing, the first of a series of wind tunnel tests has been run, and attainment of the estimated efficiency appears likely.

To gain an understanding of how the prop-fan can best be exploited, and of the problems to be expected in integrating it with a high-speed transport airframe, NASA has sponsored several industry studies of prop-fan applications, including the present investigation.

2.2 STUDY GROUND RULES

Twin engine airplanes designed to carry 180 to 200 passengers in a 10% first/90% economy class cabin configuration with 0.97/0.86 m (38/34 in.) seat pitch are the subject of this study. The mission range is 3333.6 km (1800 nmi), and the cruise speed objective is Mach 0.8. The minimum cruise altitude is 9144 m (30 000 ft) for compatibility with modern air traffic control requirements. Because this airplane is a medium range design, a maximum takeoff field length of 2134 m (7000 ft) at full payload for sea level standard day conditions was specified. An additional requirement, imposed by Boeing and based on experience with commercial operators, is that the maximum sea level standard day approach speed at the design mission landing weight should be 65 m/sec (126

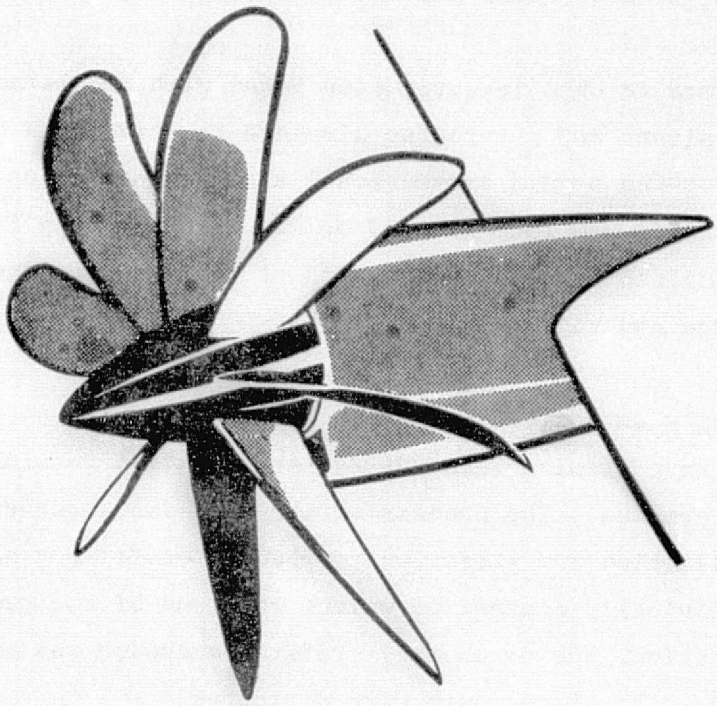

Figure 5 Prop-Fan

KEAS). This ensures that the approach speed will not exceed 70 m/sec (135 KEAS) for landings at higher weights on shorter route segments.

Equal cabin comfort levels were required. This implies that any extra noise generated by the propellers must be attenuated to the level of the reference turbofan airplane by appropriate airplane arrangement, structural design measures, or insulation.

Turbofan engine data were based on 1985 technology as embodied in the data base developed for a previous NASA-sponsored Boeing study (ref. 2). A turboshaft core engine of comparable technology, the Pratt & Whitney STS-476, served as the basis for prop-fan propulsion system performance.

2.3 TASKS AND DOCUMENT ORGANIZATION

The tasks performed in this investigation began with the parametric design of two prop-fan airplanes and a turbofan airplane to serve as a standard of comparison. One prop-fan used a conventional arrangement having engines on the wing, while the other had them mounted on struts projecting from the aft body. (A scheme with engines mounted on the tips of the horizontal stabilizer was briefly considered and rejected.)

Because of Boeing's extensive experience in turbofan transport design, the parametric reference airplane did not require detailed examination to validate weights and performance. The newness of the prop-fan, however, demanded airplane design evaluation and iteration to ensure consistency and reasonableness. It was originally planned to select only one of the two prop-fan designs for iteration, but no clearly preferable choice was evident from the parametric study. Therefore, both were evaluated.

The remaining tasks were the determination of the sensitivity of the prop-fan airplane takeoff weight, empty weight, and fuel burned to variations in propulsion system characteristics, and comparison of direct operating costs with those of the reference turbofan airplane. The details of these tasks are discussed in sections 4 to 7. Conclusions and recommendations for further research and technology work are presented in the Summary, section 1.

3.0 ABBREVIATIONS AND SYMBOLS

a_o	speed of sound (sea level, standard day) m/sec (ft/sec)
A/P	airplane
AR	aspect ratio
ATA	Air Transport Association
A_{wet}	airplane wetted area, m^2 (ft^2)
b	wing span, m (ft)
B	number of propeller blades
BL	buttock line, in.
BPR	bypass ratio
BS	body station, in.
c	local chord, m (in.)
$\bar{c}$	mean aerodynamic chord m (in.)
C_D	drag coefficient, D/qS_{ref}
C_{D_i}	induced drag coefficient, D_i/qS_{ref}
C_f	skin friction coefficient, τ/q
c.g.	center of gravity
c_e	elevator chord, m (in.)
c_ℓ	section lift coefficient, lift per unit span/qc
C_ℓ	rolling moment coefficient, rolling moment/$qS_{ref}b$
C_L	wing lift coefficient, L/qS_{ref}
C_{L_H}	horizontal tail lift coefficient, L_H/qS_H
C_{L_R}	ratio of the lift coefficient at the maximum achievable initial cruise altitude to the lift coefficient for maximum lift-to-drag ratio $(L/D)_{MAX}$
C_{L_s}	stall lift coefficient, L_s/qS_{ref}
C_M	pitching moment coefficient, pitching moment/$q\bar{c}S_{ref}$
C_n	yawing moment coefficient, yawing moment/$qS_{ref}b$

D	propeller diameter, m (ft)
dB	decibel
deg	degree
^{o}C	degrees Celsius
^{o}F	degrees Fahrenheit
^{o}K	degrees Kelvin
^{o}R	degrees Rankine
DOC	direct operating cost
EAS	equivalent airspeed, TAS $\sqrt{\rho/\rho_o}$, m/sec (ft/sec)
EPNdB	effective perceived noise, decibels
FAR	Federal Aviation Regulations
F_n	net thrust of one engine, kN (lb)
hp	horsepower
HPC	high-pressure compressor
H.S.	high speed
Hz	hertz
ICAC	initial cruise altitude capability
ILS	instrument landing system
KEAS	equivalent airspeed in knots
KTAS	true airspeed in knots
kN	kilonewton
kW	kilowatt
LE	leading edge
L/D	lift-to-drag ratio
ℓ_H	horizontal tail arm, m (in.)
ℓ_v	vertical tail arm, m (ft)
LRC	long-range cruise
L.S.	low speed
M	Mach number
MAC	mean aerodynamic chord
M_{DR}	drag-rise Mach number
M_h	propeller helical tip Mach number

M_t	propeller rotational tip Mach number
MZFW	maximum zero fuel weight, kg (lb)
N_p	propeller normal force, kg (lb)
nac	nacelle
OASPL	overall sound pressure level, dB
OEW	operational empty weight, kg (lb)
Pass	passengers
P/D^2	prop-fan power loading in cruise, kW/m^2 (hp/ft^2)
P/F	prop-fan
PSIL	preferred speech interference level, dB
q	dynamic pressure, kN/m^2 (lb/ft^2)
S_{EXP}	exposed wing area, m^2 (ft^2)
S_H	horizontal tail area, m^2 (ft^2)
Shp	shaft horsepower
S_{IMM}	immersed wing area, m^2 (ft^2)
S.L.	sea level
SLST	sea level static thrust, kN (lb)
SM	static margin
SOB	side of body
spl	sound pressure level, dB
S_{REF}	wing reference area, m^2 (ft^2)
S_V	area of vertical tail, m^2 (ft^2)
T_p	propeller thrust, kN (lb)
TAS	true airspeed, m/sec (ft/sec)
TBL	turbulent boundary layer
t/c	wing thickness-to-chord ratio, measured streamwise
T/F	turbofan engine
TOFL	takeoff field length, m (ft)
TOGW	takeoff gross weight, kg (lb)
TOR	takeoff rotation
TSFC	thrust specific fuel consumption, kg/kN-sec (lb/lb)
U	utilization

V	velocity, m/sec (ft/sec or knots)
V_{APP}	approach speed
V_{BAL}	moment balance speed, m/sec (knots)
V_E	equivalent airspeed, $V\sqrt{\rho/\rho_o}$, m/sec (knots)
Vert	vertical
$\overline{V}_H$	horizontal tail volume coefficient, $\ell_H S_H/\bar{c}S_{ref}$
V_{MC_g}	minimum control speed on runway, m/sec (knots)
vol	volume, m^3 (ft^3)
V_R	rotation speed, m/sec (knots)
V_s	stall speed, m/sec (knots)
V_T	propeller rotational tip speed, m/sec (ft/sec)
$\overline{V}_v$	vertical tail volume coefficient, $\ell_v S_v/bS_{ref}$
W	weight, kg (lb)
W/S	wing loading, kg/m^2 (lb/ft^2)
X_G	main landing gear location, fraction of $\bar{c}$
Y_E	engine spanwise perpendicular distance from centerline, m (ft)
ZFW	zero fuel weight, kg (lb)

GREEK LETTERS

α	angle of attack, deg
α_p	propeller angle of attack (measured from propeller axis to free stream relative wind), deg
α_u	upwash angle at propeller due to wing flow field
ε	downwash angle, deg
λ	taper ratio, tip chord/root chord
Λ	sweepback angle, deg
ρ	air density, kg/m^3 ($slugs/ft^3$)
ρ_o	sea level standard air density, 1.226 kg/m^3 (.002378 $slugs/ft^3$)
τ	skin friction, kN/m^2 (lb/ft^2)
$\varepsilon_{\alpha_{P,W}}$	downwash derivative at wing due to propeller
$\varepsilon_{\alpha_{P,H}}$	downwash derivative at horizontal tail due to propeller

4.0 PARAMETRIC DESIGN

The parametric study objective was to size both the turbofan and prop-fan airplanes to achieve the given mission within certain performance constraints. The sizing exercise identified critical design criteria and trades on which further detailed analyses could be made.

4.1 METHODS AND ASSUMPTIONS

A twin-turbofan airplane design meeting similar requirements was available from previous Boeing studies. This airplane was modified in wing sweep and thickness to satisfy the study objective of a design long-range cruise Mach of 0.8. The baseline airplane's aerodynamic, propulsion, and weight characteristics were developed together with appropriate scaling parameters. These characteristics were used as inputs to the THUMBPRINT sizing program. Although the resultant sized airplane was more intensively analyzed and the design refined, the critical design trades were established from this initial sizing. The design selection method is shown in figure 6. The mission profile used in this design selection process is defined in figure 7. The following design objectives and performance constraints were observed:

Objectives:	Payload, 180 passengers (90% tourist, 10% first class)
	Range, 33 336 km (1800 nmi) (still air)
Constraints:	Takeoff field length 2134 m (7000 ft) on standard day @ S.L.
	Approach speed 65 m/sec (126 KEAS)
	Initial cruise altitude 9144 m (30 000 ft)

The wing-mounted prop-fan airplane was evaluated in the same manner as the turbofan starting from the same baseline airplane, but the prop-fan propulsion units and increased tail sizes were incorporated to reflect the stability and engine-out control differences of a propeller-powered airplane.

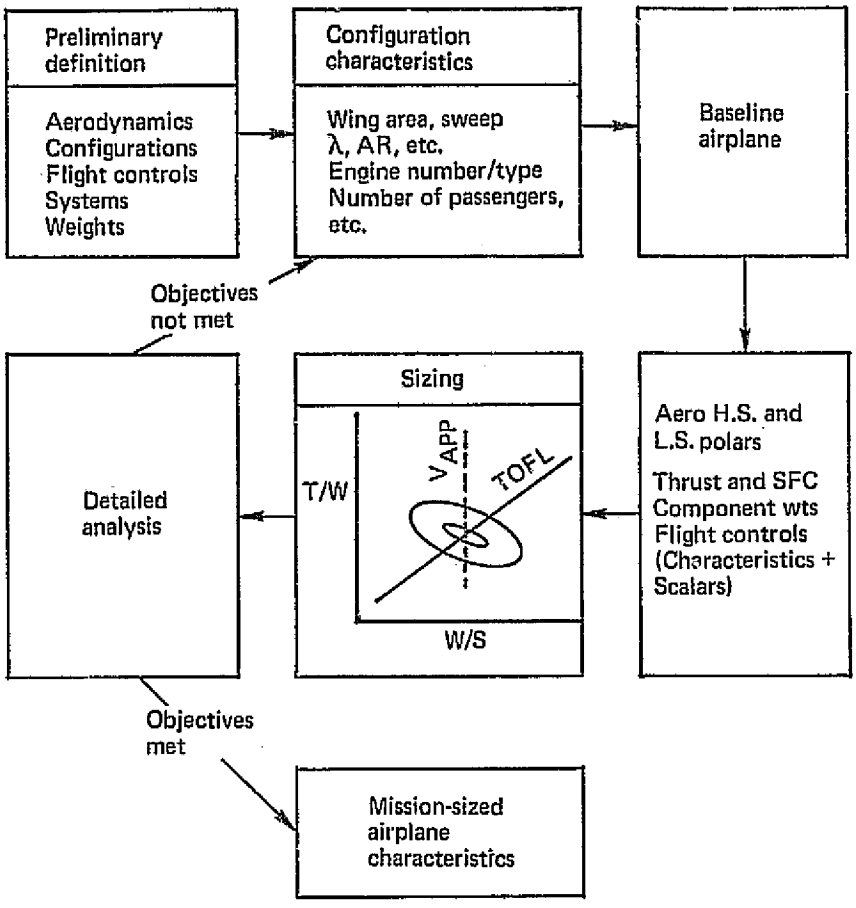

Figure 6 Design Selection Method

The THUMBPRINT program is designed to scale turbofan airplanes, so special procedures and checks had to be adopted to handle propeller airplanes. The engine size is scaled with thrust in the program. It was assumed that the prop-fan propulsion units would scale in the same manner, implying that for constant disc loading (SHP/D^2) the propeller diameter must vary. When variations in the propeller sizing were completed for the wing-mounted prop-fan, drag polars were readjusted to reflect an airplane close to the finally sized airplane.

Variations in propeller diameter also influenced the configuration layout, particularly distances between propeller and fuselage and propeller and ground. These changes also were reflected in final sizing.

Weight-scaling philosophy involving interrelationships between component weights and design parameters (e.g., gross weight, wing area, and engine

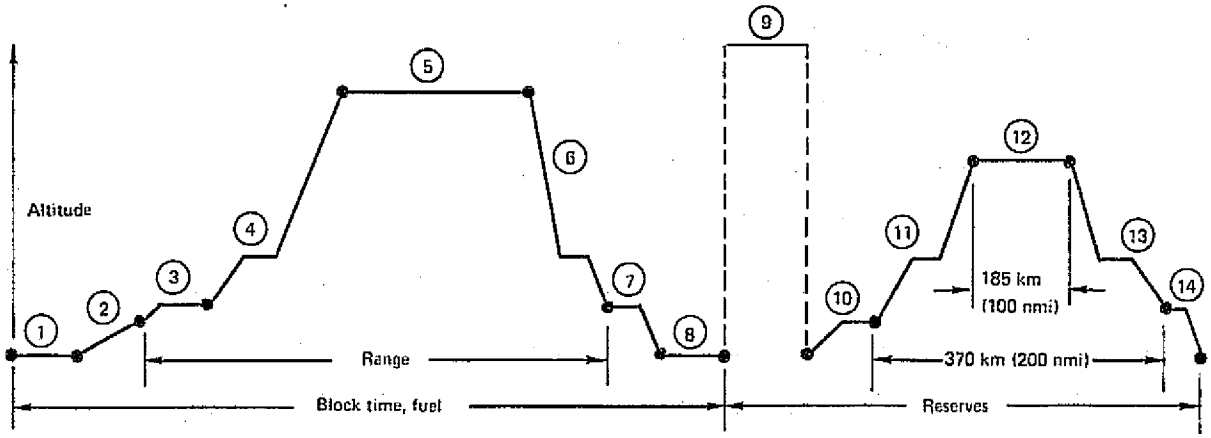

1. Taxi out (9 min taxi thrust)
2. Takeoff (1 min max thrust)
3. Climb to 457 m (1500 ft), accel to 129 m/s (250 KCAS)
4. Climb to 3048 m (10 000 ft), accel to climb speed and climb to cruise alt
5. Cruise
6. Descend to 3048 m (10 000 ft), decel to 129 m/s(250 KCAS), descend to 457 m (1500 ft), decel to V_{APP}
7. ILS approach (2 min. max. thrust)
8. 5 min taxi in (from reserves)
9. 1 hr at LRC altitude and M
10. Missed approach (2 min at max thrust)
11. Climb
12. Cruise
13. Descend
14. ILS approach

Figure 7 Flight Profile and Mission Rules

thrust) can be described as a series of partial derivatives as shown in figure 8. These weight sensitivities were developed individually for the turbofan and prop-fan airplanes in recognition of their specific configuration characteristics. This enabled development of a consistent set of airplane-operating-empty weights required as inputs to mission sizing analyses.

Because a constant payload was maintained throughout the study, primary weight effects of variations in gross weight, wing area, and engine thrust were limited to the airplane structure, surface controls, and propulsion-related items. Payload-related weight, such as fixed equipment, customer options, and standard and operational items, remained unchanged. Figure 8 shows that propulsion-related items were separated into their respective components, permitting a more accurate reflection of the weight impact due to changes in engine thrust.

The aft-mounted prop-fan was handled in the same manner as the wing-mounted version, except that there was no need to revise the drag polars for power effects after initial sizing.

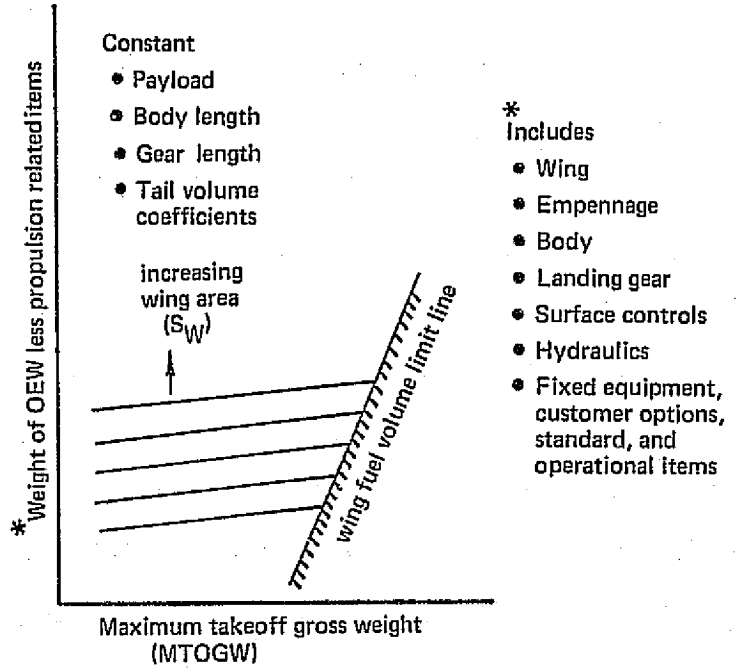

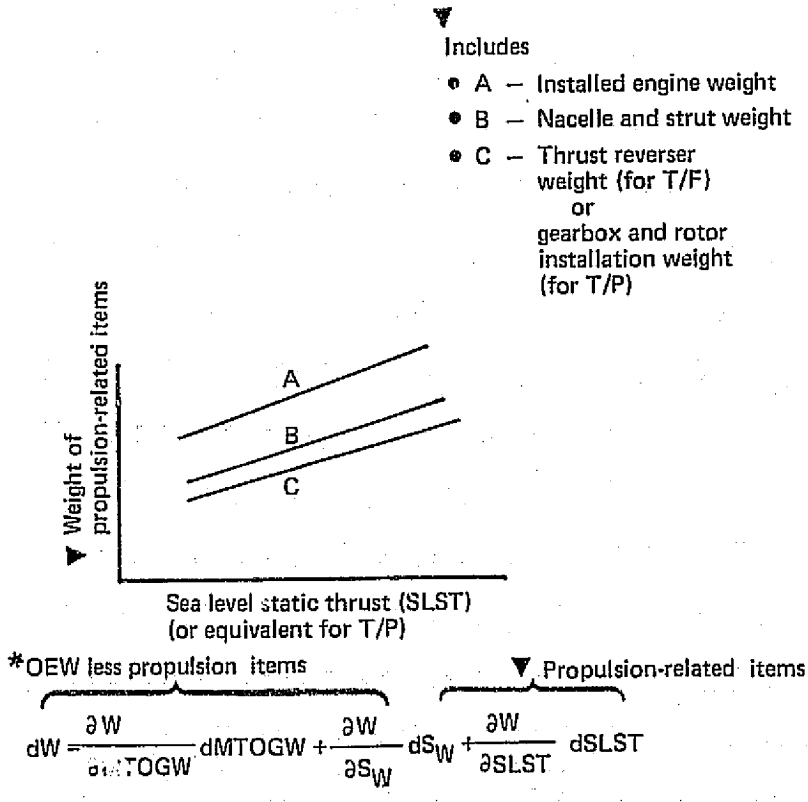

$$dW = \underbrace{\frac{\partial W}{\partial MTOGW} dMTOGW + \frac{\partial W}{\partial S_W} dS_W}_{\text{*OEW less propulsion items}} + \underbrace{\frac{\partial W}{\partial SLST} dSLST}_{\text{▼Propulsion-related items}}$$

Figure 8 Weight-Scaling Techniques

4.2 TURBOFAN SIZING, BASELINE SELECTION, AND PERFORMANCE

The baseline turbofan airplane sizing results are shown in figure 9. This chart shows the combinations of thrust-to-weight ratio (T/W) and wing loading (W/S) that satisfy the mission requirements. Superimposed on the chart are the performance constraints, airplane TOGW, and block fuel. Also shown are lines of constant C_L ratio.* To achieve a C_{L_R} of 1.0 or more means providing the airplane with sufficient thrust to cruise at the altitude for L/D_{MAX}. The chart shows that optimum block fuel occurs for airplanes designed to achieve C_{L_R} between 0.9 and 1.0. This airplane is constrained by its takeoff field-length capability if it is to be sized to achieve minimum block fuel. Figure 10 shows more clearly the selection of the optimum airplane. These design selection trades show how TOGW, wing area, block fuel, etc. vary with C_{L_R} for a constant takeoff field length. They show that the block fuel is insensitive to C_{L_R} values between 0.925 and 1.0; however, the TOGW is a minimum at a C_{L_R} = 1.0, and because this will correspond to a minimum cost airplane, the design was selected at C_{L_R} = 1.0.

The characteristics of the selected airplane in terms of weights, configurations, and performance are shown in table I.

4.3 PROP-FAN SIZING, BASELINE SELECTION, AND PERFORMANCE

A preliminary study was made to determine the desired cruise power loading (P/D^2) of the prop-fan. Based on an initial estimate of the takeoff thrust and cruise thrust required, the engine/gearbox/rotor weight, prop-fan diameter, engine size, and prop-fan efficiency were determined over a range of power loadings. The results of this study are shown in figure 11. Prop-fan

---

*(C_L ratio, or C_{L_R}, is the ratio of the C_L at the maximum achievable initial cruise altitude to the C_L for maximum lift-to-drag ratio (L/D_{MAX}).

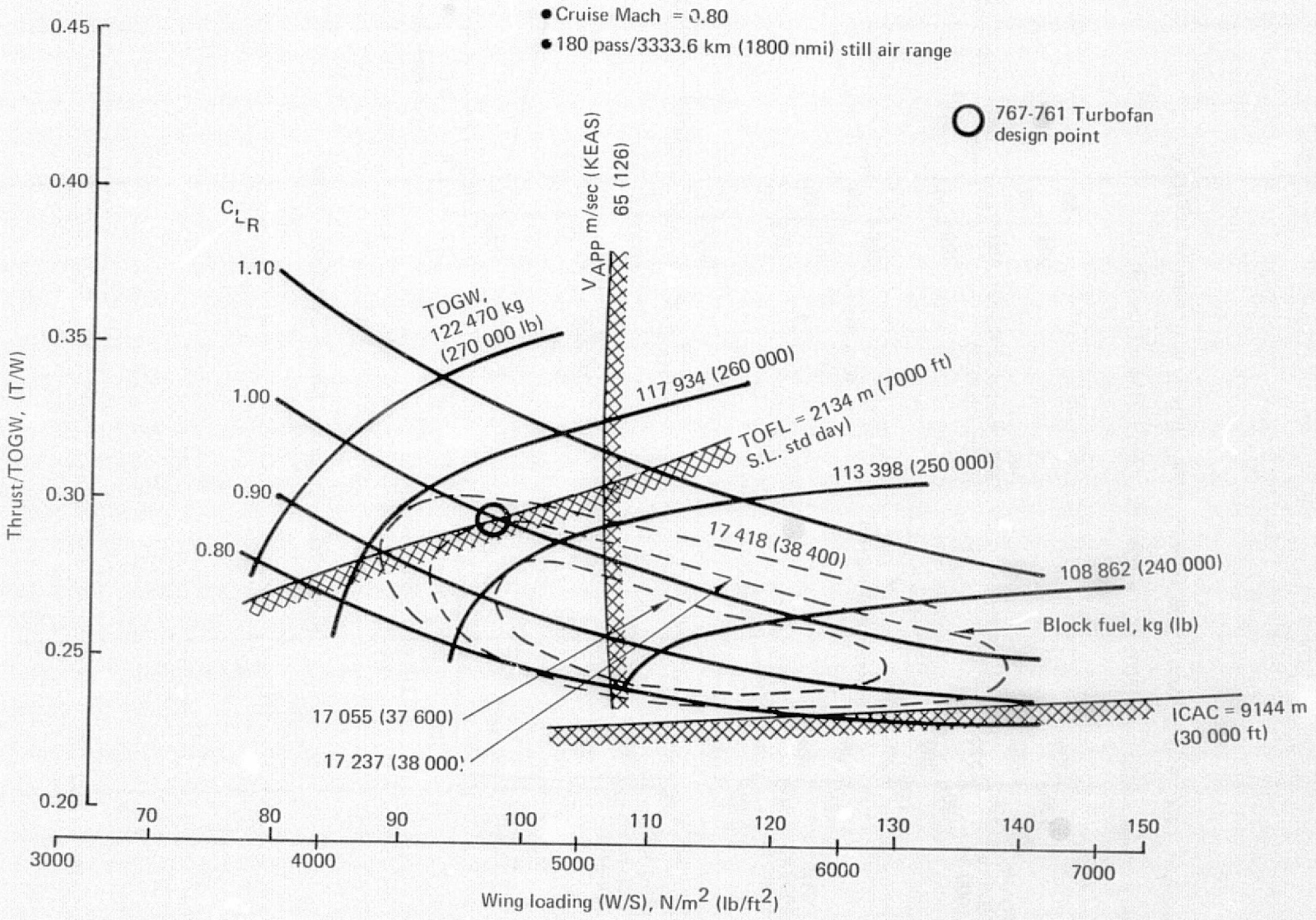

Figure 9 Turbofan Design Selection Chart

• Passengers = 180 • Cruise Mach = 0.80 @ Max altitude capab'lity or altitude for L/D_{MAX}

• Still air range = 3333.6 km (1800 nmi) • TOFL (S.L. std) = 2134 m (7000 ft)

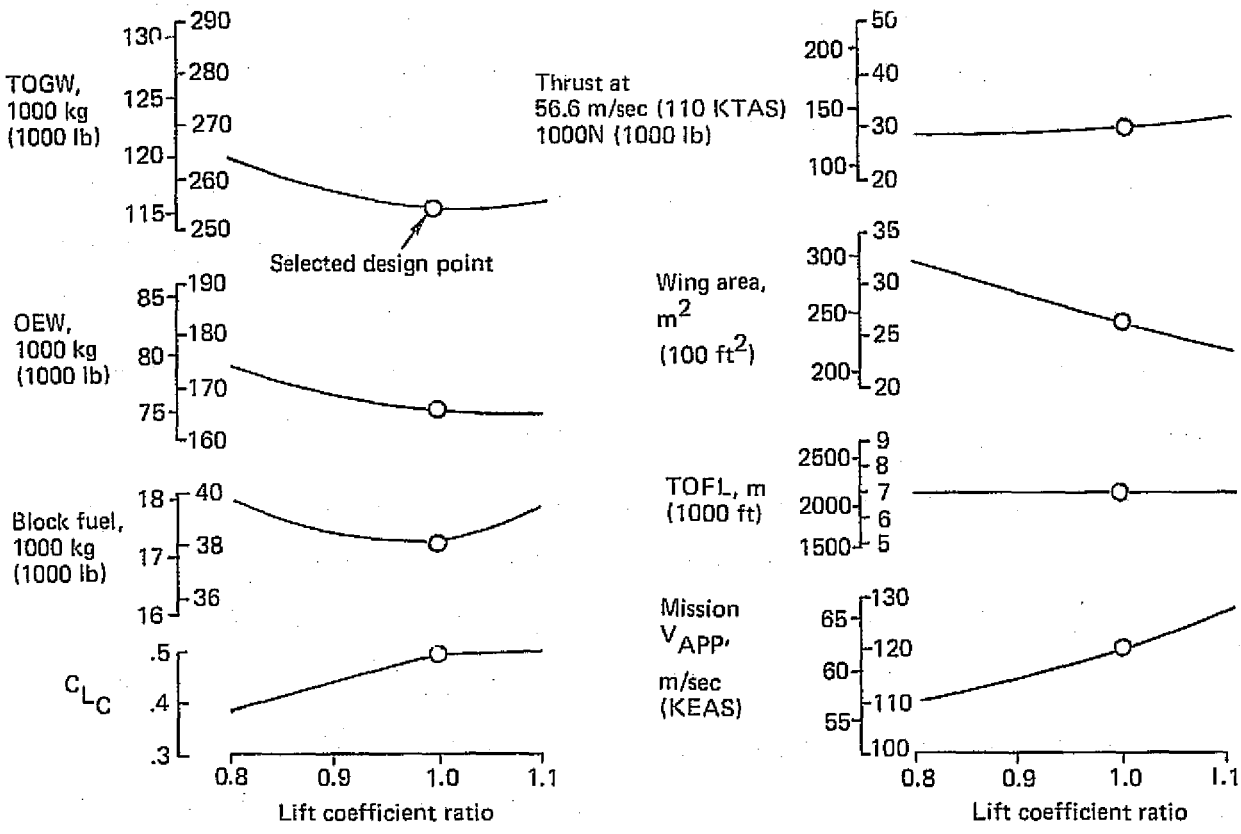

Figure 10 Turbofan Design Selection Trades

Table I Turbofan Airplane Parametric Design Characteristics and Performance

Weights	TOGW, kg (lb)	115 260 (254 100)
	OEW, kg (lb)	75 024 (165 400)
	Landing weight (mission), kg (lb)	98 250 (216 600)
	(maximum), kg (lb)	104 417 (230 200)
	Payload, pass./kg (pass./lb)	180/16 738 (180/36 900)
Configuration	Wing area/Λ, m^2/deg (ft^2/deg)	243/30 (2618/30)
	Aspect ratio/t/c outboard (–/%)	10/10.5
	S_H, m^2 (ft^2)	50.3 (541)
	S_V, m^2 (ft^2)	50.0 (538)
	Body length/diameter, m/m (ft/in.)	42.7/5.03-5.37 (140/198-211.6)
	SLST/number of engines, N (lb)	166 365 (37 388)/2
	Engine type-BPR	TAC/6
	T/W	0.294
	W/S, N/m^2 (lb/ft^2)	4649.2 (97.1)
Performance	Still air range, km (nmi)	3333.6 (1800)
	Cruise Mach number	0.80
	Cruise altitude, m (ft)	11 890 (39 000)
	Range factor, km (nmi)	23 576 (12 730)
	L/D average cruise	18.5 (18.5)
	SFC, kg/kN-sec (lb/hr/lb)	0.01886 (0.666)
	TOFL, m (ft)	2134 (7000)
	C.G. position, % MAC	15 (15)
	V_{APP}, m/sec (KEAS)	62 (120.6)
	Block fuel, kg (lb)	17 237 (38 000)
	Reserves, kg (lb)	6468 (14 260)
	Total fuel, kg (lb)	23 722 (52 740)
	Block fuel, kg/pass. km (lb/pass. nmi)	0.0287 (0.117)

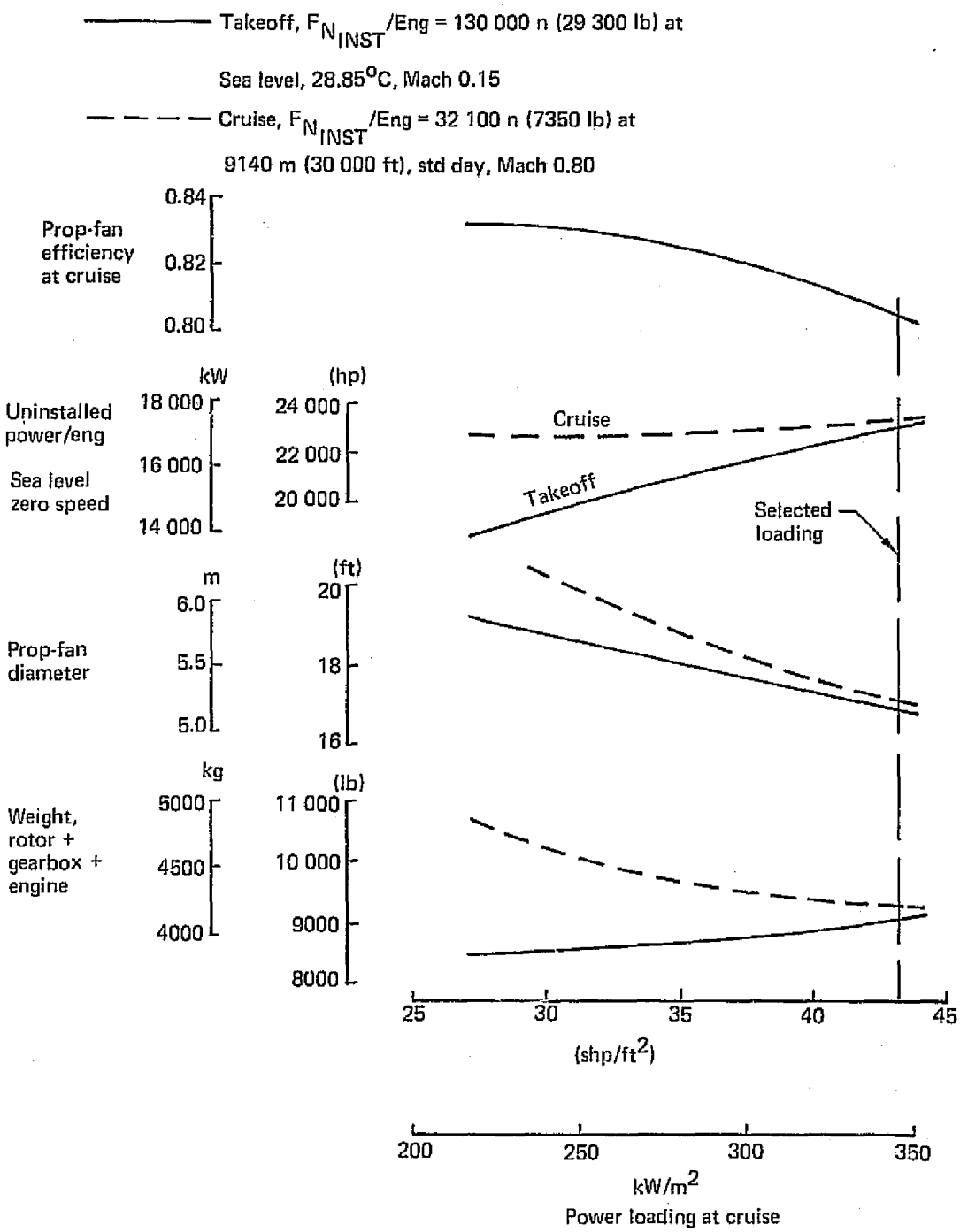

Figure 11 Basis for Selection of Prop-Fan Power Loading

diameter and propulsion system weight decrease as the power loading increases, although with an attendant reduction in prop-fan efficiency. After consideration of the possible impact of prop-fan size on the airplane configuration (i.e., ground clearance, nacelle forward locations, and clearance between the fuselage and the rotor), a relatively high loading of 345 kW/m^2 (43.2 shp/ft^2) was selected.

Although the sized airplane resulted in different values of takeoff and cruise thrust, the trades shown by the study and the considerations for selection remain unchanged. Only if the takeoff thrust requirement had become much more severe (which was not the case) would there have been a necessity to re-evaluate the power loading selection.

The sizing of the prop-fan airplane is shown in figure 12 in the same manner as the turbofan. There are significant differences between this airplane and the turbofan. Provision of sufficient thrust to cruise at an altitude that will minimize the block fuel results in an equivalent T/W at low speed that is considerably higher than the turbofan (0.392 compared to 0.294).* The loss in maximum lift coefficient caused by prop-fan nacelle interference makes this airplane approach speed limited. In this case, a C_{L_R} value of 0.95 yields the minimum block fuel at the lowest TOGW. Trades shown in figure 13, which in this case are for a constant approach speed, show how the sized airplane was chosen. The high equivalent T/W and moderate W/S ensure that the airplane is not field-length or cruise altitude limited. A slightly lower block fuel and lower TOGW might have been obtained if the $C_{L_{MAX}}$ were improved by using double or triple slotted flaps. That block fuel improvement would be offset by the additional weight, complexity, and cost of a more sophisticated trailing-edge-flap system. These detailed trades were not pursued in this study.

---

*The "equivalent T/W" was adopted because of the different thrust/speed characteristics of the prop-fan. Prop-fan and turbofan engines having the same thrust at 56 m/sec (110 KEAS) are considered to be equivalent in size.

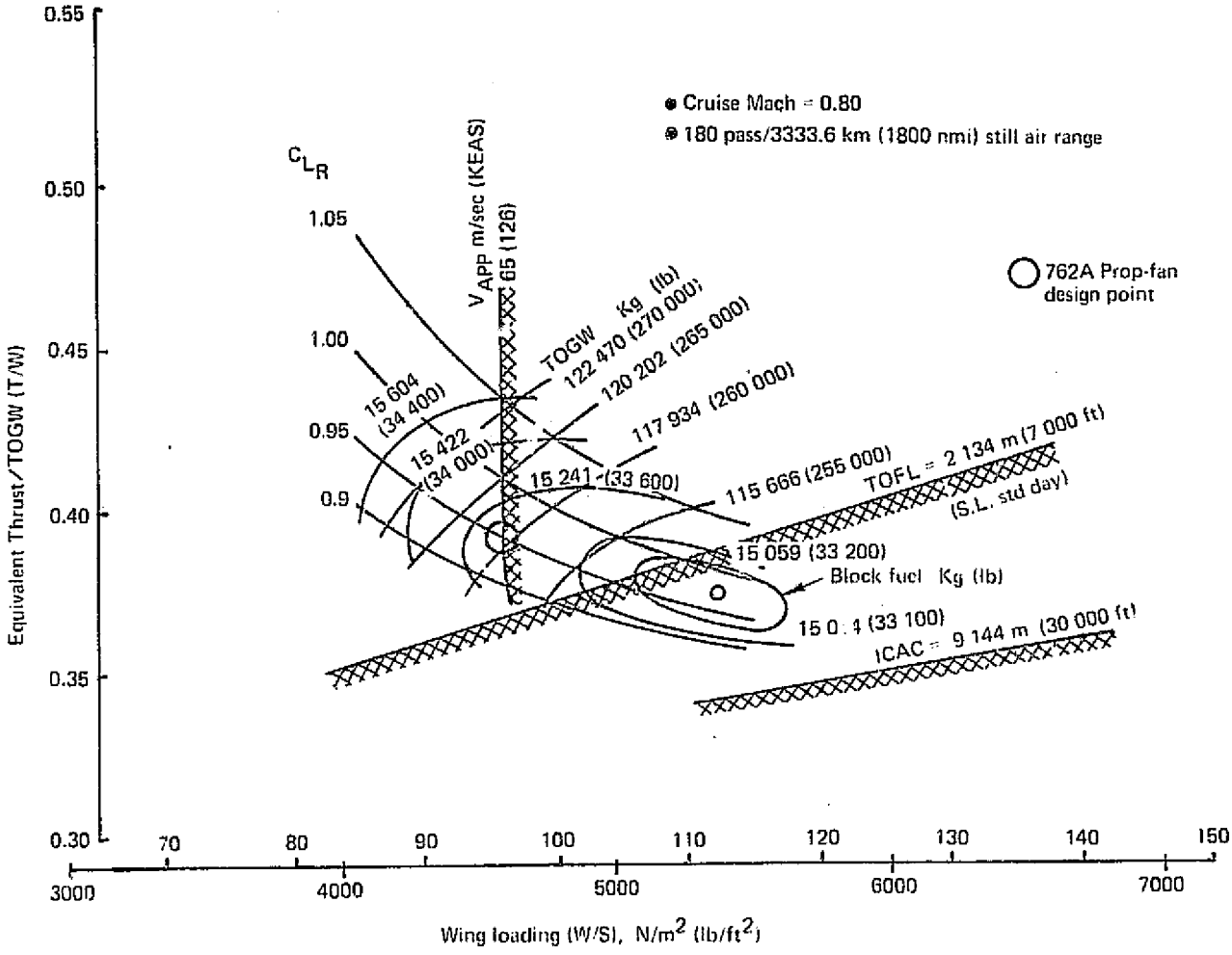

Figure 12 Wing-Mounted Prop-Fan Design Selection Chart

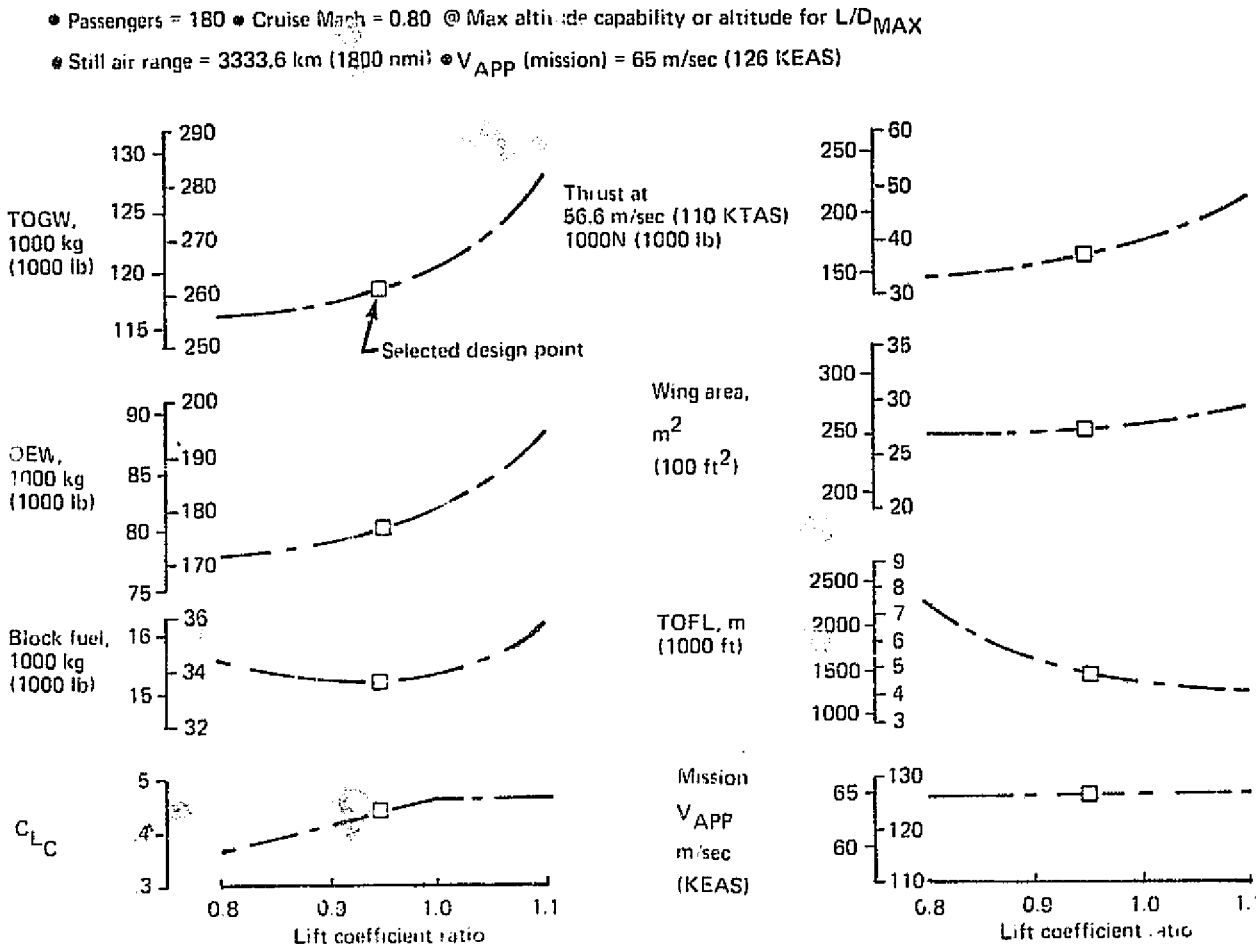

Figure 13 Wing-Mounted Prop-Fan Design Selection Trades

Characteristics of the sized airplane are shown in table II. Despite the reduction in block fuel for the prop-fan, the TOGW is higher than that of the turbofan because of the much higher operating empty weights of the prop-fan (explained fully in section 5.2.7).

4.4 ALTERNATE PROP-FAN CONFIGURATION, SIZING, BASELINE SELECTION, AND PERFORMANCE

An alternate prop-fan configuration with engines mounted on the rear of the fuselage was also sized. This airplane was also designed for minimum block fuel along the approach speed constraint (figure 14). The trades (figure 15) show that the best airplane from a fuel-burn and TOGW standpoint flies at a C_{L_R} of 0.9, has an equivalent T/W = 0.382, and W/S of 5027 N/m^2 (105 lb/ft^2). This airplane also is not takeoff field-length or cruise altitude limited. And, as with the wing-mounted prop-fan, the approach speed requirement could be met at higher W/S with a more sophisticated high-lift system. Again, however, this would be offset by additional weight, complexity, and cost and these detailed trades were not pursued in this study. The OEW of the selected airplane as given in the airplane characteristics, table III, is heavier than the wing-mounted version. Those weight differences are explained in section 5.3.7.

Table II Wing-Mounted Prop-Fan Parametric Design Characteristics and Performance

Weights	TOGW, kg (lb)	118 206 (260 600)
	OEW, kg (lb)	80 330 (177 100)
	Landing weight (mission), kg (lb)	103 190 (227 500)
	(maximum), kg (lb)	107 090 (236 100)
	Payload, pass./kg (pass./lb)	180/16 738 (180/36 900)
Configuration	Wing area/Λ, m^2/deg (ft^2/deg)	252/30 (2713/30)
	Aspect ratio/t/c outboard, (—/%)	10/10.5
	S_H, m^2 (ft^2)	63.5 (684)
	S_V, m^2 (ft^2)	54.1 (582)
	Body length/diameter, m/m (ft/in.)	42.7/5.03-5.37 (140./198.-211.6)
	kW (shp)/number of engines	22 230 (29 800)/2
	Engine type	STS 476 (Scaled)
	T/W equivalent	0.392
	W/S, N/m^2 (lb/ft^2)	4596.5 (96.0)
Performance	Still air range, km (nmi)	3333.6 (1800)
	Cruise Mach number	0.80
	Cruise altitude, m (ft)	11 280 (37 000)
	Range factor, km (nmi)	26 560 (14 341)
	L/D, average cruise	17.06 (17.06)
	SFC, kg/kN-sec (lb/hr/lb)	0.0155 (0.546)
	TOFL, m (ft)	1445 (4740)
	C.G. position, % MAC	0.08 (0.08)
	V_{APP}, m/sec (KEAS)	65 (126)
	Block fuel, kg (lb)	15 179 (33 465)
	Reserves, kg (lb)	6121 (13 495)
	Total fuel, kg (lb)	21 566 (47 545)
	Block fuel, kg/pass. km (lb/pass. nmi)	0.0252 (0.103)

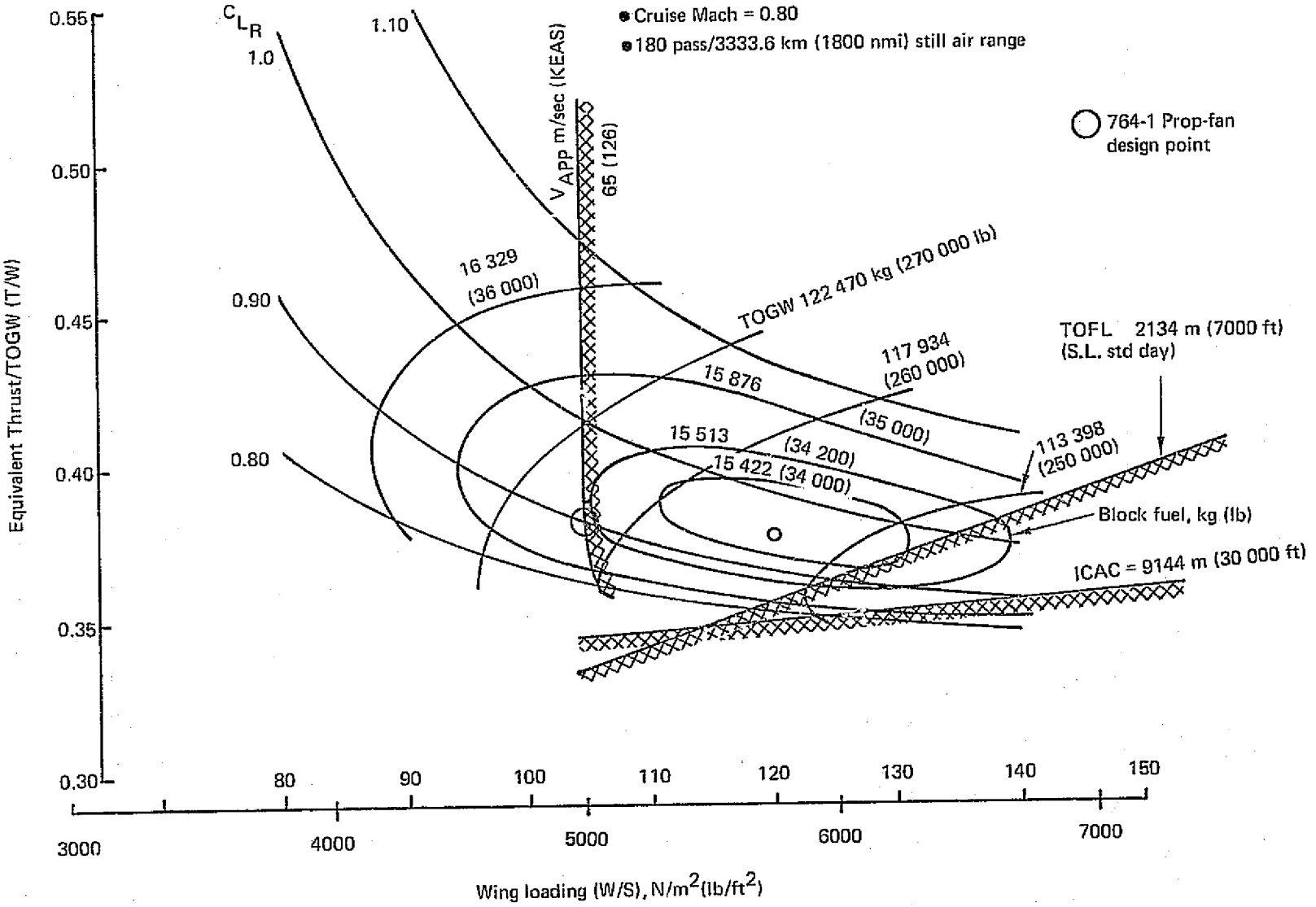

Figure 14 Aft-Mounted Prop-Fan Design Selection Chart

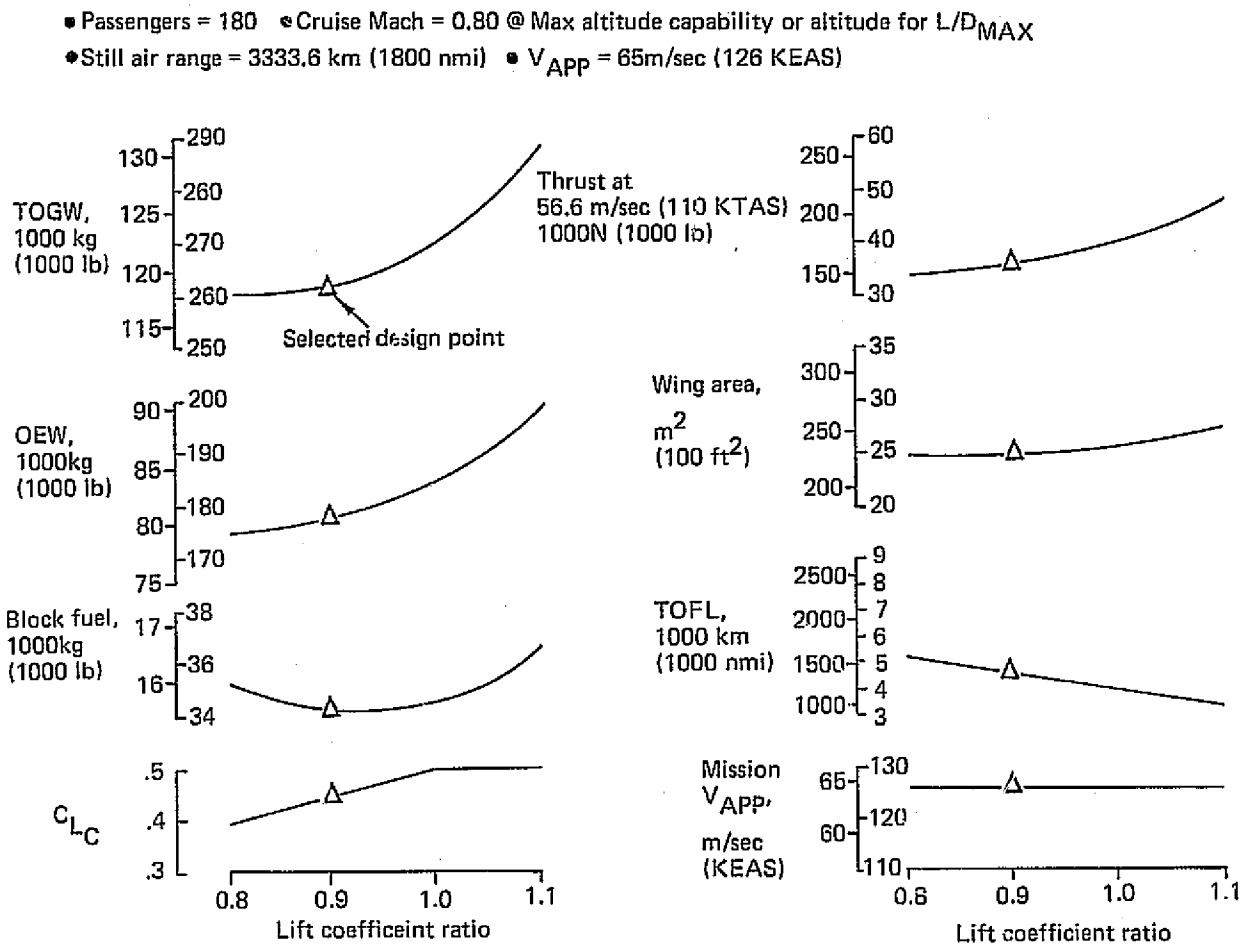

Figure 15 Aft-Mounted Prop-Fan Design Selection Trades

Table III Aft-Mounted Prop-Fan Parametric Design Characteristics and Performance

Weights	TOGW, kg (lb)	119 250 (262 900)
	OEW, kg (lb)	80 920 (178 400)
	Landing weight (mission), kg (lb)	103 870 (229 000)
	(maximum), kg (lb)	108 046 (238 200)
	Payload, pass./kg (pass./lb)	180/16 738 (180/36 900)
Configuration	Wing area/Λ, m^2/deg (ft^2/deg)	233.5/30 (2513/30)
	Aspect ratio/t/c outboard, (—/%)	10/10.5
	S_H, m^2 (ft^2)	66.8 (719)
	S_V, m^2 (ft^2)	57.5 (619)
	Body length/diameter, m/m (ft/in.)	43.9/5.03-5.37 (144.2/198.-211.6)
	kW (shp)/number of engines	21 932 (29 400)/2
	Engine type	STS 476 (Scaled)
	T/W equivalent	0.382
	W/S, N/m^2 (lb/ft^2)	5008.3 (104.6)
Performance	Still air range, km (nmi)	3333.6 (1800)
	Cruise Mach number	0.80
	Cruise altitude, m (ft)	10 972 (36 000)
	Range factor, km (nmi)	25 806 (13 934)
	L/D average cruise	16.56 (16.56)
	SFC, kg/kN-sec (lb/hr/lb)	0.0155 (0.546)
	TOFL, m(ft)	1414 (4640)
	C.G. position, % MAC	20. (20.)
	V_{APP}, m/sec (KEAS)	65 (126)
	Block fuel, kg (lb)	11 526 (34 230)
	Reserves, kg (lb)	6232 (13 740)
	Total fuel, kg (lb)	22 026 (48 560)
	Block fuel, kg/pass. km (lb/pass. nmi)	0.02596 (0.106)

5.0 DESIGN EVALUATION

The parametric investigations discussed in the preceding section were intended to permit selection of one of the two prop-fan designs for more detailed evaluation. Because neither parametric design was decisively superior, both the wing-mounted and the aft-mounted prop-fan airplanes were evaluated.

The reference turbofan airplane did not require detailed evaluation because of its similarity to conventional designs studied elsewhere. Some discussion of its characteristics is included for perspective and comparison.

5.1 REFERENCE TURBOFAN AIRPLANE

The reference turbofan configuration and characteristics are shown in figure 16 and table IV.

5.1.1 ARRANGEMENT CONSIDERATIONS

A seating capacity of 180 (18 first class, 162 tourist), with a corresponding mission payload of 16 738 kg (36 900 lb) was selected because the interior arrangement (fig. 17) permitted use of a previously laid out and analyzed body structure. The passenger compartment has two aisles, six abreast 0.96 m (38 in.) pitch seating for the first class section, and seven abreast 0.86 m (34 in.) pitch seating in the tourist section. Provision is made for galleys, toilets, closets, and attendants stations. The space under the floor is used to store eight LD-3 containers.

A wing with an aspect ratio of 10, quarter chord sweep of 30°, and thickness ratio of 10.5% outboard approximates the mission optimum based on previous Boeing design studies. The wing dihedral of 5° was selected for adequate

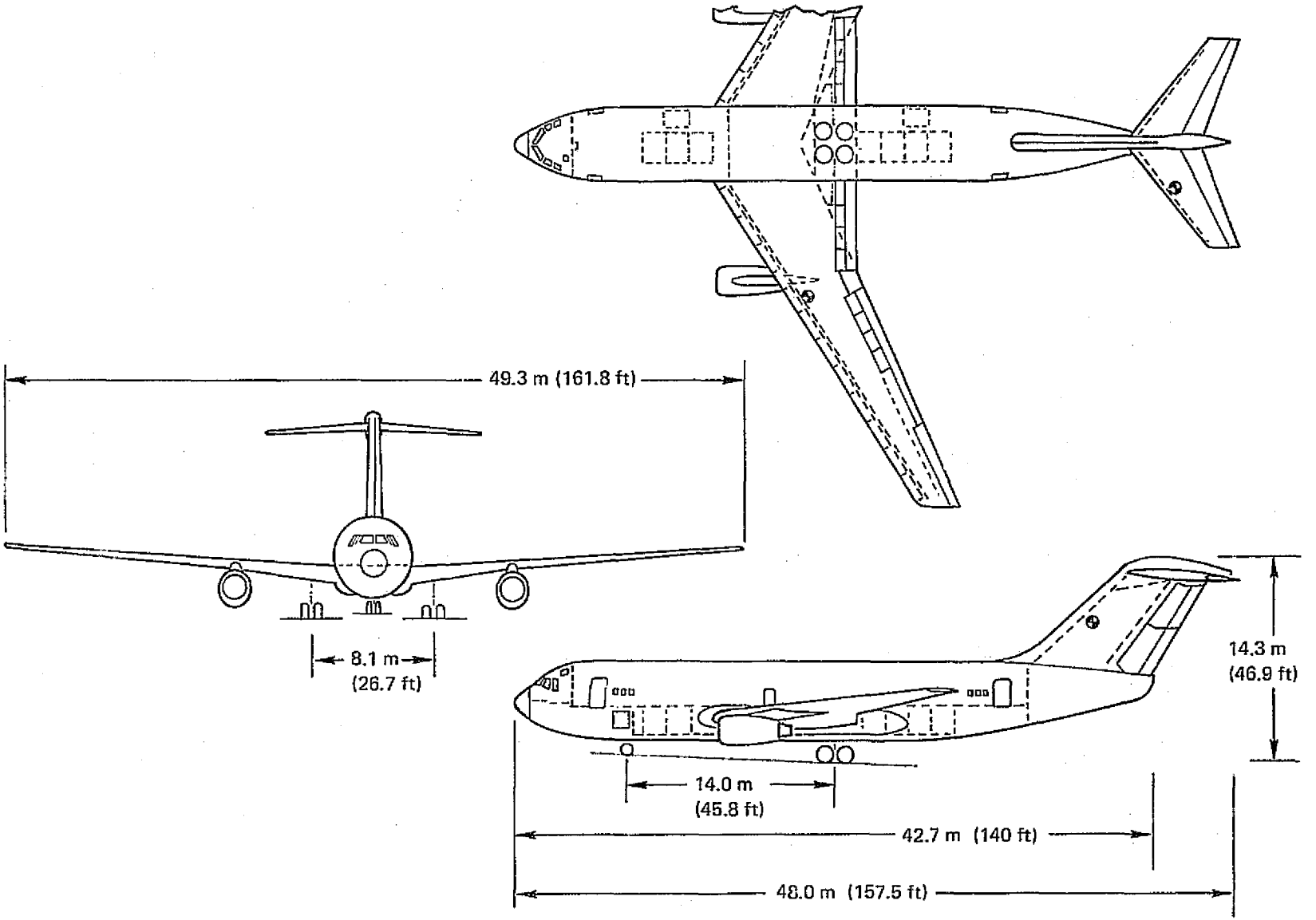

Figure 16 General Arrangement, Turbofan

Table IV 767-761 Baseline Turbofan Airplane Characteristics and Performance

Weights	TOGW, kg (lb)	115 350 (254 300)
	OEW, kg (lb)	75 070 (165 500)
	Landing weight (mission), kg (lb)	98 340 (216 800)
	(maximum), kg (lb)	104 490 (230 370)
	Payload, pass./kg (pass./lb)	180/16 738 (180/36 900)
	Maximum fuel capacity (kg (lb)	68 668 (151 388)
	C.G. limits, % MAC	15 fwd, 43 aft
	T/W	.235
	W/S, N/m^2 (lb/ft^2)	4649.2 (97.1)
Performance	Still air range, km (nmi)	3333.6 (1800)
	Cruise Mach number	0.80
	Cruise altitude, m (ft)	11 890 (39 000)
	Range factor, km (nmi)	23 240 (12 550)
	L/D average cruise	18.21
	SFC, kg/kN-sec (lb/hr/lb)	0.01886 (0.666)
	TOFL, m (ft)	2134 (7000)
	C.G. position, % MAC	15
	V_{APP}, m/sec (KEAS)	63 (122)
	Block fuel, kg (lb)	17 218 (37 960)
	Reserves, kg (lb)	6550 (14 450)
	Total fuel, kg (lb)	23 990 (52 890)
	Block fuel, kg/pass. km (lb/pass. nmi)	0.0287 (0.117)
Power plants	Number	2
	Bypass ratio	6
	SLS thrust/engine uninstalled	166 000 N (37 400 lb)
Body	Length, m (in.)	42.67 (1680)
	Maximum diameter, m (in.)	5.38 (211.6)
	Accommodations	180 passengers—10% 1st, 90% tourist
		8 LD-3 containers, 35.79 m^3 (1264 ft^3)
Landing gear m (in.)	Nose	(2)-0.86x0.28 (34x11)
	Main	(8)-1.09x0.42 (43x16.5)
	Truc. size	1.32x0.97 (52x38)
	Oleo stroke (extended to static)	0.51 (20)

Wing and empennage	Wing	Horizontal tail	Vertical tail
Area, m^2 (ft^2)	243.2 (2618)	50.3 (541.4)	50.0 (537.9)
Aspect ratio	10	4.0	0.8
Taper ratio	0.353	0.4	0.65
c/4 sweep, deg	30	35	45
Incidence, deg	1	variable	0
Dihedral, deg	5	-3	—
t/c, %	2	10.5	12
MAC, m (in.)	5.308 (208.963)	3.763 (148.157)	8.022 (315.830)
Span, m (in.)	49.317 (1941.628)	14.184 (558.438)	6.323 (248.930)
Tail arm, m (in.)	—	24.767 (975)	19.202 (756)
Tail vol coefficient	—	0.965	0.080

1 Wing incidence: SOB 3.75
MAC 2.00
TIP -1.00

2 Wing t/c, %: SOB -13.1 (total chord)
BL 387-10.5 (const outboard)

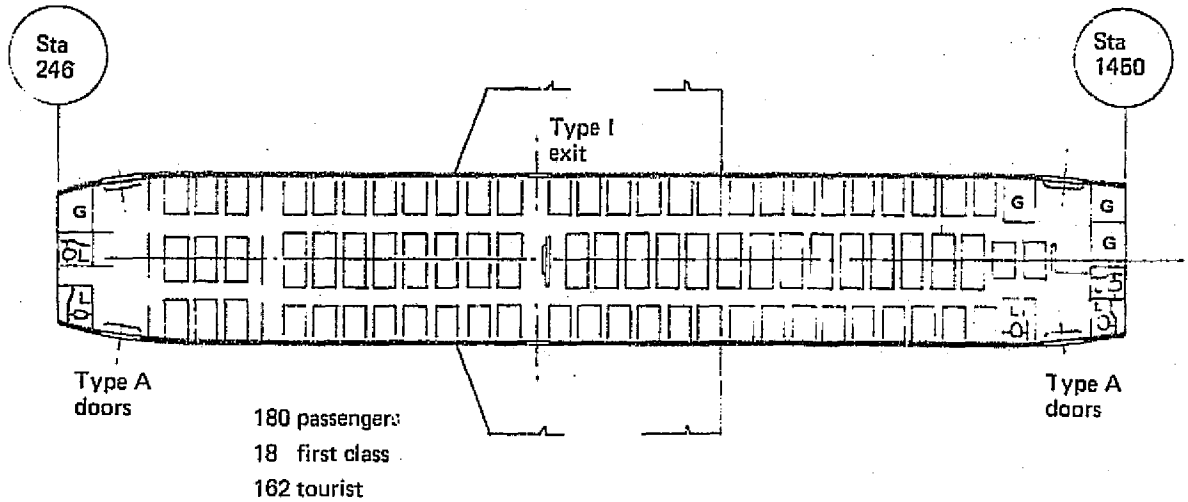

Figure 17 Cabin Interior Arrangement

engine clearance. The wing planform includes a straight trailing-edge fillet to provide adequate room for the inboard flap behind the landing gear trunnion.

The main landing gear is cantilevered off the rear spar behind the aft c.g. and is of sufficient length to provide a takeoff rotation angle of 13°. The landing gear tire and truck were sized to provide flotation on rigid pavement 0.305 m (12 in.) thick with a subgrade of 300.

5.1.2 AERODYNAMIC CHARACTERISTICS

Aerodynamic characteristics for the baseline turbofan were based on Boeing wind tunnel test data for a similar twin-engined medium-range configuration. Analytical corrections were applied to account for the relatively minor differences in wing sweep, wing thickness, empennage size, engine size, etc., between the wind tunnel model and the study baseline airplane.

5.1.2.1 High-Speed Drag

High-speed drag polars for the sized turbofan airplane are shown in figure 18. Total parasite drag coefficient at Mach 0.7 and 12 000 m (40 000 ft) altitude is 0.0167. Maximum lift-to-drag ratio at Mach 0.8 is 18.3.

5.1.2.2 Low-Speed Characteristics

The low-speed drag characteristics are summarized in figure 19, which shows lift-to-drag ratio versus lift coefficient for an engine-out climbout condition at sea level. Reference climbout speed is 74 m/sec (143 kt). The airplane is trimmed at the forward c.g. (0.15 MAC) location with the landing

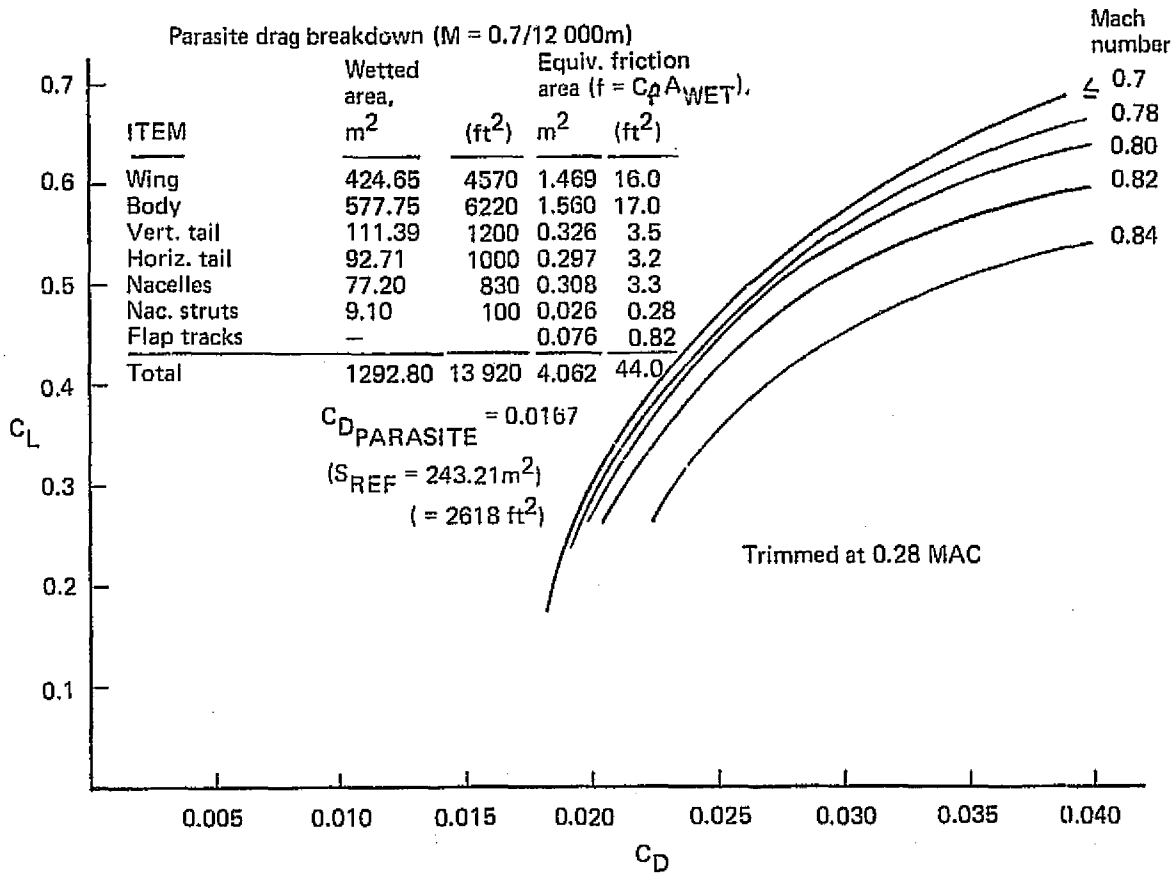

Figure 18 Sized Turbofan Airplane High-Speed Drag Polars

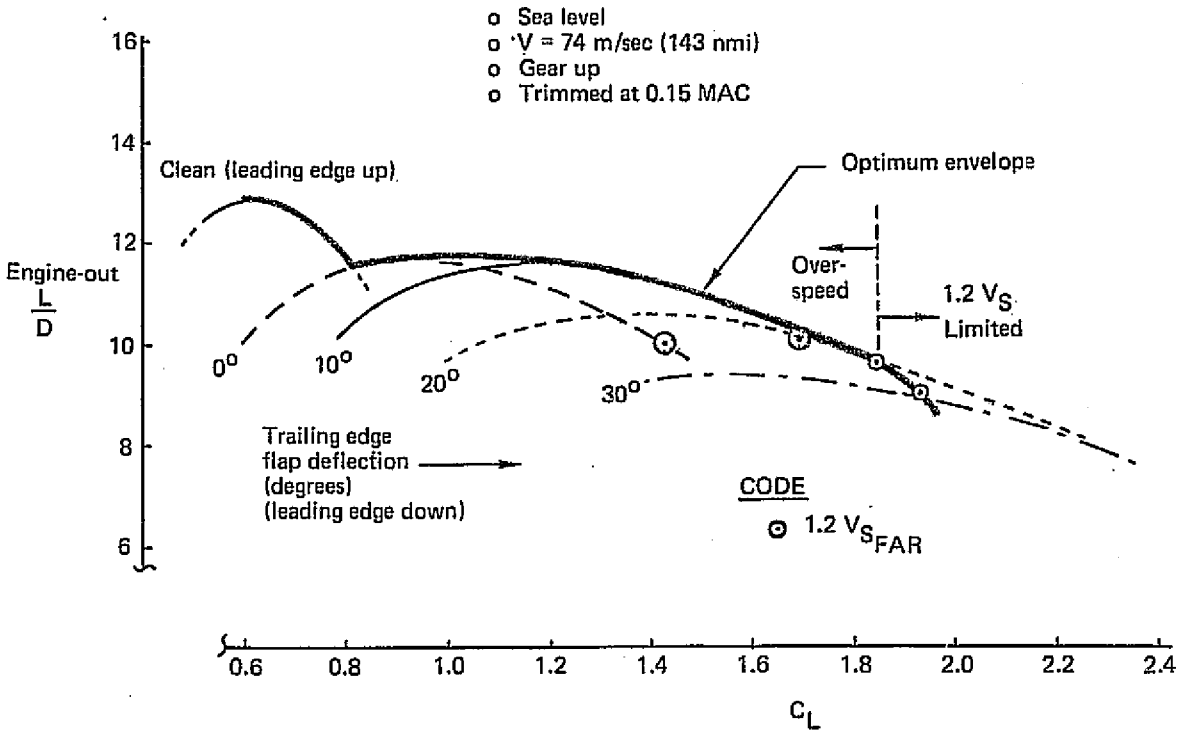

Figure 19 Sized Turbofan Airplane Engine-Out Climbout Lift-to-Drag Ratios

gear retracted. Under these conditions, the airplane meets the climbout gradient requirement of 0.024 with a slight overspeed, at a lift coefficient of 1.4 and 10° flap setting. Climbout lift-to-drag ratio, engine out, is 11.2.

The turbofan airplane FAR stall lift coefficients trimmed at the forward c.g. location were estimated to be:

Leading-edge device deflection, degrees	Trailing-edge flap deflection, degrees	$C_{L_{S_{FAR}}}$
0	0	1.64
50/60	0	2.05
50/60	10	2.42
50/60	20	2.64
50/60	30	2.77
50/60	40	2.84

5.1.3 ENGINE CHARACTERISTICS

A Boeing study engine having a bypass ratio of 6 was selected as the turbofan engine for this contract. This selection was based on results of a bypass ratio study (ref. 2) performed under Contract NAS 1-12018 and similar studies using shorter ranges that showed that minimum fuel was burned with an engine having a bypass ratio of approximately 6.

The technology level of the turbofan engine family is representative of inservice engines in the 1980 to 1985 time period. The cycle and component performance assumed for the engine is shown in table V.

The uninstalled takeoff thrust per engine required for minimum block fuel is 166 000 N (37 400 lb). Installation effects per engine included in the engine performance are: (1) an inlet pressure recovery of 0.99 during static operation increasing to 0.9975 at M = 0.4 and above; (2) high-pressure compressor

Table V Turbofan Cycle Assumptions

9144 m (30 000 ft) Maximum Cruise Thrust, Standard day, 0.8M	
Overall compressor pressure ratio	24
Turbine inlet temperature *	1420 K (2550°R)
Bypass ratio	6
Fan pressure ratio	1.66
Fan specific flow rate	200 kg/sec-m^2 (41 lb/sec-ft^2)
Fan hub/tip ratio	0.38
Fan adiabatic efficiency	0.836
Fan duct pressure loss, %	1.85
Fan nozzle velocity coefficient	0.9925
High-pressure compressor polytropic efficiency	0.89
Combustor efficiency	0.995
Combustor pressure loss, %	4.2
High-pressure turbine cooling, % of HPC flow	5.5
Low-pressure turbine cooling, % of HPC flow	1.4
High-pressure turbine adiabatic efficiency	0.90
Low-pressure turbine adiabatic efficiency	0.91
Shaft efficiencies	0.995
Nozzle discharge coefficients	1.0
Primary nozzle velocity coefficient	0.99
Primary duct pressure loss, %	0.6

* The maximum turbine inlet temperature at takeoff power is 1556°K(2800°R)

airbleed of 1.24 kg/sec (2.73 lb/sec), and (3) power extraction of 48.5 kW (65 hp) from the high-pressure compressor shaft. The installed engine performance during takeoff and cruise is shown in figures 20 and 21, respectively.

5.1.4 FLIGHT CONTROLS

The scope of the stability and control investigation was restricted to the topics below, using the criteria listed:

- Longitudinal stability at aft c.g., including elastic effects
  - No augmentation
  - 6% MAC static margin--approach (Boeing criterion)
  - 3% MAC static margin--cruise (Boeing criterion)
  - 0% MAC static margin--dive (Boeing criterion)
- Takeoff rotation at forward c.g.
  - $\ddot{\theta}$ = 1.5 deg/sec^2 capability (Boeing criterion)
  - Mistrimmed
- Approach trim at forward c.g.
  - Trim with stabilizer--zero elevator deflection
- Stall recovery capability at aft c.g.
  - $V = V_{Min\ Dem}$
  - $\ddot{\theta} = -0.08$ rad/sec^2
- Engine-out control at aft c.g.
  - $V_R = 1.05\ V_{MC_g}$
  - 1.25 OEW (Boeing criterion)
  - $V_{MC_g} = V_{BAL} - 10$ kt
- Directional stability at aft c.g.
  - $C_{n_\beta} = 0.002$ deg^{-1} (all speeds)
- The assumption was made that the airplane will have an alpha-limiter if required for positive stall identification and recovery.

Tail sizing studies were actually done during the parametric design phase of the program, and used the dimensions and weights then considered applicable. The tail volume coefficients are considered applicable to subsequently

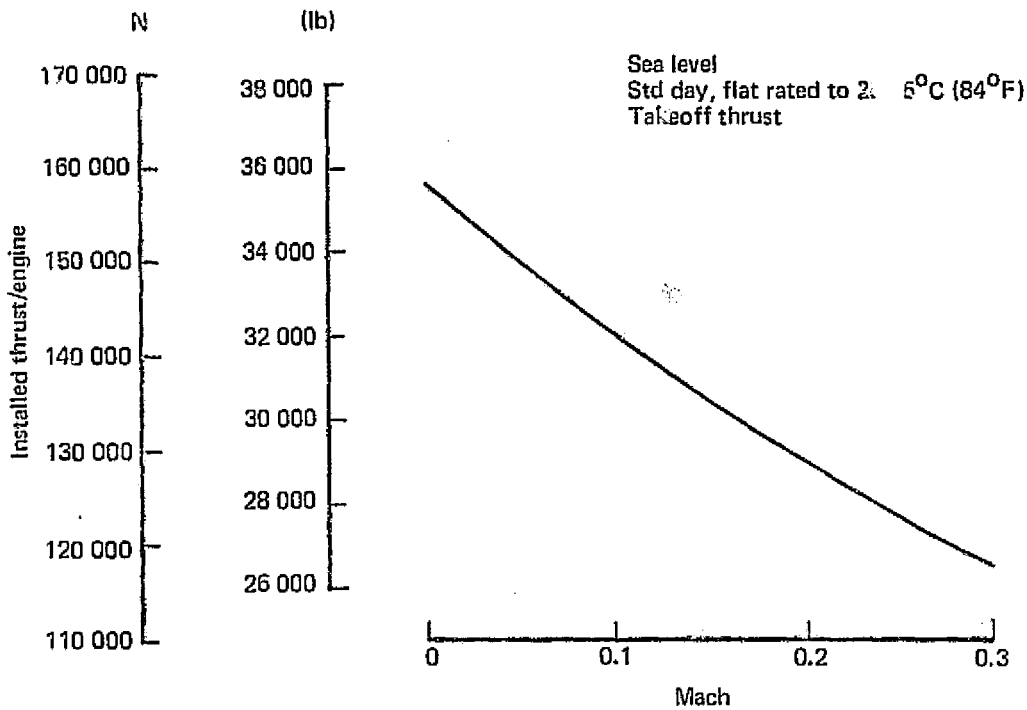

Figure 20 Turbofan Takeoff Thrust

resized designs, and enable the determination of required tail areas without a new configuration analysis. Table VI lists weights and wing areas used for the tail-sizing exercise, together with the resulting tail areas and volume coefficients.

Static stability and control analysis for the pitch axis of the reference turbofan airplane resulted in the tail-sizing chart shown in figure 22, from which the horizontal tail volume coefficient, $\bar{V}_H = 0.965$, was chosen. The designing conditions for the horizontal tail were approach stability (including aeroelastic effects that determine the aft c.g.) and takeoff rotation at light takeoff weight that determines the forward c.g. The tail volume coefficient for the required loading range of the configuration sized with the wing area of $S_W = (793\ m^2)$ is $\bar{V}_H = 0.965$.

The vertical tail was sized by rudder power requirements for ground engine-out control at 1.25 OEW. The directional static balance (figure 23) includes a 10 kt difference between the moment balance speed, V_{BAL}, and minimum control speed, V_{MC_g} (Boeing criterion).

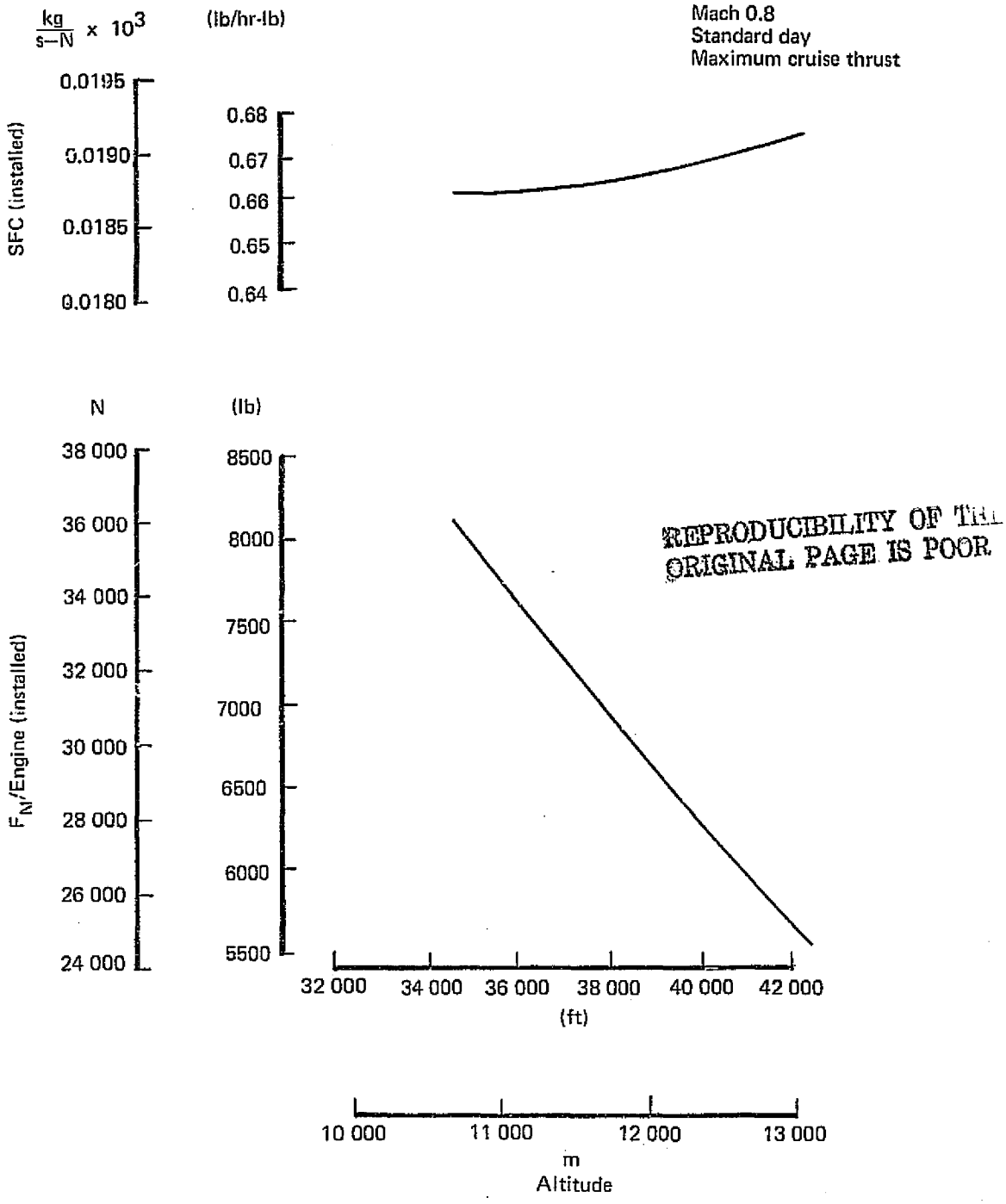

Figure 21 Turbofan Engine Cruise Performance

Table VI Tail Sizing Summary--Parametric Airplanes

Model	S_W m^2 (ft^2)	TOGW kg (lb)	$\bar{V}_H$	S_H	$\bar{V}_V$	S_V	V_R (light wt.)	C.G. limits
Turbofan (baseline airplane)	793 (2602)	113 636 (250 000)	0.96	50.30 m^2 (541.4 ft^2)	0.08 (control)	49.97 m^2 (537.9 ft^2)	55.60 m/sec (107 KEAS) (perf.)	0.15$\bar{c}$ - 0.43$\bar{c}$
Prop-fan (wing mounted)	774 (2540)	113 636 (250 000)	1.17	59.10 m^2 (636.12 ft^2)	0.08 (control)	48.36 m^2 (520.52 ft^2)	61.78 m/sec (120 KEAS) (T.O.R.)	0.08$\bar{c}$ - 0.34$\bar{c}$
Prop-fan (aft body mounted)	747 (2460)	114 273 (251 400)	1.20	68.93 m^2 (698.91 ft^2)	0.08 (stability)	54.94 m^2 (591.32 ft^2)	61.78 m/sec (120 KEAS) (T.O.R.)	0.20$\bar{c}$ - 0.52$\bar{c}$

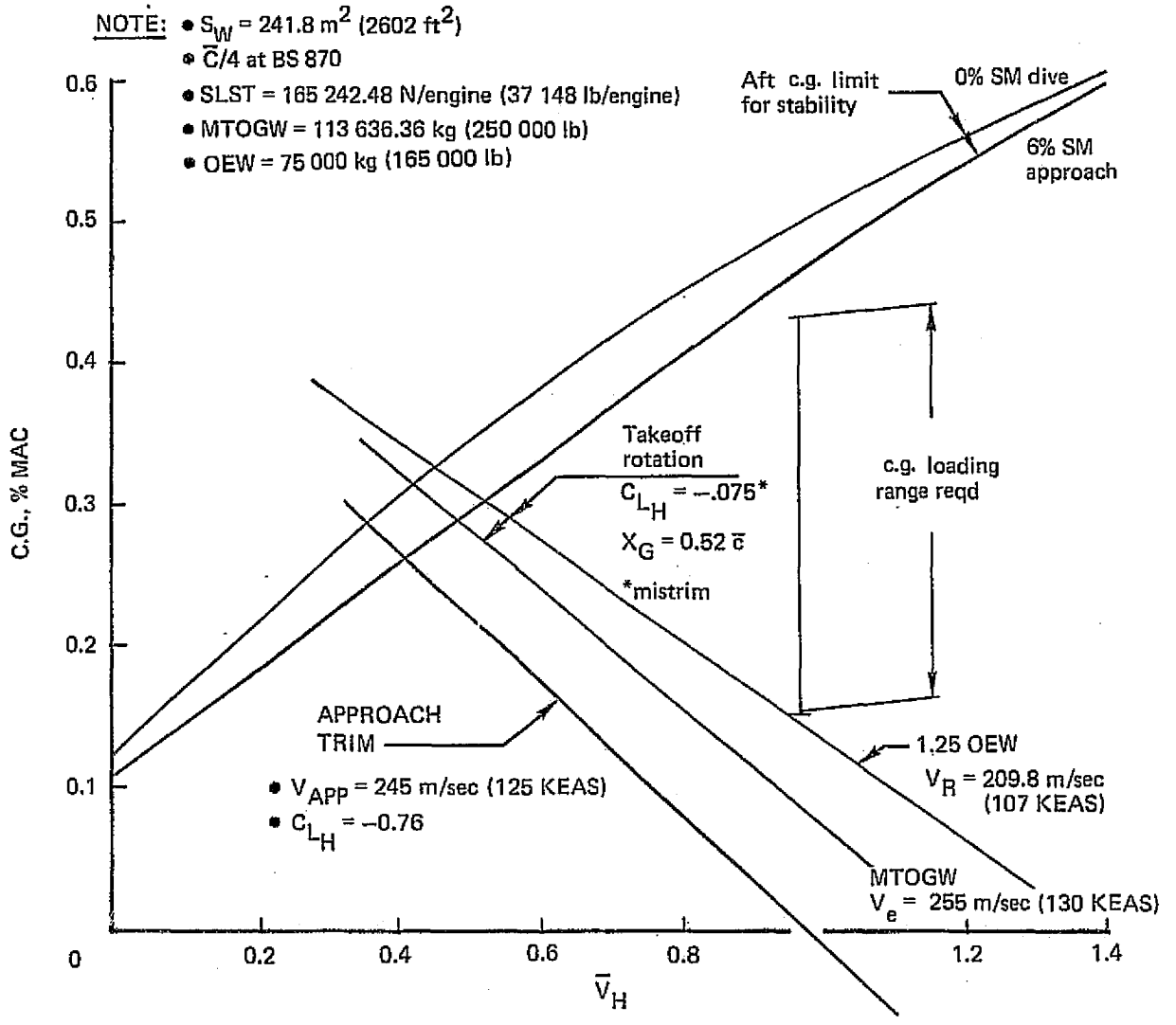

Figure 22 Horizontal Tail Sizing for Turbofan Baseline Configuration 767-761

		$V_{R_{MIN}}$	C_{L_V} MAX RUD	Engine Location	$\bar{V}_V$
(1)	T/F	209.8 m/sec (107 KEAS)	0.62	0.373 b/2	0.08
(2)	P/F	235.3 m/sec (120 KEAS)	0.62	0.41 b/2	0.08

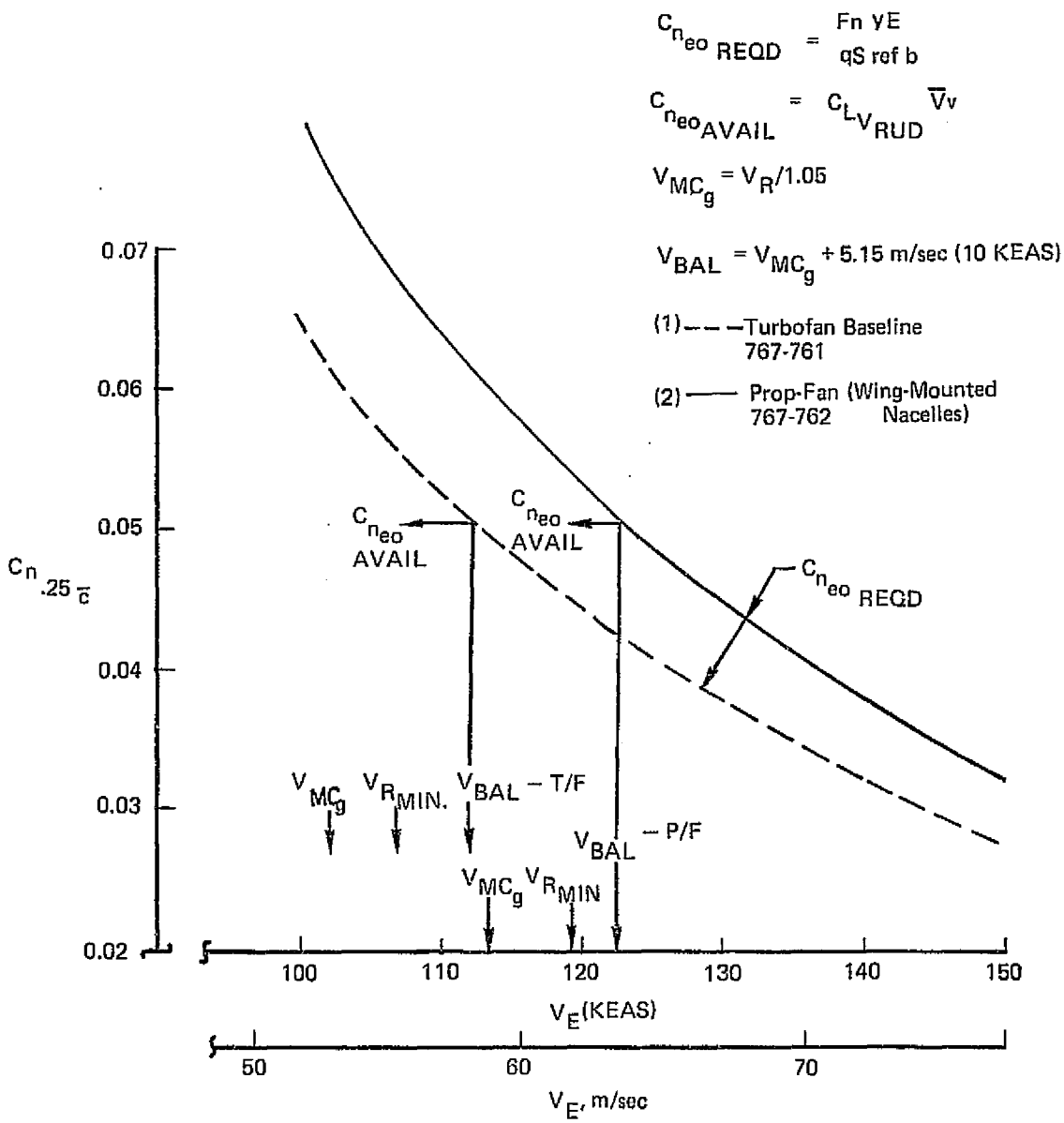

Figure 23 Vertical Tail Size Engine-Out Balance, 767-761 vs 767-762

5.1.5 CABIN NOISE

Estimated cabin internal overall sound pressure level (OASLP) and PSIL values for the reference turbofan airplane are shown in figure 24. The relative effects of the external noise source components on OASPL are also shown. The two wing-mounted high-bypass-ratio engines have a slightly lower jet velocity than current commercial transport engines, so the jet influence on interior noise is reduced. Peripheral lining in the inlet and fan duct reduce fan tones and inlet "buzzsaw" noise. Therefore, the most significant contributor to cabin noise is estimated to be turbulent boundary layer fluctuations.

Cabin sidewall treatment was assumed to provide a uniform noise reduction throughout the length of the fuselage. This treatment consists of fiberglass insulation and interior trim separated by airspaces, installed in a conventional skin/stringer/frame body structure.

5.1.6 WEIGHT AND BALANCE

Table VII is the weight statement for the reference turbofan. These weights represent current technology conventional aluminum structure and 1985 engine technology.

Figure 25 shows that the airplane has acceptable loadability within the design c.g. range. Airplane loading range requirements, while considering stability and control forward and aft limits, also provide for conceptual design OEW c.g. tolerances including the effect of possible customer variations.

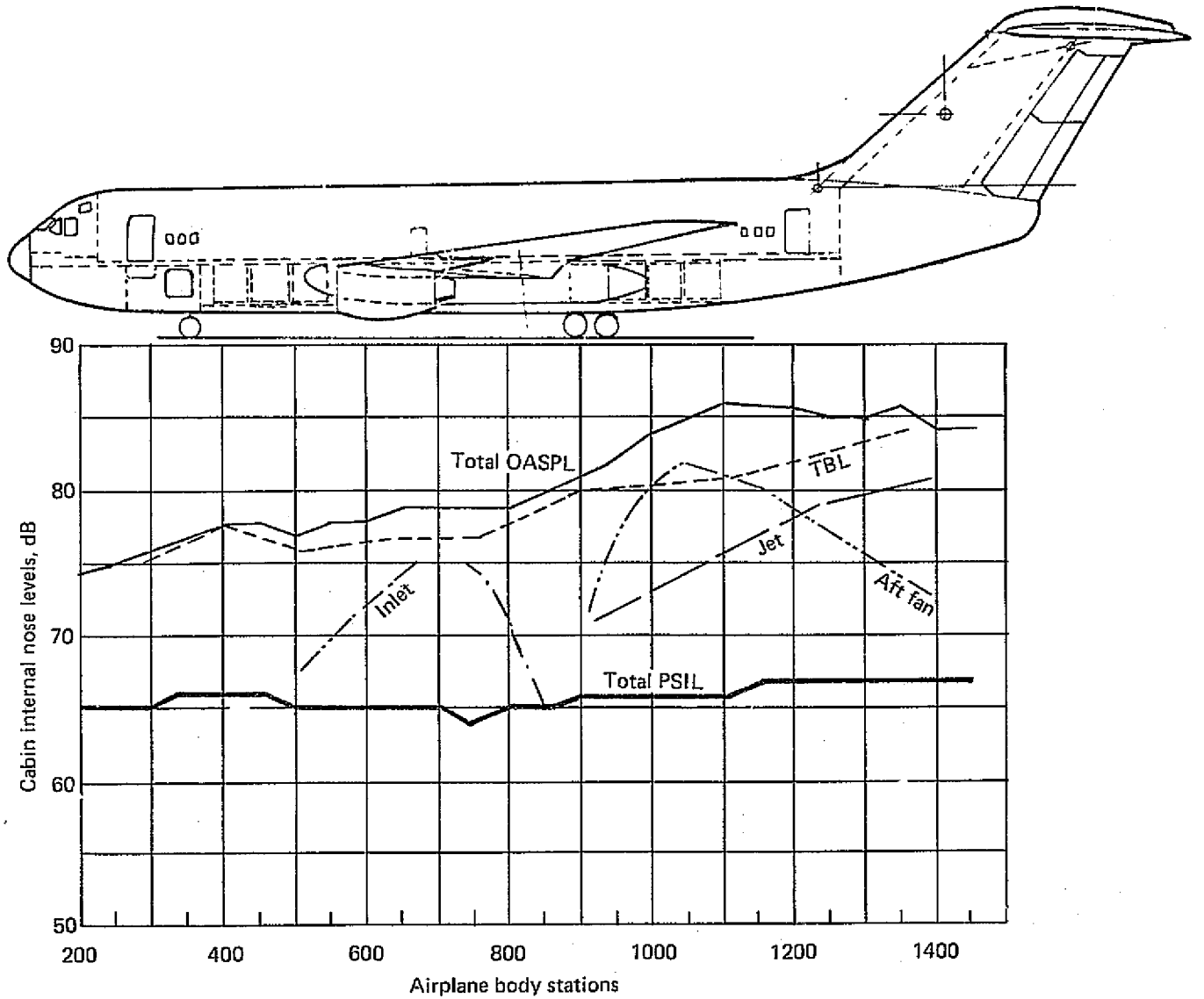

Figure 24 Cabin Environment and Exterior Noise Sources of Turbofan (767-761)

Table VII Weight Statement for the Baseline Turbofan (767-761)

	kg	lb
Wing	17 050	37 580
Horizontal tail	1370	3020
Vertical tail	1660	3670
Body	13 720	30 250
Main landing gear	5930	13 070
Nose landing gear	710	1570
Nacelle and strut	3260	7190
Total structure	43 700	(96 350)
Engine	6290	13 880
Engine accessories	480	1070
Engine controls	40	80
Starting system	50	100
Fuel system	570	1250
Thrust reverser	1340	2960
Total propulsion system	(8770)	(19 340)
Instruments	530	1170
Surface controls	1880	4150
Hydraulics	1320	2900
Pneumatics	270	600
Electrical	1140	2520
Electronics	960	2120
Flight provisions	310	690
Passenger accommodations	6950	15 310
Cargo handling	1230	2700
Emergency equipment	300	670
Air conditioning	1110	2450
Anti-icing	230	500
Auxiliary power unit	930	2060
Total fixed equipment	(17 160)	(37 840)
Exterior paint	70	150
Options	910	2000
Manufacturer's empty weight	(70 610)	(155 680)
Standard and operational items	4450	9800
Operational empty weight	(75 060)	(165 480)
Maximum taxi weight	116 260	256 300

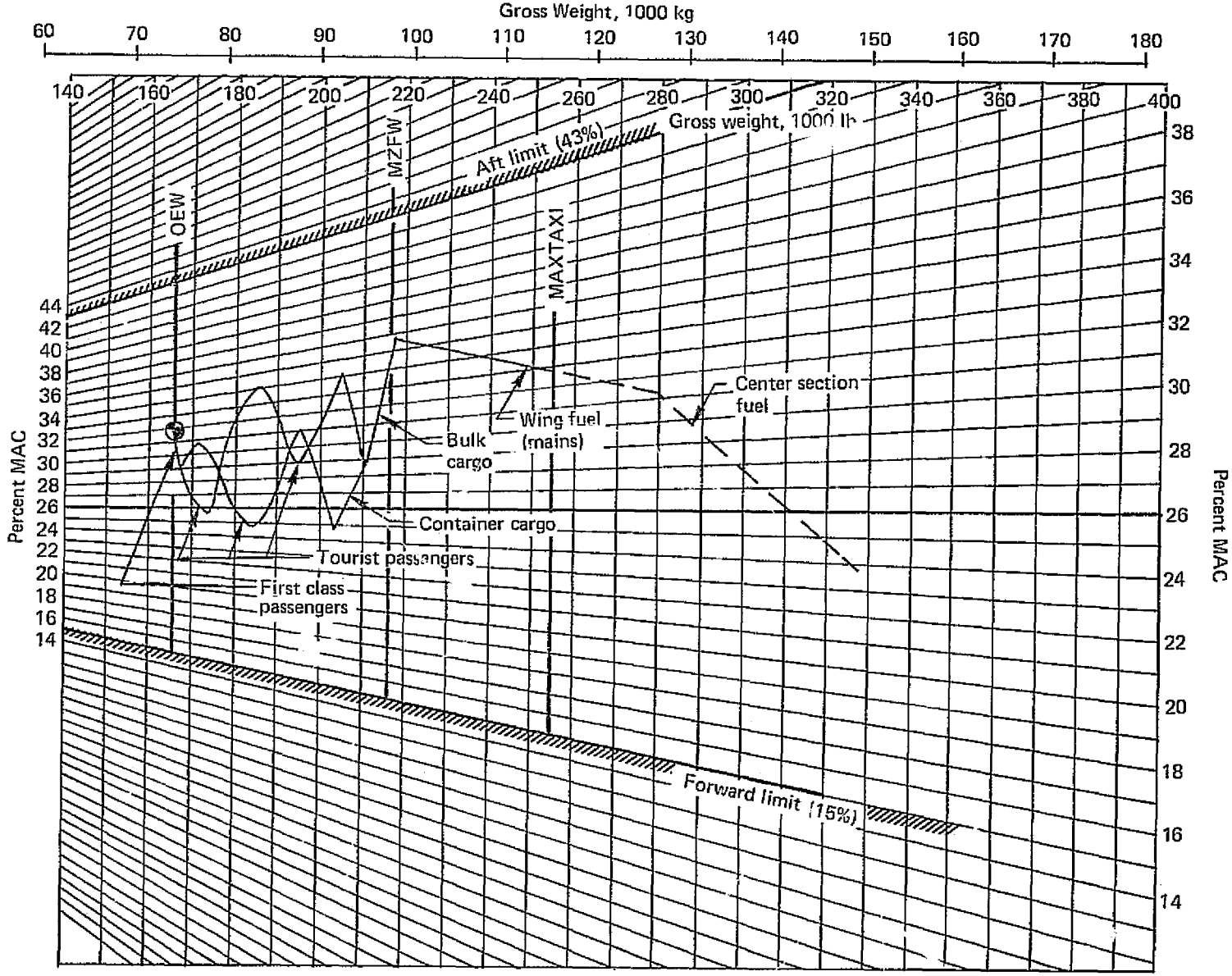

Figure 25 Loadability Diagram for the Baseline Turbofan (767-761)

5.2 WING-MOUNTED PROP-FAN AIRPLANE

5.2.1 ARRANGEMENT CONSIDERATIONS

The configuration and geometric characteristics of the prop-fan powered airplane with the wing-mounted engines are shown in figure 26 and table VIII.

The wing-mounted prop-fan has the same general arrangement as the turbofan airplane except for the engine installation. The spanwise location of the engine was selected to provide a blade-tip-to-body clearance of 0.8 propeller diameters as recommended by Hamilton Standard. Three different nacelle installations were studied. Initially, the engine turbine section was placed forward of the wingbox, but the resulting nacelle was long and heavy, contained much waste space, and had excessive wetted area. Review of engine failure possibilities indicated that a dry bay (fuel-free volume) in the wingbox over the engine would provide adequate safety for underwing placement of the turbine section (fig. 27). It was necessary to "gull" the wing slightly to provide the 0.76 m (30 in) propeller ground clearance considered the minimum acceptable value by Hamilton Standard for prevention of pebble-strike damage. The third arrangement considered was to place the engine over the wing. Fire protection (in case of burning fuel flowing from the turbine exhaust) required that the tailpipe extend to the trailing edge, resulting in extra weight and wetted area, and likely causing severe interference drag at cruise. Therefore, the arrangement in figure 27 was selected. The propellers have opposite rotation, upward on the inboard side. This sense of rotation is expected to give less cabin noise than the opposite one, and symmetry of wing tailoring is preserved.

5.2.2 AERODYNAMIC CHARACTERISTICS

The aerodynamic characteristics of the wing-mounted prop-fan airplane were based on those of the turbofan airplane with corrections applied to account for the "over-under" nacelle installation and the presence of the propeller slipstream.

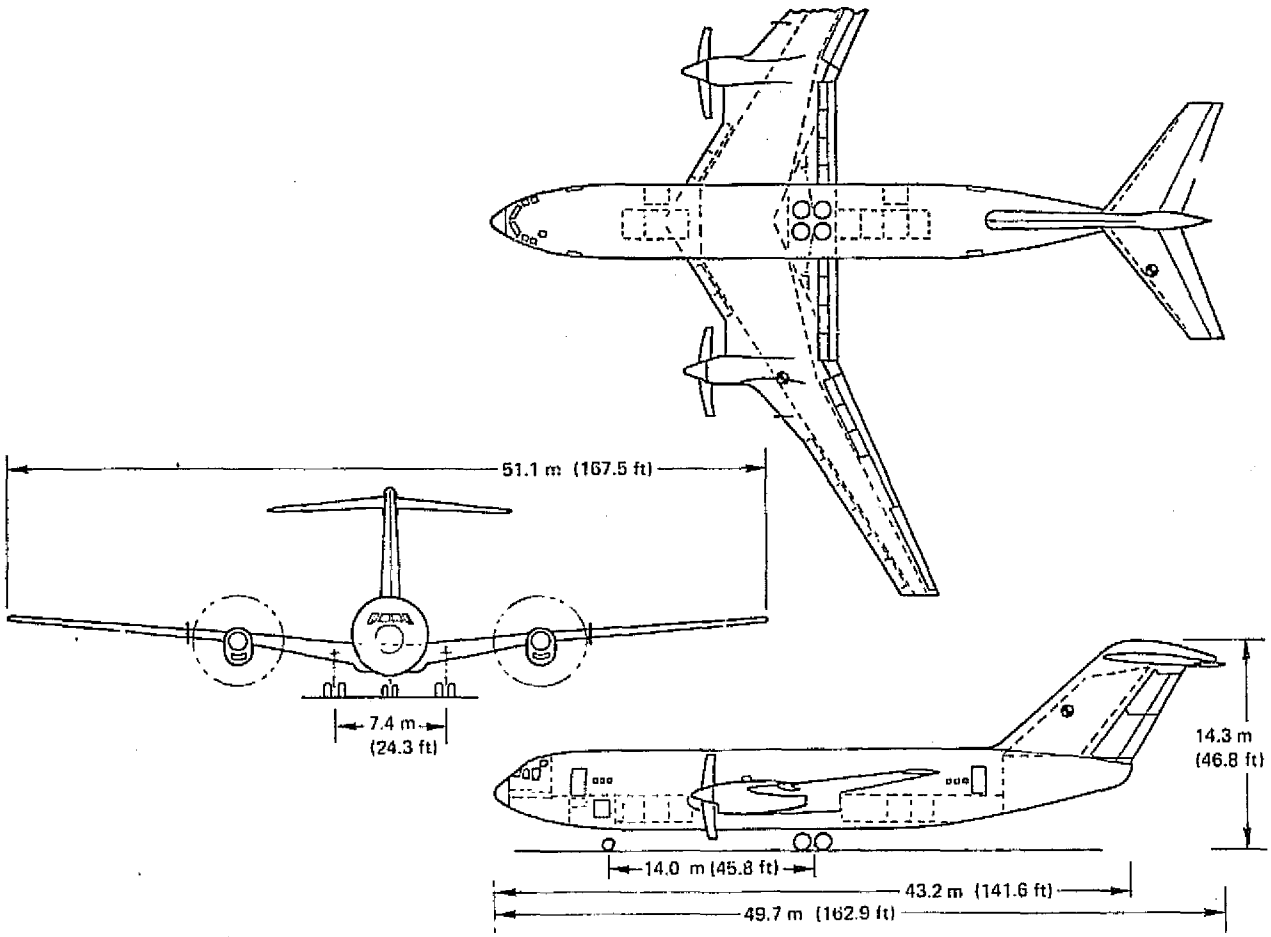

Figure 26 General Arrangement, Wing-Mounted Prop-Fan (767-762)

Table VIII 767-762 Wing-Mounted Prop-Fan Airplane Characteristics and Performance

Weights	TOGW, kg (lb)	122 060 (269 100)
	OEW, kg (lb)	83 690 (184 500)
	Landing weight (mission, kg (lb)	116 685 (235 200)
	(maximum), kg (lb)	110 580 (243 780)
	Payload, pass./kg (pass./lb)	180/16 738 (180/36 900)
	Maximum fuel capacity, kg (lb)	69 592 (153 423)
	C.G. limits, % MAC	8 fwd, 34 aft
	T/W equivalent	.279
	W/S, N/m^2 (lb/ft^2)	4592 (95.9)
Performance	Still air range, km (nmi)	3333.6 (1800)
	Cruise Mach number	0.80
	Cruise altitude, m (ft)	11 280 (37 000)
	Range factor, km (mni)	26 780 (14 460)
	L/D average cruise	17.20
	SFC, kg/kN-sec (lb/hr/lb)	0.0155 (0.546)
	TOFL, m (ft)	1476 (4841)
	C.G. position, % MAC	8
	V_{APP}, m/sec (KEAS)	65 (126)
	Block fuel, kg (lb)	15 550 (34 280)
	Reserves, kg (lb)	6250 (13 780)
	Total fuel, kg (lb)	22 060 (48 630)
	Block fuel, kg/pass. km (lb/pass. nmi)	0.02596 (0.106)
power plants	Number	2
	Type	Scaled P & W STS476
	Power	22 722 kW (30 470 SHP)
Landing gear, m (in.)	Nose	(2)–0.86 x 0.28 (34 x 11)
	Main	(8)–1.09 x 0.42 (43 x 16.5)
	Truck size	1.32 x 0.97 (52 x 38)
	Oleo stroke (extended to static)	0.51 (20)
Body	Length, m (in.)	43.15 (1699)
	Maximum diameter, m (in.)	5.38 (211.6)
	Accommodations	180 passengers–10% 1st, 90% tourist
		8 LD-3 containers, 35.79 m^3 (1264 ft^3)

Wing and empennage	Wing	Horizontal tail	Vertical tail
Area, m^2 (ft^2)	260.8 (2807)	64.3 (692)	55.1 (593)
Aspect ratio	10	4.0	0.8
Taper ratio	0.353	0.4	0.65
c/4 sweep, deg	30	35	45
Incidence, deg	1	–	–
Dihedral, deg	2	-3	–
t/c, %	3	10.5	12
MAC, m (in.)	5.496 (216.37)	4.254 (167.49)	8.425 (331.71)
Span, m (in.)	51.066 (2010.49)	16.036 (631.32)	6.641 (261.45)
Tail arm, m (in.)	–	25.171 (990.98)	19.327 (760.90)
Tail vol coefficient	–	1.129	0.080

1 Wing incidence: SOB 3.75°
MAC 2.00°
TIP -1.00°

2 Wing dihedral: Inboard–7.5°
BL 402.1 –4.3° outboard

3 Wing t/c%: SOB–13.1 (total chord)
BL 427–10.5
(const outboard)

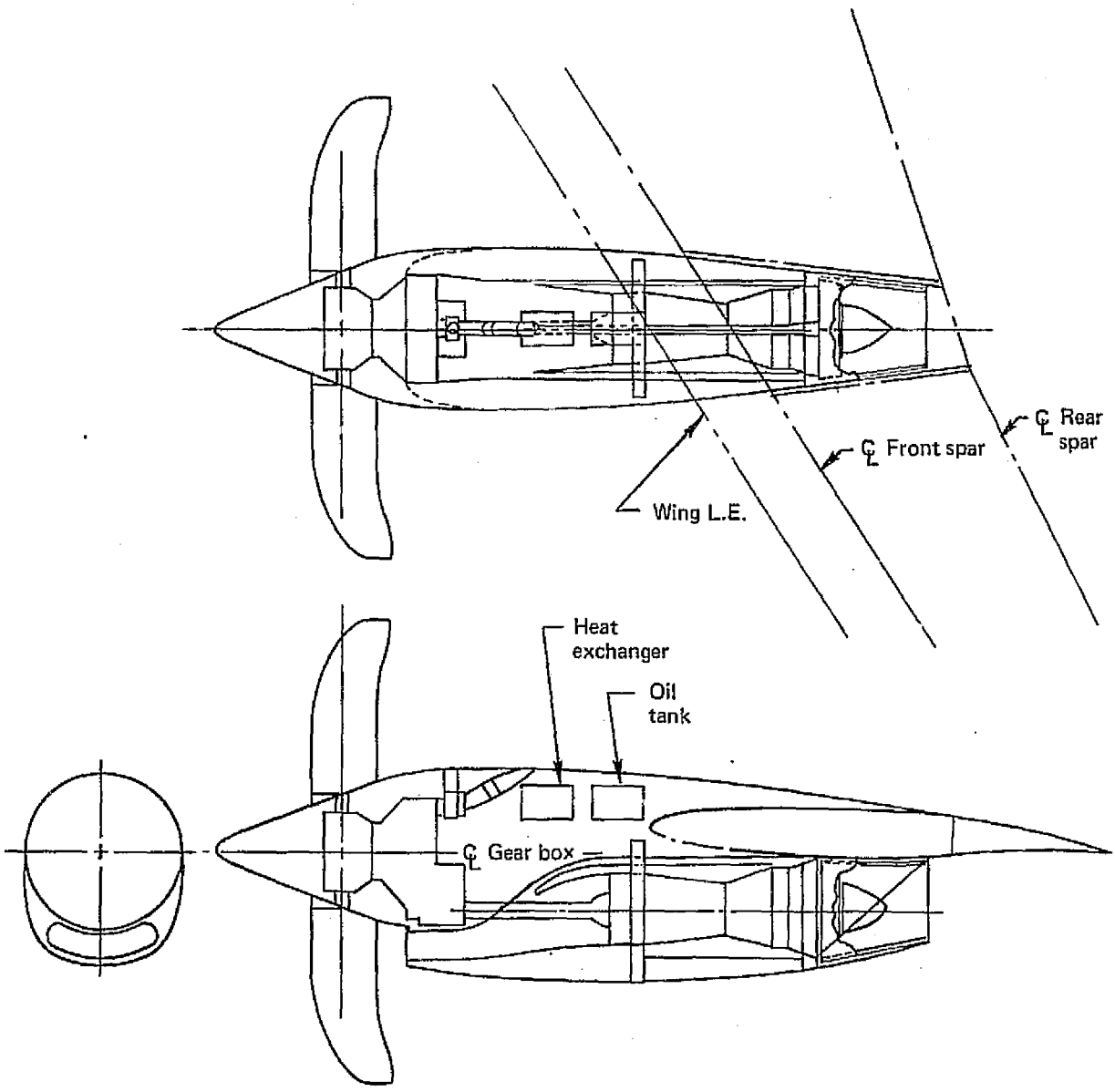

Figure 27 Prop-Fan Installation

5.2.2.1 High-Speed Characteristics

Because of the many uncertainties in predicting slipstream effects in high-speed compressible flow, a simplified approach was adopted to estimate the cruise-drag polars for the wing-mounted prop-fan. Figure 28 summarizes the corrections applied to the turbofan drag polars to arrive at the corresponding wing-mounted prop-fan data.

The portion of wing immersed in the slipstream experiences an effective Mach number in excess of freestream. To account for this locally higher Mach number, degradation in airplane drag-rise Mach number was applied, with the degradation in the form of a wing-area-weighted fraction of slipstream Mach number increment. Values used in the study were 0.26 for the ratio of immersed wing area to total exposed area, and 0.045 for the average slipstream Mach number increment (calculated from simple momentum considerations). Any nacelle drag rise contribution was ignored.

Similarly, because immersed surfaces also experience an elevated slipstream dynamic pressure, a scrubbing drag correction was applied to the immersed portions of wing and nacelles. At Mach 0.8 cruise, this amounted to a drag coefficient increment of 0.0003.

The over-under nacelle installation also gives rise to a degradation in high-speed drag characteristics, even when careful aerodynamic tailoring is employed. This takes the form of an increase in configuration profile drag due to lift (polar shape). The penalty applied, based on Boeing test results for over-under nacelle installations, increases with lift coefficient and amounts to a 0.0008 drag coefficient increment at a lift coefficient of 0.5.

The resultant wing-mounted prop-fan high-speed drag polars are shown in figure 29. Total parasite drag coefficient at Mach 0.7 and 11 280 m (37 000 ft) altitude is 0.0166, and maximum lift-to-drag ratio at Mach 0.8 is 17.4.

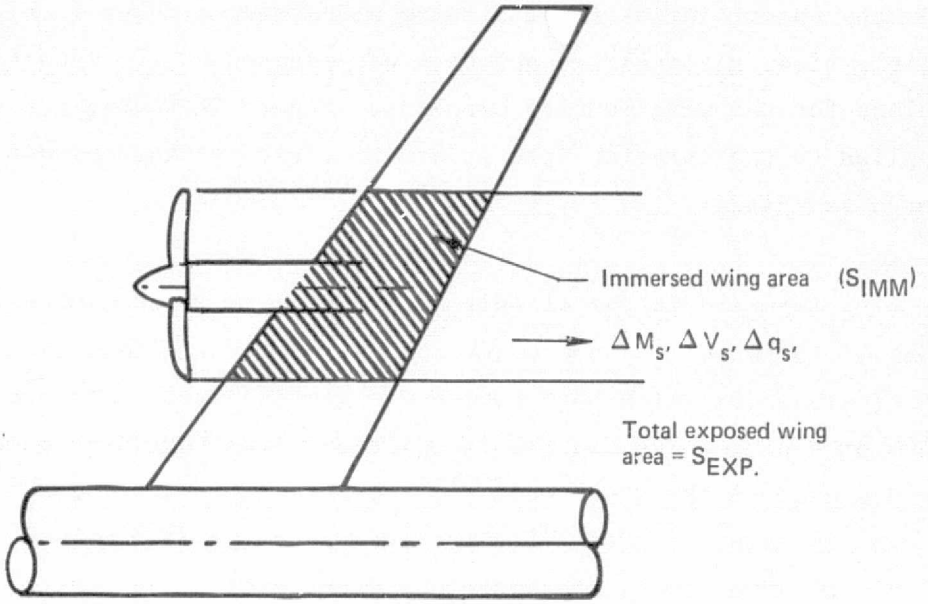

CRUISE DRAG INCREMENTS

- $\Delta M_{DD} = -\frac{S_{IMM.}}{S_{EXP}} \Delta M_S$

- $\Delta C_{D_{SCRUB}} = \sum \frac{f_{IMM.}}{S_{REF}} \frac{\Delta q_s}{q_\infty}$ (Wing and nacelles)

- PROFILE DRAG-DUE-TO-LIFT INCREMENT DUE TO OVER-UNDER NACELLE

TYPICAL VALUES

$\left.\begin{array}{l} \Delta M_S = 0.045 \\ \frac{S_{IMM}}{S_{EXP}} = 0.26 \end{array}\right\} \quad \Delta M_{DD} = -0.012$

$\frac{\Delta q_s}{q_\infty} = 0.116 \sim \Delta C_{D_{SCRUB}}$ (Wing and nacelles) = 0.0003

$\Delta C_{D_{L_{NACELLES}}} = 0.0008$ AT $C_L = 0.5$

Figure 28 Prop-Fan Airplane Simplified High-Speed Power Effects Method

Parasite drag breakdown (M = 0.7/11280 m)

Item	Wetted area, m^2	(ft^2)	Equiv friction area ($f = C_f A_{WET}$), m^2	(ft^2)
Wing	459.76	4950	1.508	16.0
Body	577.75	6220	1.544	17.0
Vert. tail	129.97	1400	0.370	4.0
Horiz. tail	120.68	1300	0.341	3.7
Nacelles	135.36	1460	0.394	4.2
Flap tracks	–	–	0.078	0.84
Scrubbing	–	–	0.083	0.89
Total	1423.52	15 330	4.318	46.73

$C_{D_{PARASITE}} = 0.0166$

$S_{REF} = 260.77\ m^2\ (=2807\ ft^2)$

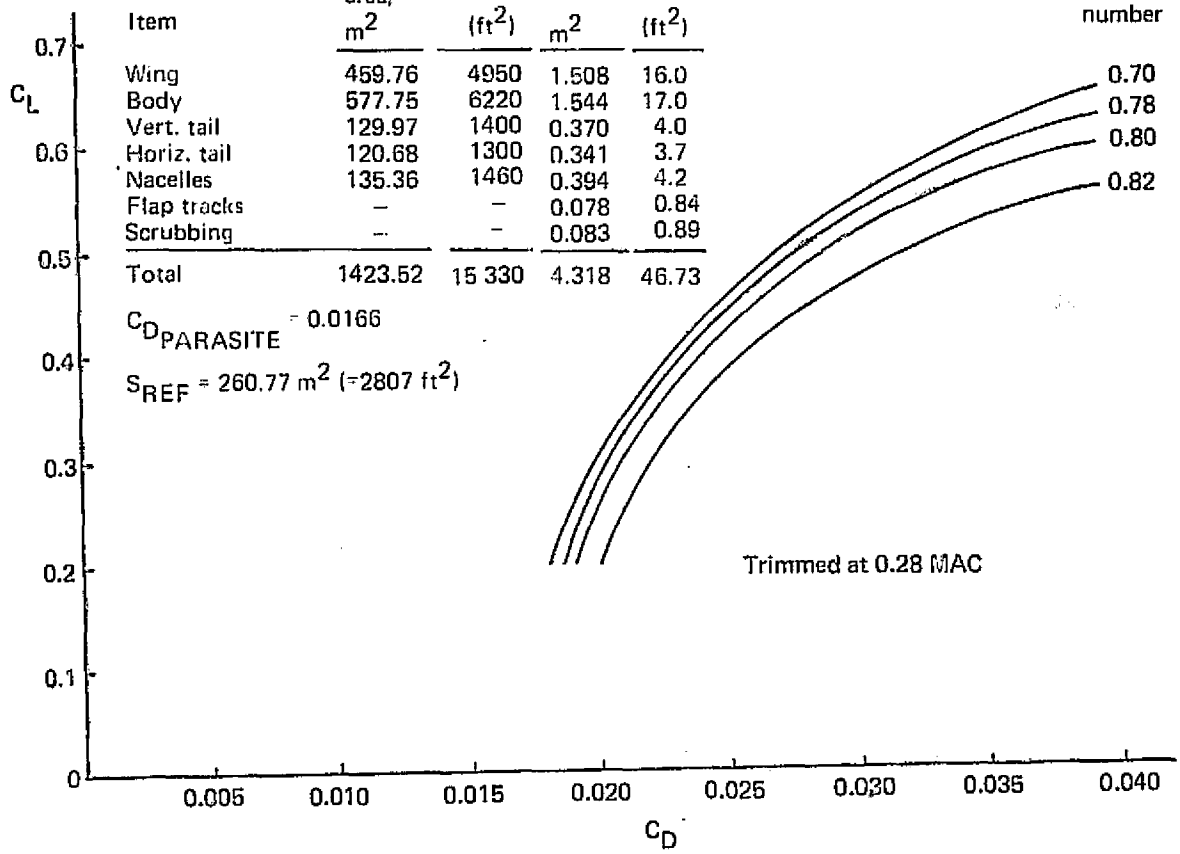

Figure 29 Sized Wing-Mounted Prop-Fan High-Speed Drag Polars

No credit was taken for the potentially favorable thrust forces resulting from wing-induced slipstream derotation (section 5.2.5.1). Analysis of applicable experimental data (ref. 3) indicates that the effect is small, and other compensating unfavorable drag phenomena could arise because of local loading effects.

5.2.2.2 Low-Speed Characteristics

In the low-speed flight regime, airplane characteristics are much more sensitive to power effects than in cruise because the slipstream velocity increment is a substantial fraction of the flight speed. In addition, flying with an engine out necessitates the trimming not only of asymmetric yawing moments, but also of appreciable rolling moments.

For these reasons, careful attention was paid to power effects in the prediction of low-speed aerodynamic characteristics. The power effects method of reference 4, together with untrimmed power-off data generated by the method of reference 5, were used to calculate power-on lift and drag characteristics and to provide data for use in the calculation of engine-out characteristics. Again, no credit for swirl momentum recovery was taken.

The results of the calculations are summarized in figure 30, which shows engine-out lift-to-drag ratio versus lift coefficient for the takeoff climbout condition with gear retracted and c.g. at the forward limit.

Because the parametric method used in the airplane sizing process does not adequately allow for the complex power effects associated with the wing-mounted prop-fan, the final airplane characteristics were determined by an iterative process: as a first approximation, power-off low-speed characteristics were used to arrive at a "first iteration sized" airplane; this was then analyzed in detail, resulting in the chain-dashed flaps-down characteristics shown in figure 30. The first iteration envelope shown in the figure was then used to

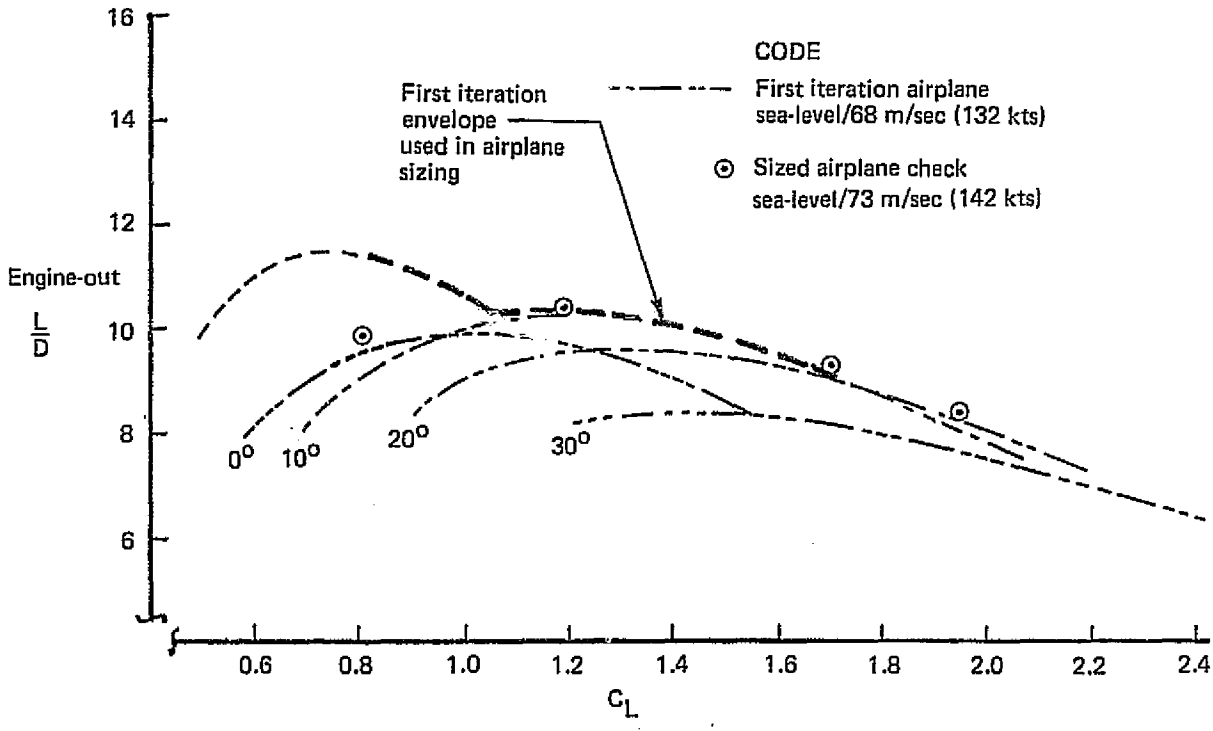

Figure 30 Wing-Mounted Prop-Fan Airplane Engine-Out Climbout Lift-to-Drag Ratios

generate final airplane characteristics, which were subsequently checked at selected conditions (circled data points).

Although both sizing and reference speed changes occurred between the first iteration and final airplanes, a satisfactory degree of convergence was achieved for the sea level takeoff case. For the final sized airplane at mission gross weight, optimum flap setting, climbout lift coefficient and lift-to-drag ratio, engine-out, are 10°, 1.63 and 9.4, respectively.

Figure 31 shows low-speed lift and drag breakdowns for the wing-mounted prop-fan and turbofan airplanes. The comparison is made at 10^{o} flap setting and the same engine-out lift coefficient. The increased engine-out drag of the wing-mounted prop-fan is attributable chiefly to slipstream drag (par. 5.2.5), increased rudder trim drag, and aileron trim drag. Lesser contributory factors are the increment in feathered propeller drag over turbofan windmilling drag and the increased longitudinal trim drag resulting from the further forward c.g. location.

In the approach condition, the only factor that has a direct impact on airplane sizing is the stall speed, which under FAR requirements must be demonstrated power-off. Wind tunnel tests have shown a sizable degradation in achievable maximum lift coefficient due to the wing-mounted over-under nacelle installation. For an untailored configuration, the degradation can amount to a C_L of -0.6. Suitable tailoring of wing planform, leading-edge devices and nacelle (section 5.2.5) can reduce this to -0.2 to -0.15. For the purposes of this study, a 1 g $C_{L_{MAX}}$ decrement of 0.15 at all flap settings was assumed for the wing-mounted prop-fan. Resulting FAR stall lift coefficients, for the airplane trimmed at the forward c.g. location (0.08 MAC), are as follows:

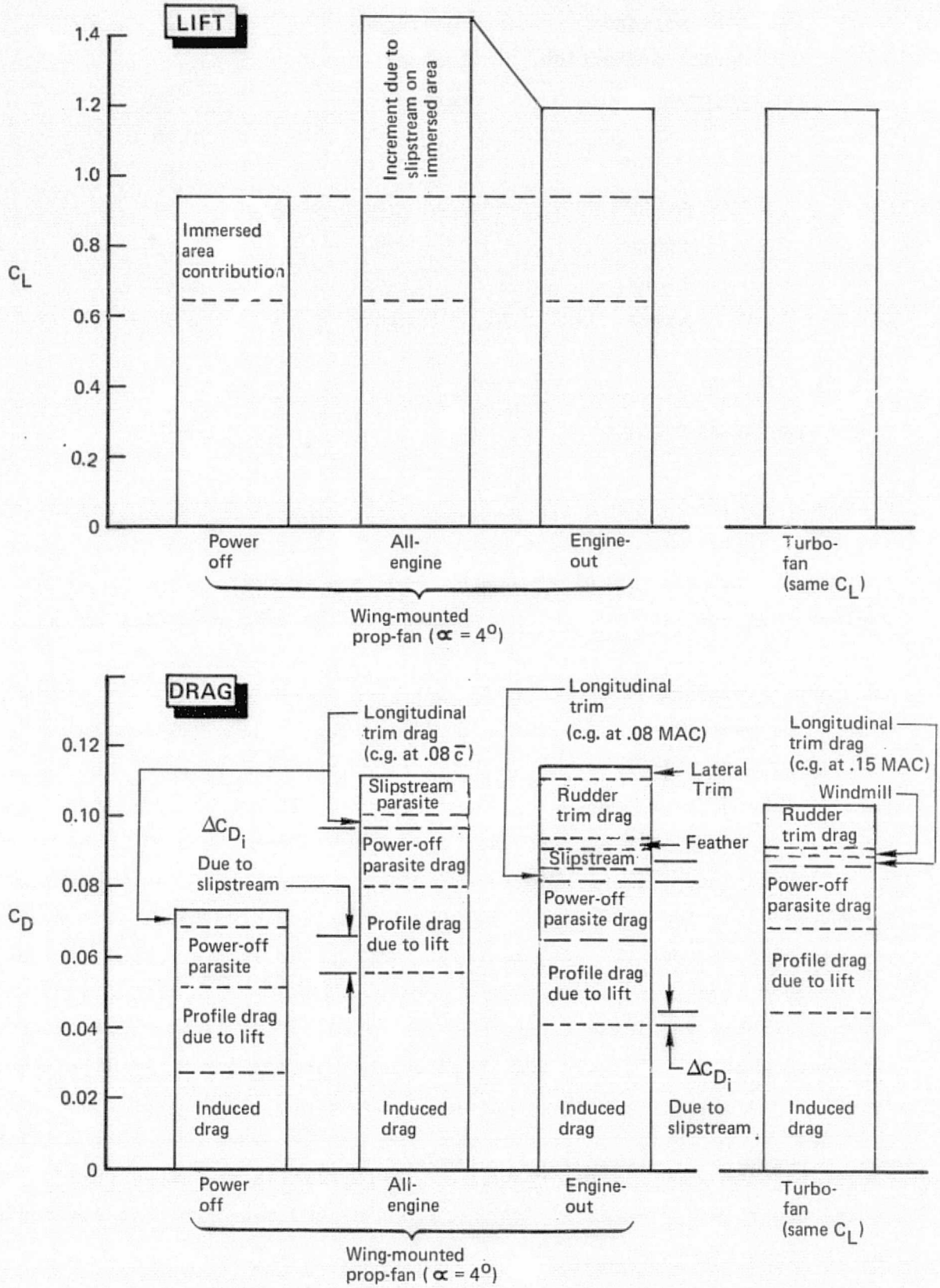

Figure 31 Comparison of Low-Speed Lift and Drag Breakdowns for Wing-Mounted Prop-Fan and Turbofan

Leading-edge device deflection, degrees	Trailing-edge flap deflection, degrees	C_{L_S} FAR
0	0	1.46
50/60	0	1.86
50/60	10	2.22
50/60	20	2.44
50/60	30	2.57
50/60	40	2.63

5.2.3 ENGINE/PROPELLER

A scaled version of the Pratt & Whitney Aircraft STS 476 study engine was used for the prop-fan studies. The engine's technology level is consistent with that of the turbofan airplane studies and is also representative of inservice engines that are expected to be available in the 1980-1985 time period.

The engine incorporates two shafts, the prop-fan being driven by a free turbine. The overall pressure ratio is 20 and the maximum trubine inlet temperature is 1644 K (2960°R). Two modifications have been made to the engine performance shown in reference 6. First, Pratt & Whitney and Hamilton Standard now believe that the reduction gear efficiency should be 0.99 rather than 0.98 and the performance shown herein reflects the better efficiency. Second, the power available for takeoff is less than what would result if a conventional relationship between the turbine inlet temperature at the takeoff rating and the maximum climb rating were used. Pratt & Whitney Aircraft advised that the power available for takeoff could be increased 17% if the turbine inlet temperature at takeoff were 130° greater than at maximum climb (the temperature relationship assumed for the turbofan). Therefore, the higher takeoff rating was used for performance calculations. No changes were made to the climb or cruise ratings given in reference 6. The turbine inlet temperature at maximum cruise power is approximately 1417°K (2550°R) and equal to that assumed for the turbofan engine.

The prop-fan performance was based on a design having eight blades, each of 200 activity factor/0.12 integrated design lift coefficient, operating at 800 fps tip speed. The efficiency of the prop-fan is defined by the nondimensional curves of reference 7.

Installed engine/prop-fan performance is based on 100% engine inlet recovery, 280 kW (376 hp) power extraction, and zero engine airbleed. Supercharging of the engine flow by the rotor is approximately equal to the engine inlet pressure loss. Air for cabin pressurization and air conditioning was provided by an engine-driven compressor to avoid the power losses associated with engine bleed, which are particularly large with turboshaft engines.

The required uninstalled power per engine at sea level, zero speed, and standard day was found to be 22 700 kW (30 470 shp) and the prop-fan diameter corresponding to the selected cruise power loading was 5.97 m (19.6 ft). The installed engine performance is shown in figures 32 and 33.

5.2.4 FLIGHT CONTROLS

The 767-762 wing-mounted prop-fan has the same lateral-directional and pitch control systems as the 767-761 turbofan airplane. Table VI summarizes and compares the empennage characteristics for all three airplanes.

The scope of the investigation and the ground rules for the analysis were the same as for the turbofan airplane. Emphasis was placed on the propeller effects on longitudinal stability. The propeller effects on speed stability and lateral-directional stability are believed to be second order effects and were neglected.

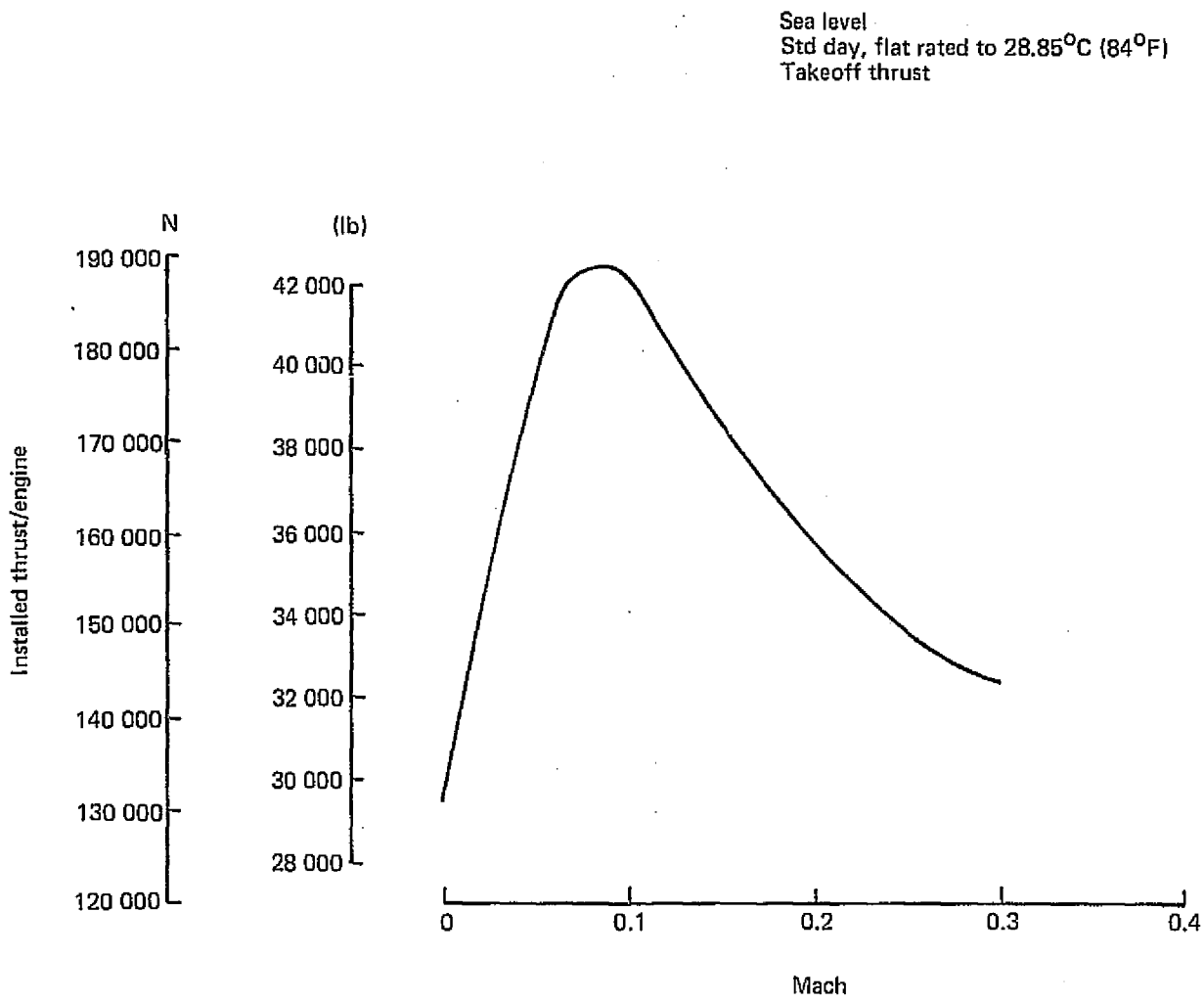

Figura 32 Prop-Fan/Engine Takeoff Thrust

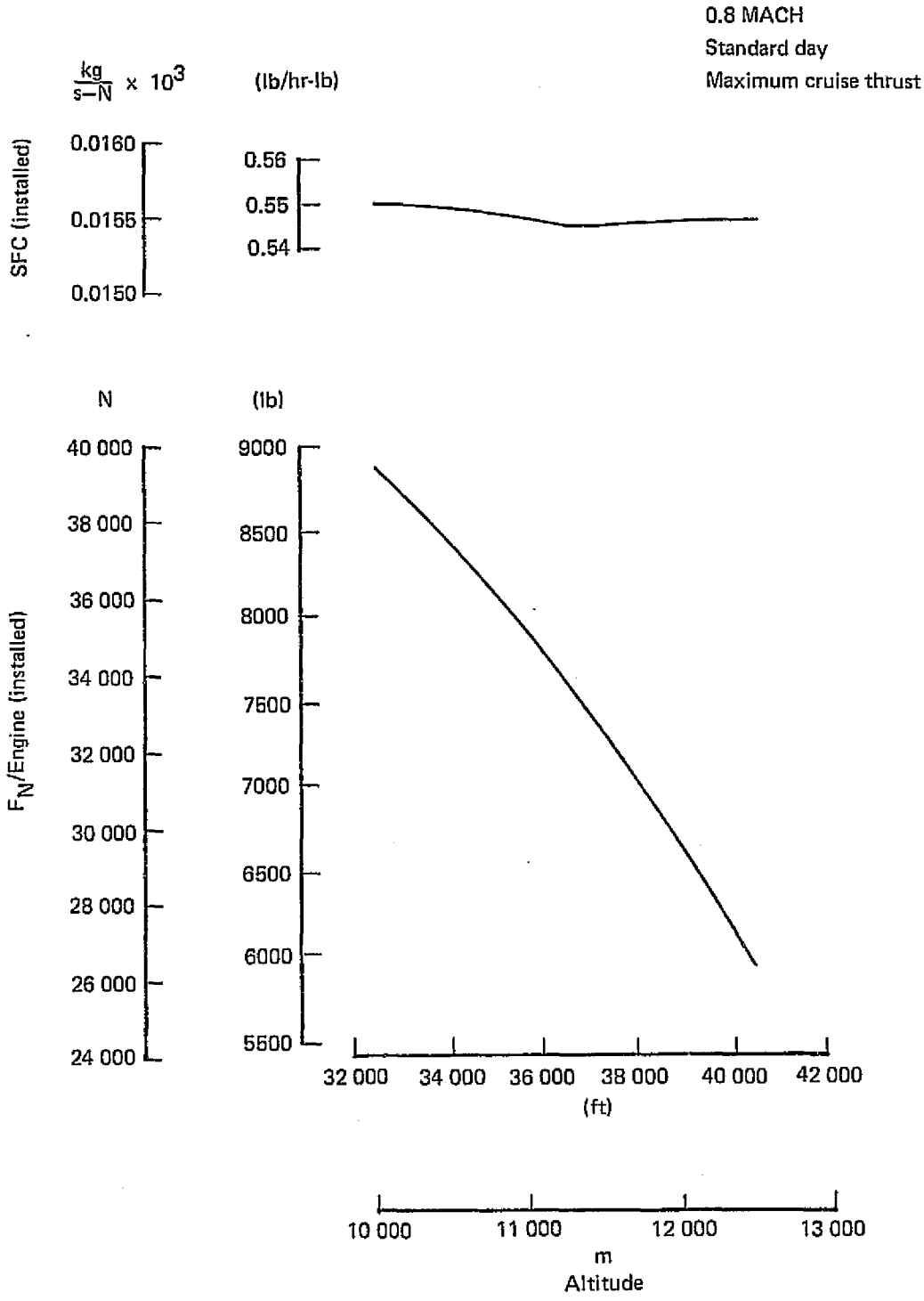

Figure 33 Prop-Fan/Engine Cruise Performance

Wing lift (ΔC_{L_α}) and tail downwash ($\Delta\varepsilon_\alpha$) increments due to the propeller slipstream were computed along with the propeller normal forces, $C_{N_{\alpha_p}}$. All of these increments were found to be destabilizing. The wing-lift increment (ΔC_{L_α}), due to the slipstream, acts at the 0.25 MAC of the wing resulting in small moment arms for all c.g. positions. Since the wing pitching moment is computed about the 0.25 MAC of the wing, the increment (ΔC_{M_α}) due to the slipstream was neglected.

Figure 34 is the horizontal tail sizing chart for the wing-mounted prop-fan. The propeller slipstream is the dominant factor at low speeds and high-power settings. Consequently, takeoff and go-around stability at full power sets the aft c.g. limit. The dive and cruise aft c.g. limits were less critical than the power-off approach case, and are not shown. The forward c.g. limit is set by the ability of the tail to rotate the airplane to the liftoff angle of attack at maximum TOGW. The lines on figure 34 show that the favorable effect of power noticeably reduces the tail volume required to rotate. With an engine inoperative, rotation could be achieved at about 3% greater speed than the 130-knot design value shown for full-power capability. Because the takeoff field length is not a design consideration (the -762 has a 30% cushion), no tail size adjustment was considered necessary.

The vertical tail was sized by engine-out directional control at the ground minimum control speed, V_{MC_g}. Because of the increased thrust and moment arm compared to the turbofan airplane, the tail size required to meet performance rotation speeds at light takeoff weights (1.25 OEW) became excessive. Consequently, a minimum rotation speed of V_R = 62 m/sec (120 KEAS) was established, resulting in an increased minimum control speed ($V_R = 1.05\ V_{MC_g}$) and a tail volume coefficient, $\overline{V}_v = 0.08$, equal to that of the 767-761 turbofan airplane.

Lateral trim requirements to cope with an engine failure at takeoff and go-around for the wing-mounted prop-fan is a problem. An estimated 20° of aileron deflection is required to trim the large rolling moment created by asymmetrical wing lift alone. Though no solutions have been identified, automatic flap retraction at engine failure (similar to YC-14) and special aileron-spoiler gearing are possible answers.

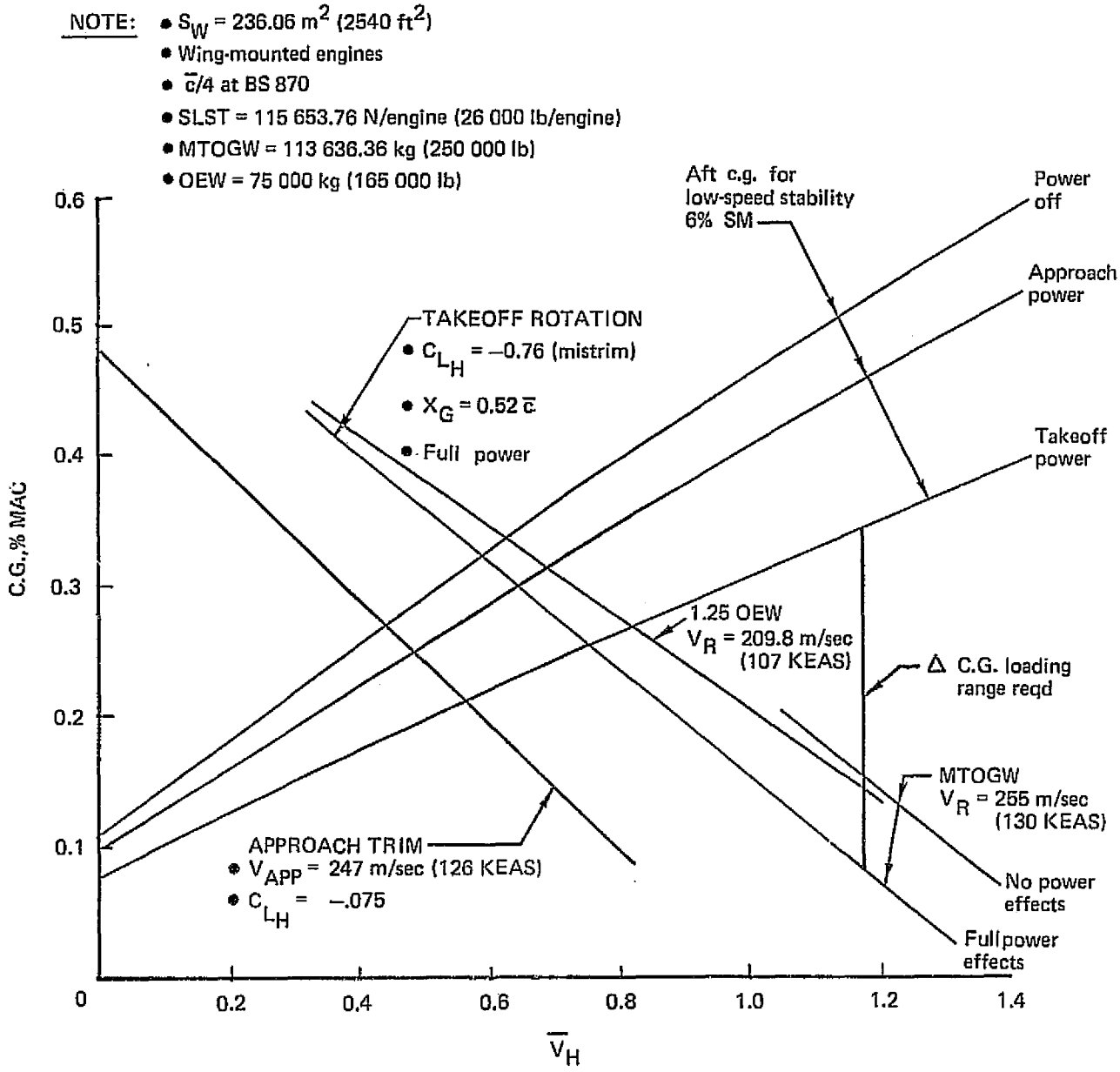

Figure 34 Horizontal Tail Sizing, for the Wing-Mounted Prop-Fan (767-762)

5.2.5 ENGINE-PROPELLER-AIRFRAME INTEGRATION

Previous generations of propeller-driven airplanes have been built and operated successfully with relatively little attention paid to aerodynamic integration of the wing and slipstream. However, a successful prop-fan airplane will demand more careful handling of this problem.

In the first place, the disc loading of the prop-fan is about four times that of previous turboprops. This means that, at the same flight condition, the axial velocity (or Mach number) increment in the slipstream is about four times higher. Approximately the same factor also can be applied to the slipstream dynamic pressure increment and swirl velocity components. The effects of "blowing" and "scrubbing" on the aerodynamic characteristics of surfaces immersed in the slipstream are thus much larger than the corresponding effects on the turboprops of the past.

Furthermore, the cruise Mach number of the prop-fan (M = 0.8) is substantially higher, Mach 0.6 being typical for inservice turboprops. Slipstream interference effects are therefore complicated by an environment of mixed transonic flows, shock-boundary-layer interactions, drag rise, and rapidly changing aerodynamic characteristics.

Finally, because the wing loading and sweep of the modern prop-fan airplane are likely to be high, a premium is likely to be placed on high-lift characteristics, relative to straight-wing turboprops with half the wing loading. The prop-fan airplane will therefore need sophisticated leading- and trailing-edge devices to achieve competitive approach speeds and field lengths. These devices must have reasonable power-on drag characteristics and at the same time provide adequate maximum lift capability for power-off FAR stall demonstration. Therefore, tailoring of the high-lift configuration in the presence of the high-energy ($q_s/q \approx 3.0$) swirling slipstream is important.

The following discussion quantifies important slipstream parameters, outlines the performance implications of wing-mounted prop-fan installations, and describes aerodynamic nacelle-wing integration concepts designed to minimize the performance penalties.

5.2.5.1 Slipstream Characteristics and Power Effects

The ideal propeller method of reference 8 was used to predict the slipstream characteristics of the prop-fan. This method does not account for the periodic nature of the real slipstream flow. Nevertheless the momentum considerations embodied in the method should provide a reasonable approximation to the velocities in the slipstream.

Figure 35 shows radial distributions of swirl angle and axial velocity increment immediately behind the propeller disc for takeoff, cruise and climb at Mach 0.45, 3050 meters (10 000 ft) altitude. Axial velocity increments in the slipstream far downstream from the propeller are approximately twice those shown in the figure.* Maximum swirl angles vary from 6^{o} during cruise to over 20^{o} at takeoff. Maximum axial velocity increments in the fully-contracted slipstream (two times the value shown in the lower portion of figure 35) can be expected to be as much as 10% of freestream velocity in cruise and 75% of freestream at takeoff.

The large swirl velocities in the slipstream imply that a considerable portion of the power input is not converted into thrust. This effective thrust loss increases with propeller power loading (decreasing ideal efficiency). Swirl thrust losses are plotted in figure 36 versus Mach number for a typical sea level takeoff, 464 to 500 km/hr (250 to 270 KEAS) IAS climb schedule and Mach 0.8 cruise condition. They amount to about 8% in cruise and 13% at takeoff.

A considerable increase in propulsive efficiency could be achieved if the slipstream swirl energy were recovered. Dual rotation propellers achieve this result directly, at considerable cost in weight and mechanical complexity. Stators mounted on the nacelle have been proposed as a simpler alternative.

---

*At one diameter downstream ughly at the leading edge), the axial velocity increment will have reached 1.7 times the value just behind the disc.

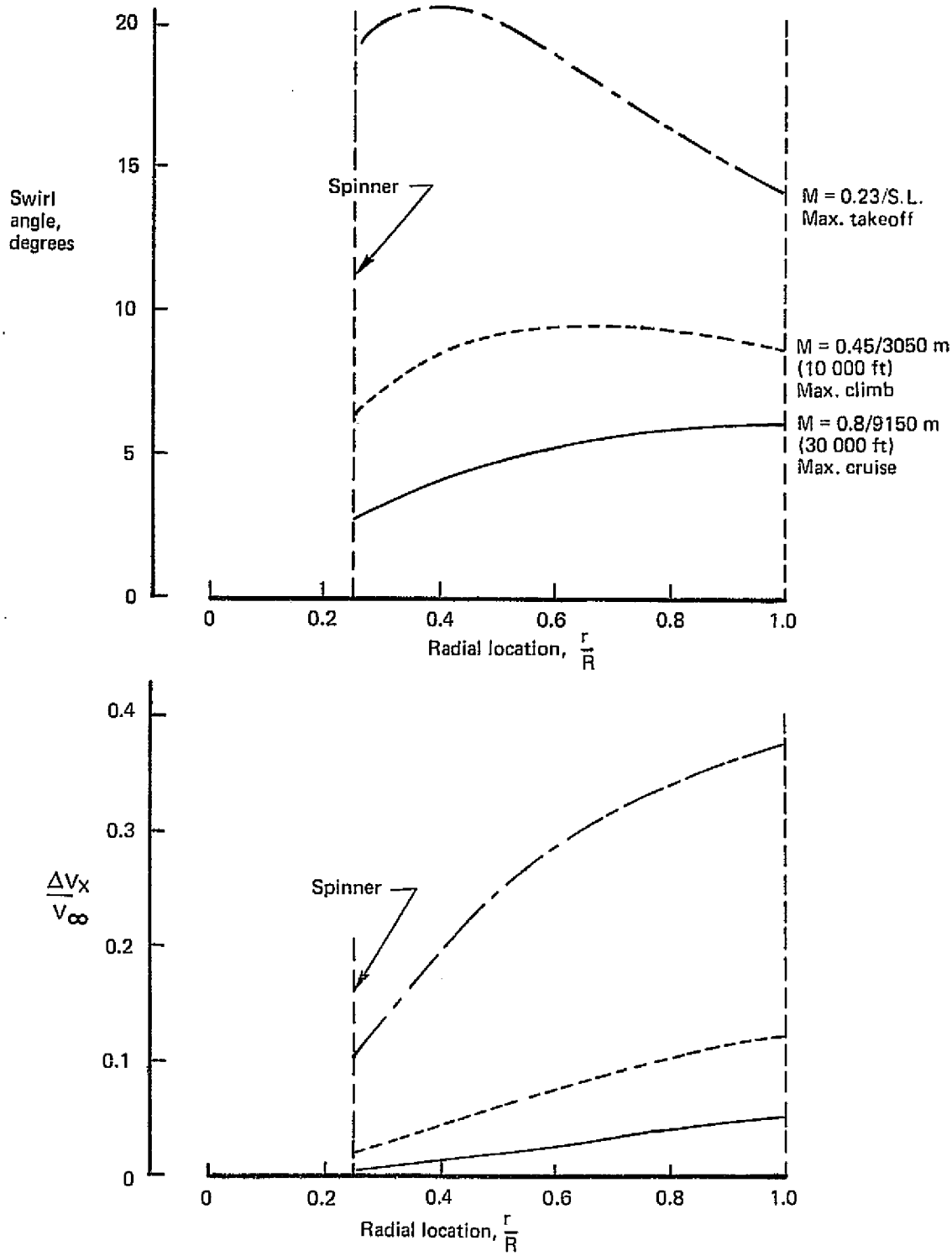

Figure 35 Radial Distributions of Swirl Angle and Axial Velocity Increment—Ideal Propeller Calculations

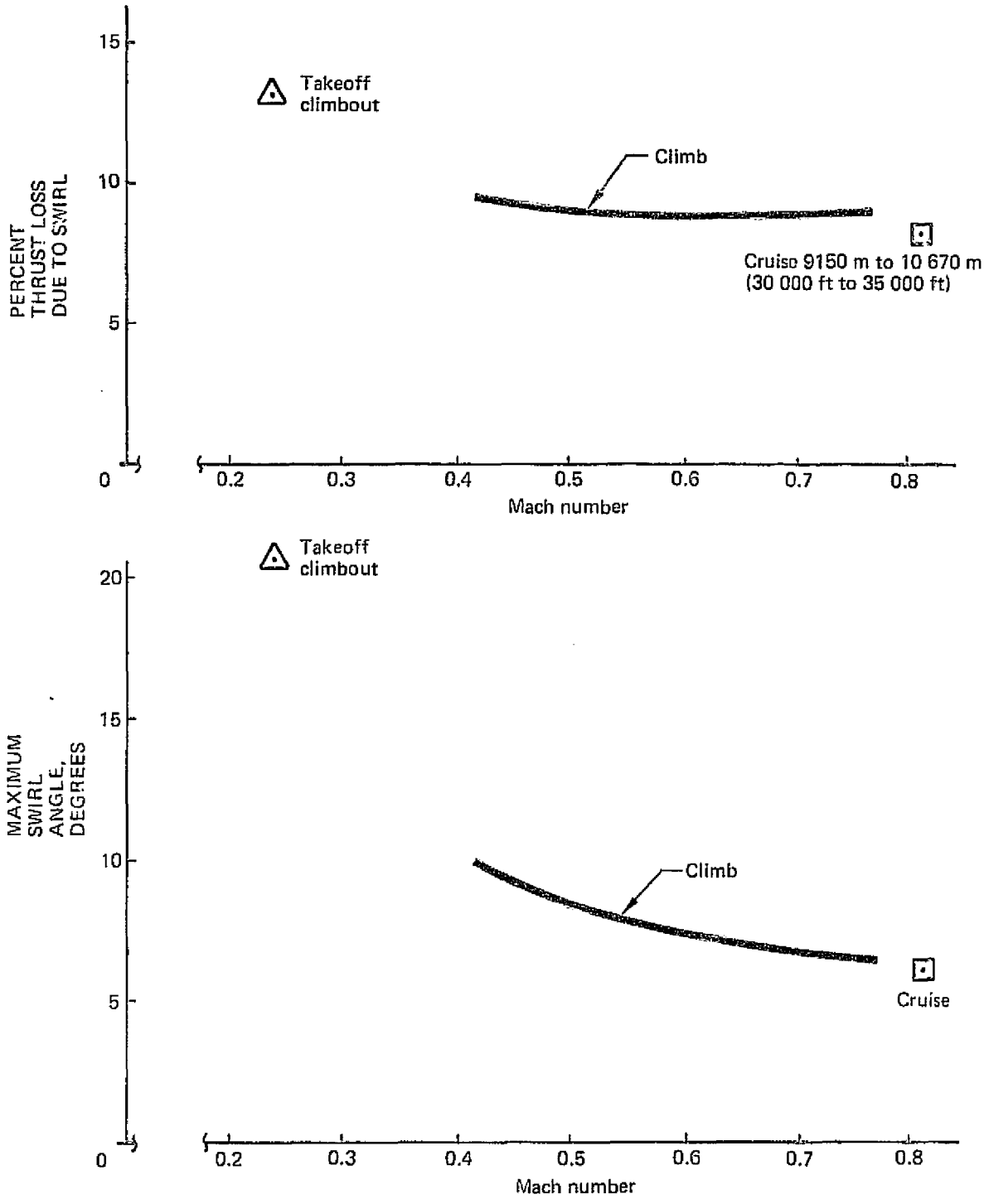

Figure 36 Thrust Loss Due to Swirl and Maximum Swirl Angle— Ideal Propeller Calculations

The wing itself may be considered a very large chord stator, and can be expected to develop some thrust from derotating the slipstream, compensating for the problems discussed above to an unknown extent.

Results of a preliminary vortex-lattice analysis of a swept wing immersed in a swirling slipstream are summarized in figure 37. Thrust coefficient and slipstream characteristics correspond to prop-fan cruise conditions. The axial force results tabulated in the figure indicate that about 50% of the swirl thrust loss is potentially recoverable (in shock and separation-free flow), equivalent to about 4% in propeller efficiency. The problem of swirl thrust recovery is complex and subject to practical constraints on achievable local loadings. Wind tunnel testing will be required for drag validation. Therefore, no performance credit for the thrust recovery was taken in this study.

Other propeller slipstream parameters are important in low-speed flight. Figure 38 shows the low-speed power-effects method used. The slipstream magnifies aerodynamic forces on immersed surfaces by virtue of its increased dynamic pressure. In addition, for cases in which the propeller is at an effective angle of attack, a rotation of these forces due to the deflection of the slipstream away from the freestream direction occurs. Resolved propeller thrust and normal forces also must be taken into account.

At small propeller angles of attack, the largest drag component is simply the magnified scrubbing drag force. At negative propeller angles of attack, forward rotation of the lift vector produces an effective thrust; at positive angles of attack, the same force is rotated aft, giving rise to an appreciable drag component. At large propeller angles, both the propeller normal force and the reduction in resolved thrust add to the drag.

At most usable angles of attack, the increased lift forces outweigh the added drag, giving an increase in L/D due to power. However, in the engine-out condition, appreciable yawing and rolling moments must be trimmed, causing a large increase in drag, generally outweighing any beneficial power effects.

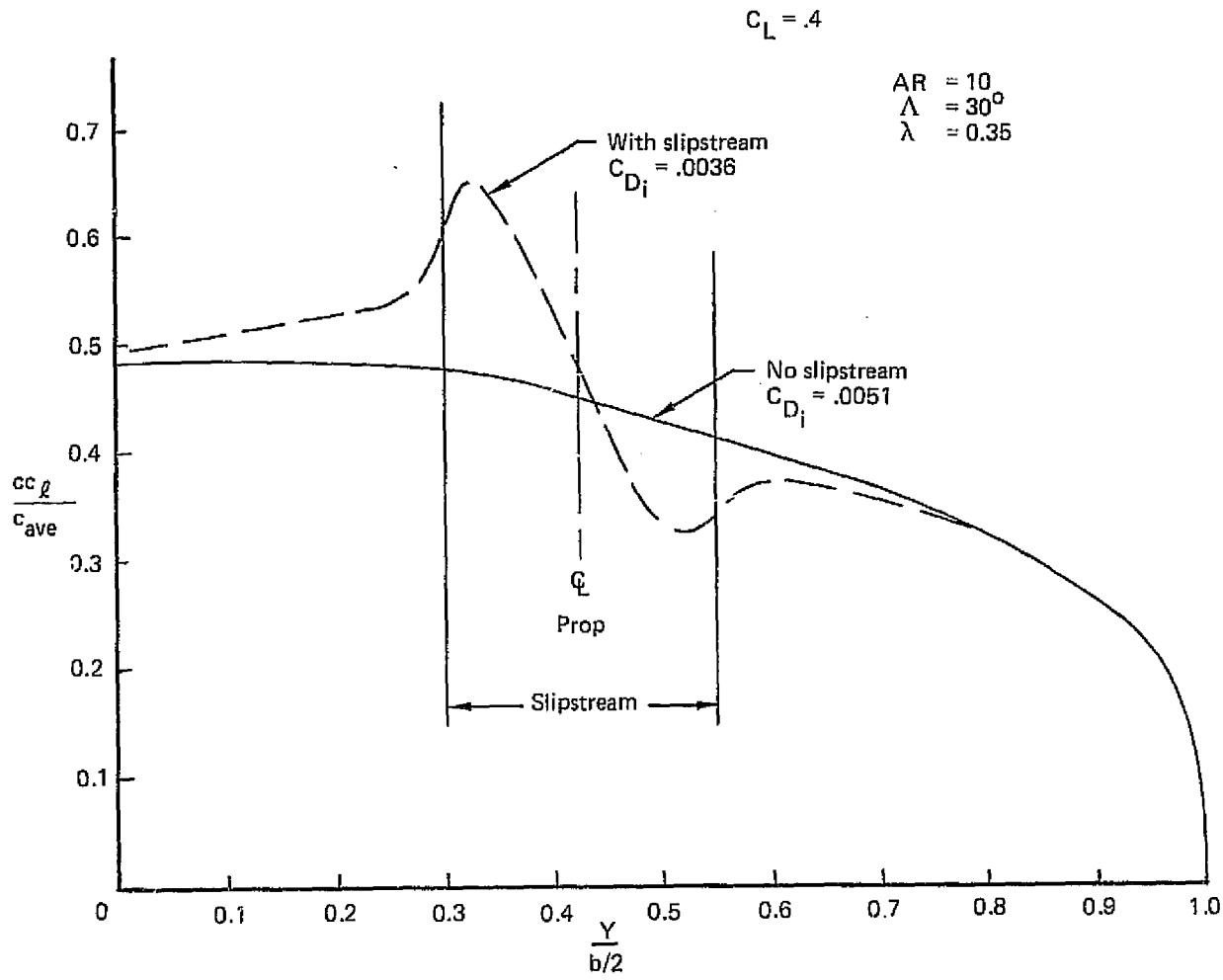

Figure 37 Effect of Slipstream on Span Load Distribution

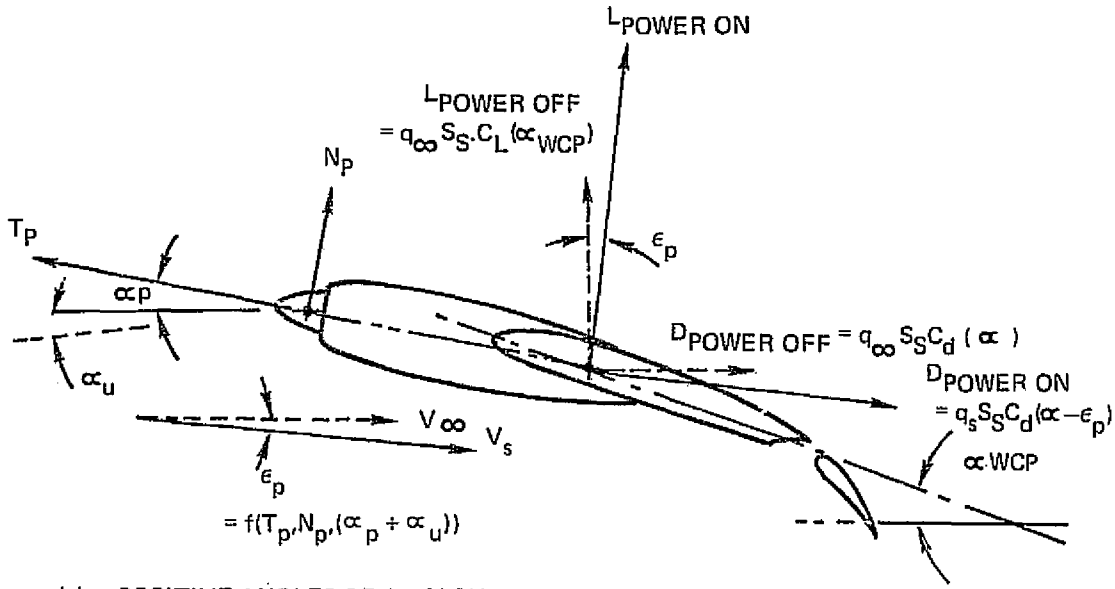

(a) POSITIVE ANGLES OF ATTACK
(Downwash behind prop.)

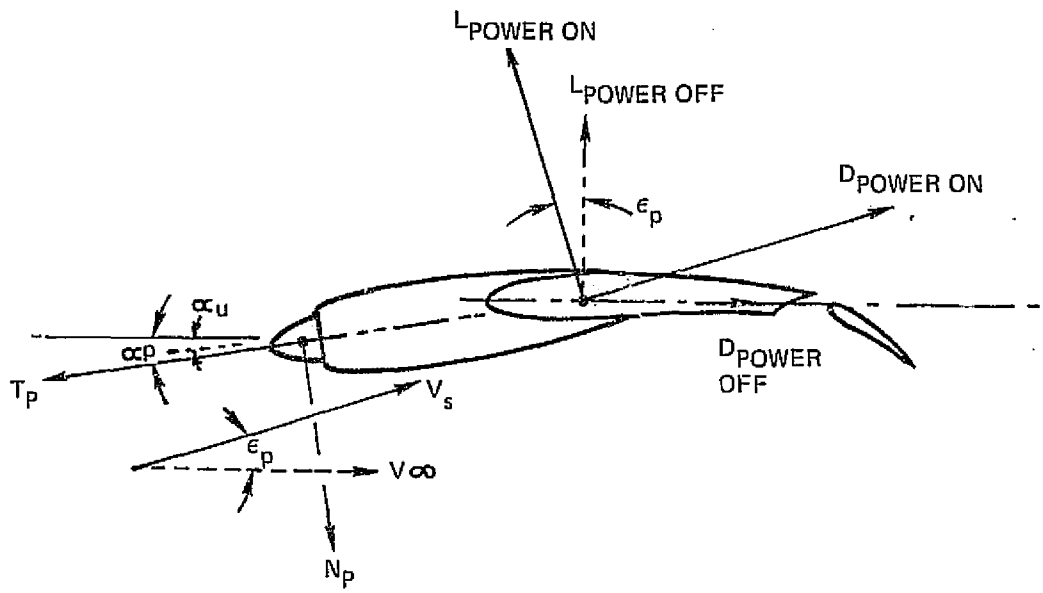

(b) SMALL OR NEGATIVE ANGLES OF ATTACK
(Upwash behind prop.)

Figure 38 Propeller Power Effects Schematic

In addition, sizing of trimming control surfaces such as vertical fin, rudder and ailerons may be dictated by these engine-out moments, leading to further increases in drag and weight.

Accurate determinations of propeller thrust variations, normal force, and slipstream deflection with angle of attack and power are of crucial importance in any power effects calculation or analytical flow modelling work. Exploration of slipstream characteristics should therefore command equal priority to the determination of direct propeller forces in any future wind tunnel testing of the prop-fan.

5.2.5.2 "Over-Under" Nacelle Installations

Even in the absence of slipstream effects, the presence of an over-under nacelle, such as that of the wing-mounted prop-fan airplane, can degrade the lift and drag characteristics of a swept wing. Vortices spring from the wing leading-edge-nacelle juncture areas and flow back over the wing. These vortices constrain the flow in a manner similar to a "fence," an effect particularly noticeable in the boundary layer flow over the aft region of the upper surface. Wind tunnel oil-flow visualization pictures typically show regions of low energy or separated flow near the wing trailing edge and adjacent to the two well-defined vortices, while force measurements show a reduction in lift and an increase in drag compared to corresponding clean-wing data. These phenomena are observed over the whole range of speed and are present even when careful aerodynamic tailoring is employed. Because the vortex strengths increase with angle of attack lift coefficient, the drag penalty is felt as a degradation in drag due to lift.

In the high-lift configuration, the over-under nacelle can cause an appreciable reduction in maximum lift, as well as a drag increase.

5.2.5.3 Nacelle Integration Concepts

A successfully integrated wing-mounted prop-fan nacelle design will probably embody some concepts shown in figure 39. The inboard leading-edge "crank" was developed in Boeing low-speed wind tunnel tests as a practical remedy for the maximum lift penalty associated with the over-under nacelle. The crank makes the angle of the notch between the wing leading edge and the nacelle sidewall less acute, reducing the severity of the inboard vortex. Leading-edge device effectiveness also is improved.

The cranked leading-edge extension, together with a swept-leading-edge fillet outboard of the nacelles, also will permit incorporation of local leading-edge camber without distorting the wing structural box. This leading-edge camber will be required to prevent excessive front-loading of the wing sections in the swirling slipstream. A drooped leading edge will be used on the upcoming blade side, where the swirl produces a positive effective angle-of-attack increment. Some negative camber will be desirable outboard of the nacelle.

5.2.5.4 Leading-Edge Devices

Leading-edge devices will be required over the whole exposed span to provide power-off maximum lift comparable to that of turbofan airplanes. With power on, these devices must not produce excessive drag in the high-energy slipstream.

Figure 40 shows a possible leading-edge arrangement near the nacelle. On the inboard side a large-chord sealed slat is proposed, which will be deployed in both power-on and power-off conditions. The slat will be designed for minimum drag power-on and will be suitably aligned with the local swirling slipstream flow ($\Delta\alpha_{swirl} \approx 20^{\circ}$), but also will provide adequate leading-edge protection under power-off conditions.

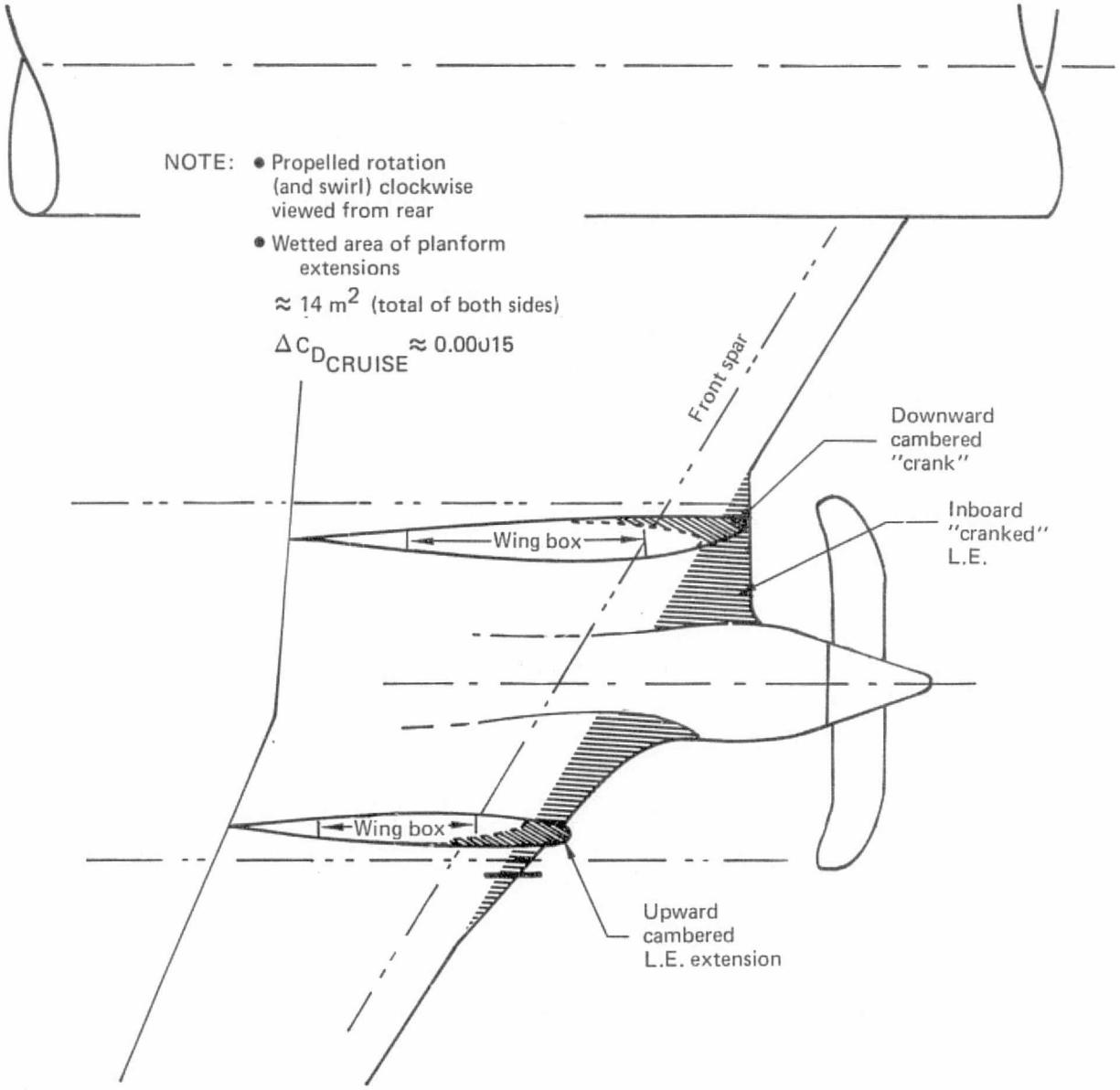

Figure 39 Prop-Fan Wing Nacelle Integration

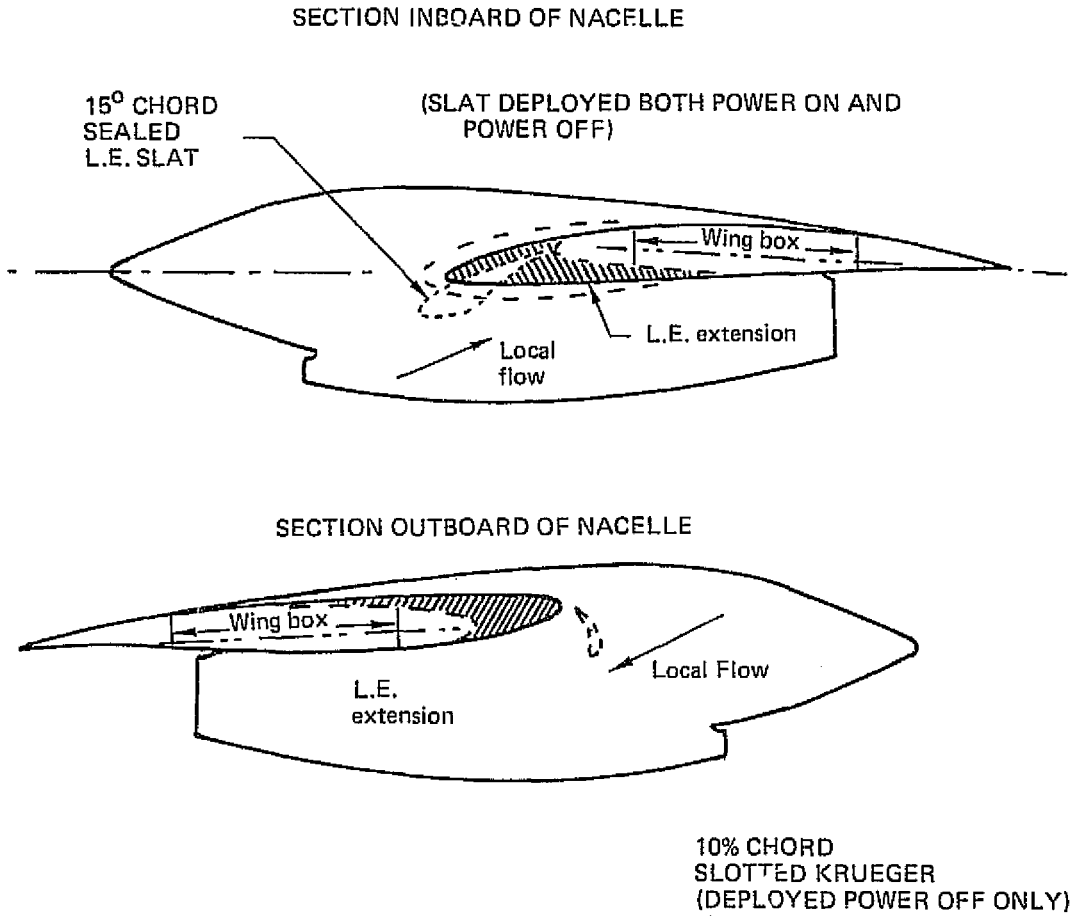

Figure 40 Prop-Fan Leading-Edge Device Integration

Outboard of the nacelle, where the swirl is downward, a leading-edge device would probably cause too much drag. It is expected that leading edge camber alone will suffice for the power-on condition, but power-off stall protection will require a high-performance device like a curved Kruger flap. To take full advantage of the wing's potential minimum speed performance, this flap would probably have to be extended automatically, under the control of an engine torque sensing system.

5.2.6 CABIN ACOUSTIC ENVIRONMENT

The external noise level from which the cabin interior must be isolated is much more severe on the prop-fan airplane than on the reference turbofan because of the propeller. (Propeller noise and cabin wall treatment for noise reduction are discussed in the appendix.)

Figure 41 shows a comparison of interior overall sound pressure levels (OASPL). The upper line shows the level that would prevail in the prop-fan if cabin structure and noise treatment were the same as the turbofan's. Shading indicates attenuation required to provide equal comfort levels in the two airplanes. Equal OASPLs were not required on a seat-by-seat basis, but rather at the same body station as the peak of the prop-fan curve.

Shading on the figure is coded to indicate noise attenuation measures required.

5.2.7 WEIGHT AND BALANCE

Table IX shows the weights for the model 767-762B wing mounted prop-fan.

The wing weight allows for:

- "Gulling" to ensure adequate propeller-tip ground clearance
- A heat shield to protect the trailing-edge area from the hot engine exhaust

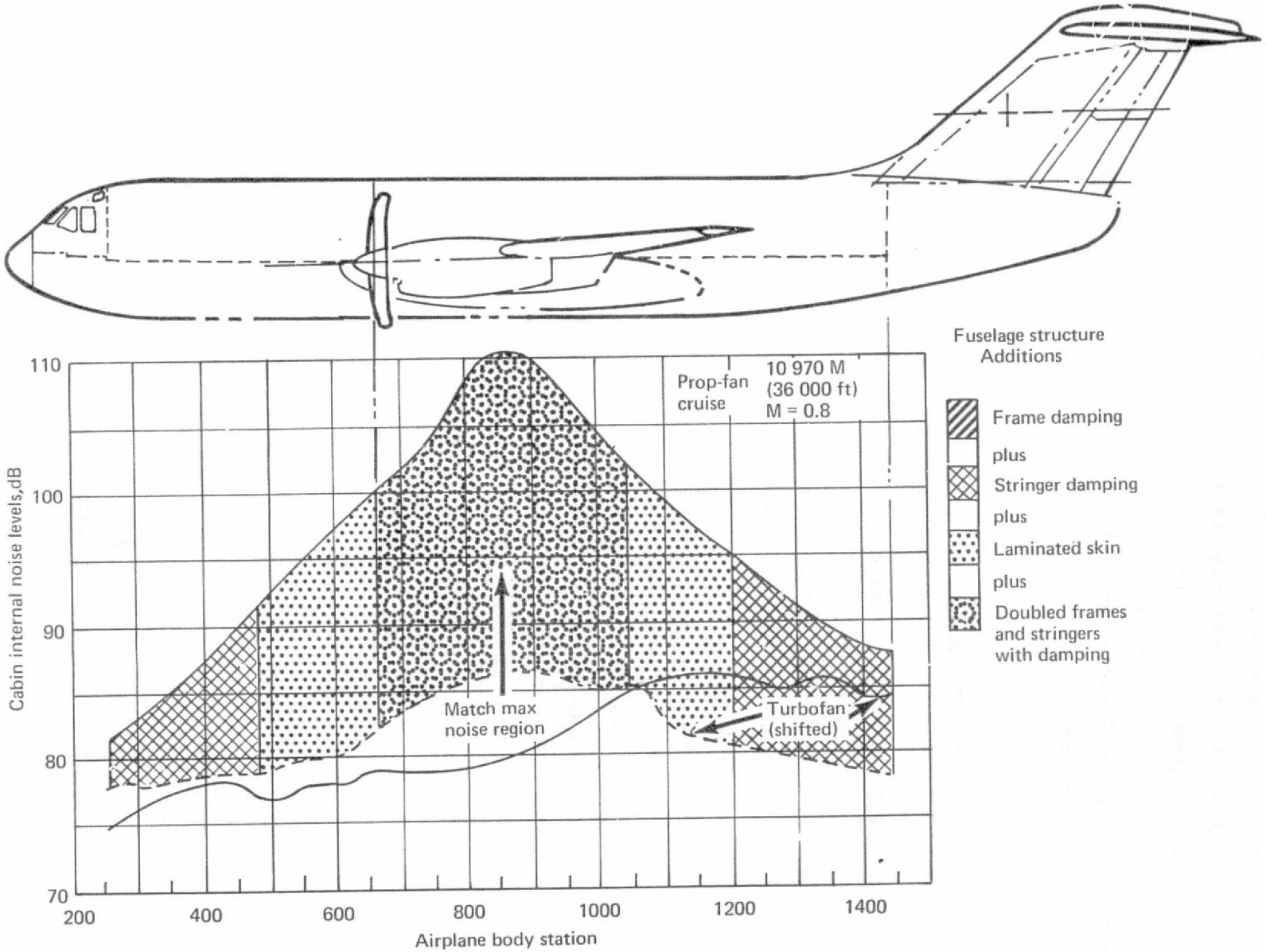

Figure 41 Prop-Fan 767-762 Fuselage Noise Reduction Requirements, Peak Cabin Noise Region Comparable to Turbofan Peak Region

Table IX Weight Statement for the Wing-Mounted Prop-Fan (767-762)

	kg	lb
Wing	18 470	40 730
Horizontal tail	1800	3960
Vertical tail	1910	4200
Body	16 470	36 320
Main landing gear	6310	13 920
Nose landing gear	750	1650
Nacelle and strut	1950	4300
Total structure	(47 660)	(105 080)
Engine	5670	12 510
Engine accessories	480	1070
Engine controls	50	110
Starting system	50	100
Fuel system	580	1280
Propeller	3170	6990
Gear box	3450	7600
Total propulsion system	(13 450)	(29 660)
Instruments	530	1170
Surface controls	1770	3890
Hydraulics	1300	2870
Pneumatics	410	900
Electrical	1140	2520
Electronics	960	2120
Flight provisions	310	690
Passenger accommodations	6950	15 310
Cargo handling	1230	2700
Emergency equipment	300	670
Air conditioning	1110	2450
Anti-icing	230	500
Auxiliary power unit	930	2060
Total fixed equipment	(17 170)	(37 850)
Exterior paint	70	150
Options	910	2000
Manufacturer's empty weight	(79 260)	(174 740)
Standard and operational items	4450	9800
Operational empty weight	(83 710)	(184 540)
Maximum taxi weight	122 960	271 070

- Local nacelle/wing tailoring for nacelle placement and slipstream effects
- Special nacelle ribs in the wingbox to support the nacelle and propulsion pod
- Flutter and fatigue penalties (the flutter penalty is incurred because the prop-fan engine is further outboard than the turbofan)

Body weight includes a 2670kg (5880 lb) increment for the heavier structure required to attenuate propeller noise to a level providing passenger comfort comparable to the turbofan's. This increment is considerably more than would have been needed for protecting the structure from sonic fatigue.

Propeller and gearbox weights were developed using data provided by Hamilton Standard and represent the level of technology expected to be available for commercial service in the mid-1980s. A total of 136 kg (300 lb) for two compressors has been included in pneumatics system weight to provide cabin air pressurization.

Figure 42 is the loadability diagram for the 767-762. Comments in section 5.1.6 regarding the tolerance in OEW c.g. and establishment of c.g. limits also apply here.

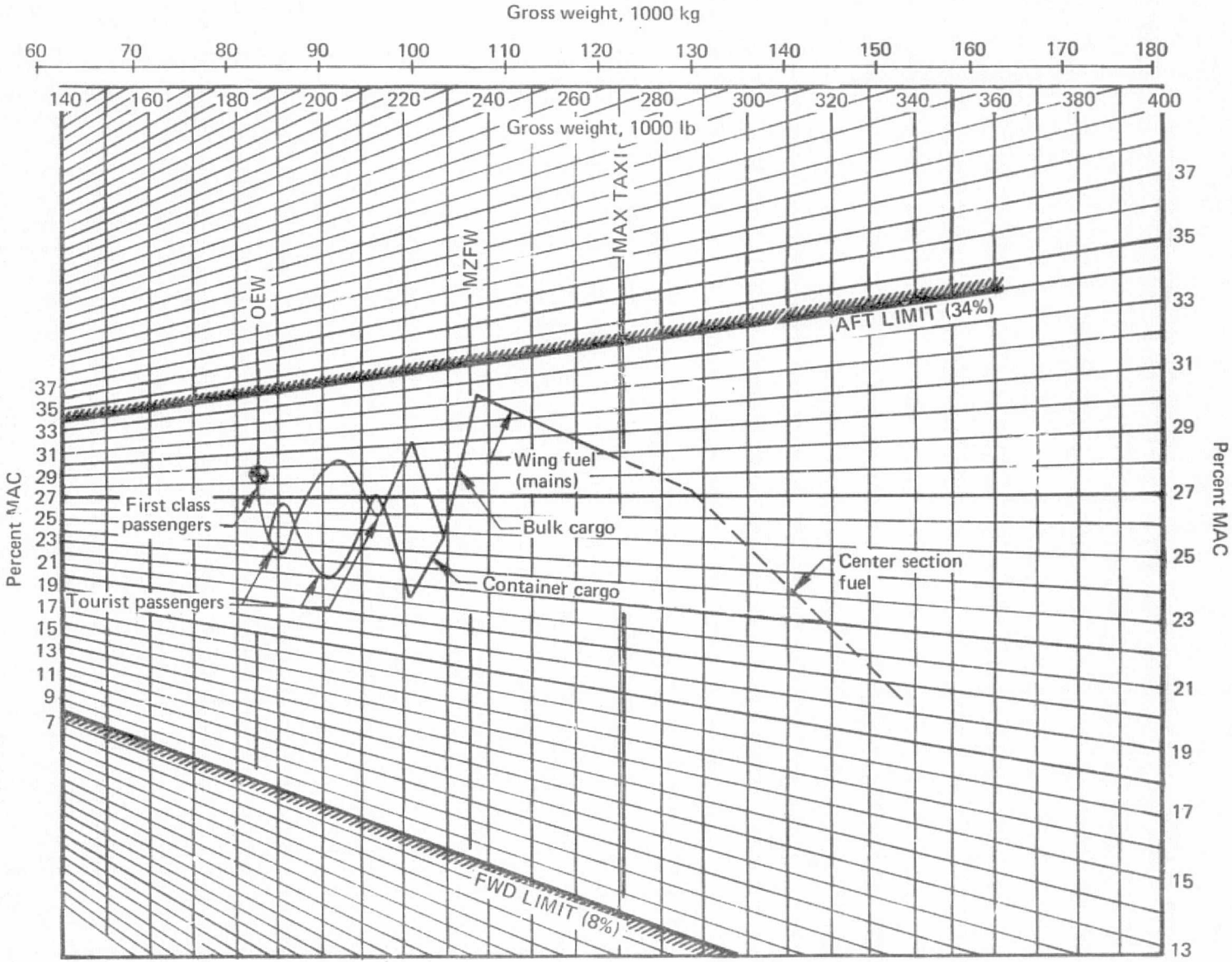

Figure 42 Loadability Diagram for the Wing-Mounted Prop-Fan (767-762)

5.3 AFT-MOUNTED PROP-FAN AIRPLANE

The model 767-764 aft-mounted prop-fan configuration and geometric characteristics are shown in figure 43 and table X.

5.3.1 ARRANGEMENT CONSIDERATIONS

Two aft-mounted prop-fan arrangements were studied. The first had the engines mounted on the horizontal tail. Variable tail incidence was not considered feasible because of the large variations of inflow angle to the propeller and the greatly augmented moving mass. The T-tail arrangement could not be retained because of the nose-down thrust moment at takeoff rotation. A second configuration, placing the engines on struts attached to the aft body (fig. 44) was therefore adopted.

The aft body is contoured (area ruled) in a manner allowing for nacelle cross section and slipstream contraction in cruising flight. Such tailoring probably will be required to avoid a drag penalty due to interference affects at high subsonic Mach number.

5.3.2 AERODYNAMIC CHARACTERISTICS

Aerodynamic characteristics of the aft-mounted prop-fan were based on those of the baseline turbofan airplane. Unlike the wing-mounted prop-fan, a detailed examination of low-speed power effects was not performed, because, apart from considerations of swirl thrust recovery, these effects are expected to be small.

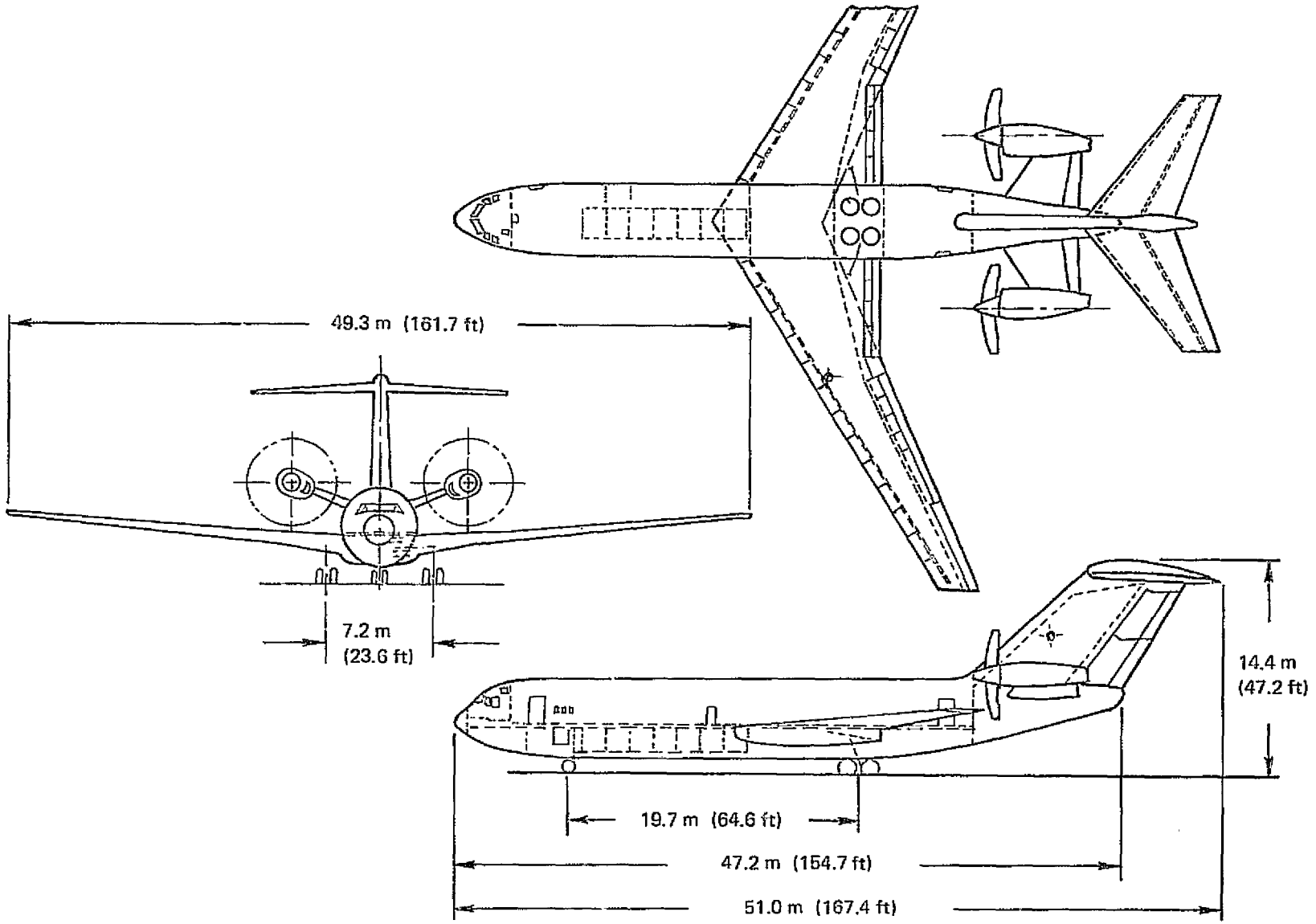

Figure 43 General Arrangement, Aft-Mounted Prop-Fan

Table X 767-764 Aft-Mounted Prop-Fan Airplane Characteristics and Performance

Weights	TOGW, kg (lb)	123 970 (273 300)
	OEW, kg (lb)	84 690 (186 700)
	Landing weight (mission), kg (lb)	107 930 (237 950)
	(maximum), kg (lb)	112 300 (247 580)
	Payload, pass./kg (pass./lb)	180/16 738 (180/36 900)
	Max fuel capacity	66 680 (147 005)
	C.G. limits, % MAC	20 fwd, 52 aft
	T/W equivalent	.279
	W/S, N/m^2 (lb/ft^2)	5008.3 (104.6)
Performance	Still air range, km (nmi)	3333.6 (1800)
	Cruise Mach number	0.80
	Cruise altitude, m (ft)	10 970 (36 000)
	Range factor, km (nmi)	25 600 (13 820)
	L/D average cruise	16.41
	SFC, k: kN-sec (lb/hr/lb)	0.0154 (0.545)
	TOFL, m(ft)	1397 (4584)
	C.G. position, % MAC	20
	V_{APP}, m/sec (KEAS)	65 (126)
	Block fuel, kg (lb)	10 216 (35 750)
	Reserves, kg (lb)	6510 (14 350)
	Total fuel, kg (lb)	22 980 (50 660)
	Block fuel, kg/pass. km (lb/pass. nmi)	0.0270 (0.110)
Power-plants	Number	2
	Type	Scaled P&W STS 476
	Power	23 110 kW (30 990 shp)
Body	Length, m (in.)	47.14 (1856)
	Maximum diameter, m (in.)	5.38 (211.6)
	Accommodations	180 passengers—10% 1st, 90% tourist 7 LD-3 containers, 35.79 m^3 (1264 ft^3)
Landing gear, m (in.)	Nose	(2) -0.86x0.28 (34x11)
	Main	(8) -1.09x0.42 (43x16.5)
	Truck size	1.32x0.97 (52x38)
	Oleo stroke (extended to static)	0.51 (20)

Wing and empennage	Wing	Horizontal tail	Vertical tail
Area, m^2 (ft^2)	242.8 (2613)	72.8 (783.56)	66.7 (717.73)
Aspect ratio	10	4.0	0.8
Taper ratio	0.353	0.4	0.65
c/4 sweep, deg	30	35	45
Incidence, deg	1	—	—
Dihedral, deg	5	-3	—
t/c, %	2	10.5	12
MAC, m (in.)	5.303 (208.76)	4.527 (178.24)	9.266 (364.82)
Span, m (in.)	49.270 (1939.77)	17.064 (671.80)	7.304 (287.55)
Tail arm, m (in.)	—	20.778 (818.01)	14.347 (564.84)
Tail vol coefficient	—	1.175	0.080

1 Wing incidence: SOB 3.75
MAC 2.00
Tip -1.00

2 Wing t/c %: SOB-13.1 (total chord)
BL407.6-10.5 (const outbd)

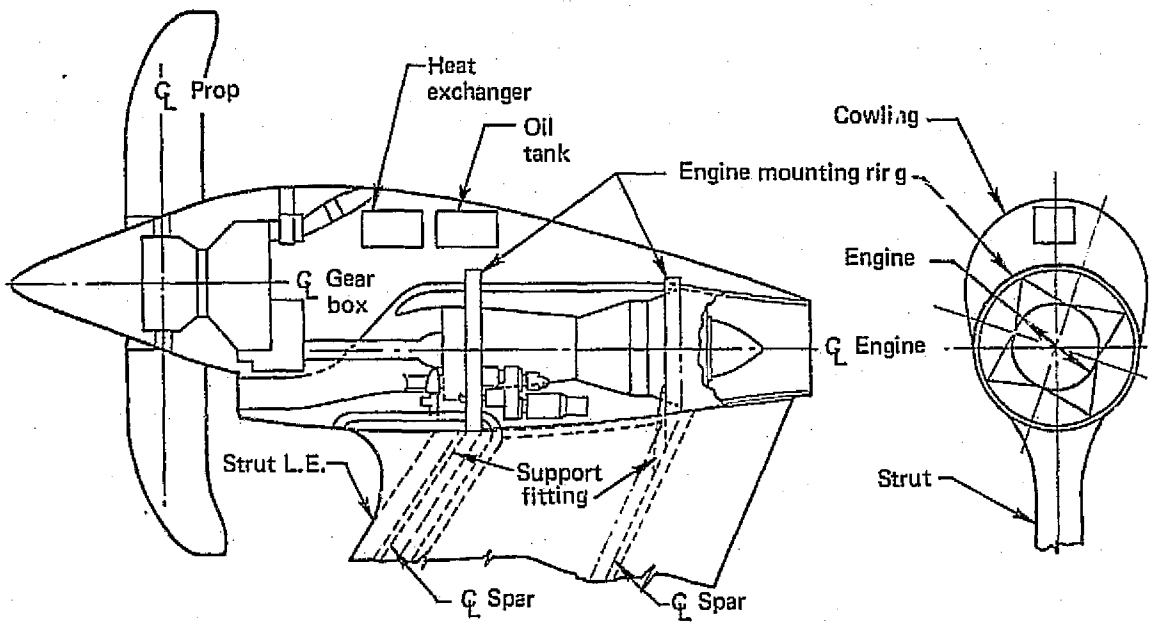

Figure 44 Aft-Mounted Prop-Fan Installation

5.3.2.1 High-Speed Drag

Figure 45 shows high-speed drag polars for the sized, aft-mounted prop-fan airplane. The minimum parasite drag coefficient, 0.0186, is considerably higher than the corresponding values for both the baseline turbofan and wing-mounted prop-fan airplanes. Factors contributing to the increase in parasite drag are:

- Increased tail areas
- Increased body length
- Nacelle struts

The drag coefficient contribution due to slipstream scrubbing is slightly more than 0.0002. Maximum lift-to-drag ratio at Mach 0.8 is 16.5.

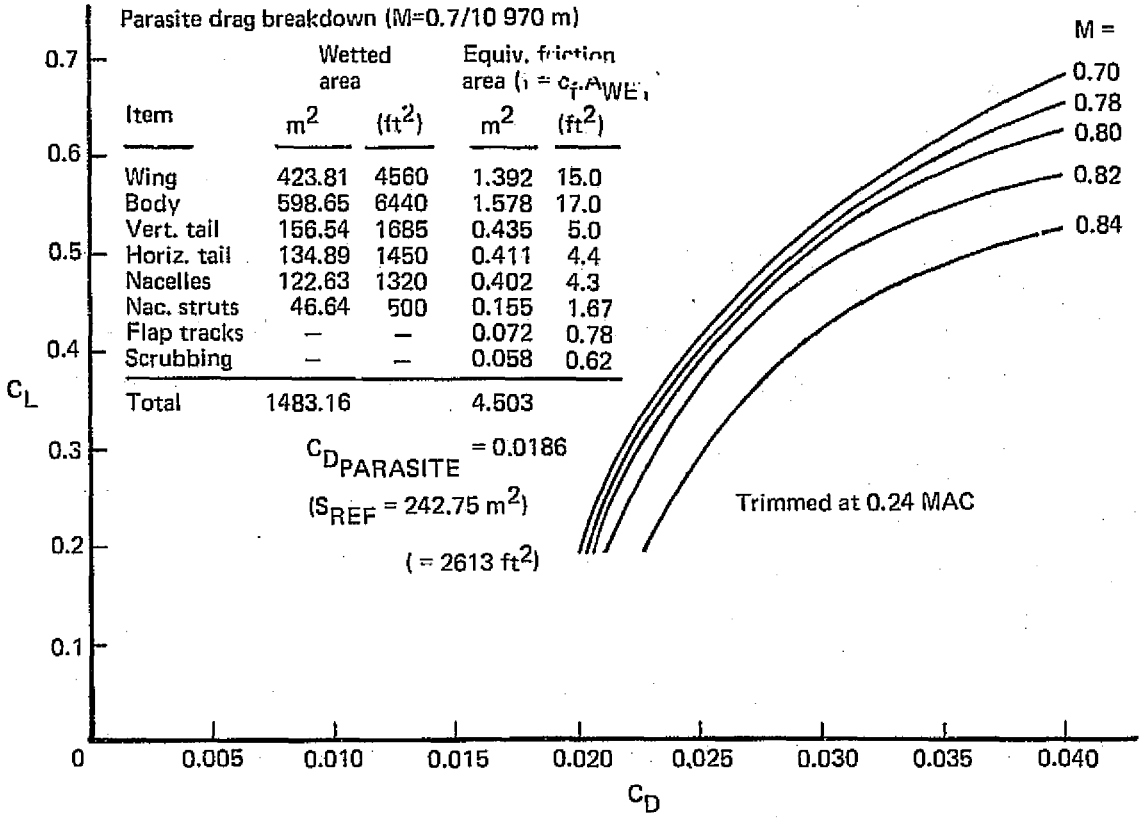

Figure 45 Sized Aft-Mounted Prop-Fan High-Speed Drag Polars

5.3.2.2 Low-Speed Characteristics

Engine-out lift-to-drag ratio is plotted versus lift coefficient in figure 46 for the takeoff climbout condition. Reference conditions are 237 km/hr (130 KEAS) at sea level, with gear up and trimmed at the forward c.g. location (0.20 MAC). At mission gross weight, the optimum flap setting, climbout lift coefficient and lift-to-drag, engine-out, are 22^{o}, 1.88, and 9.2 respectively. FAR stall lift coefficients are:

Leading-edge device deflection, degrees	Trailing-edge flap deflection, degrees	$C_{L_{S_{FAR}}}$
0	0	1.66
50/60	0	2.06
50/60	10	2.44
50/60	20	2.67
50/60	30	2.79
50/60	40	2.86

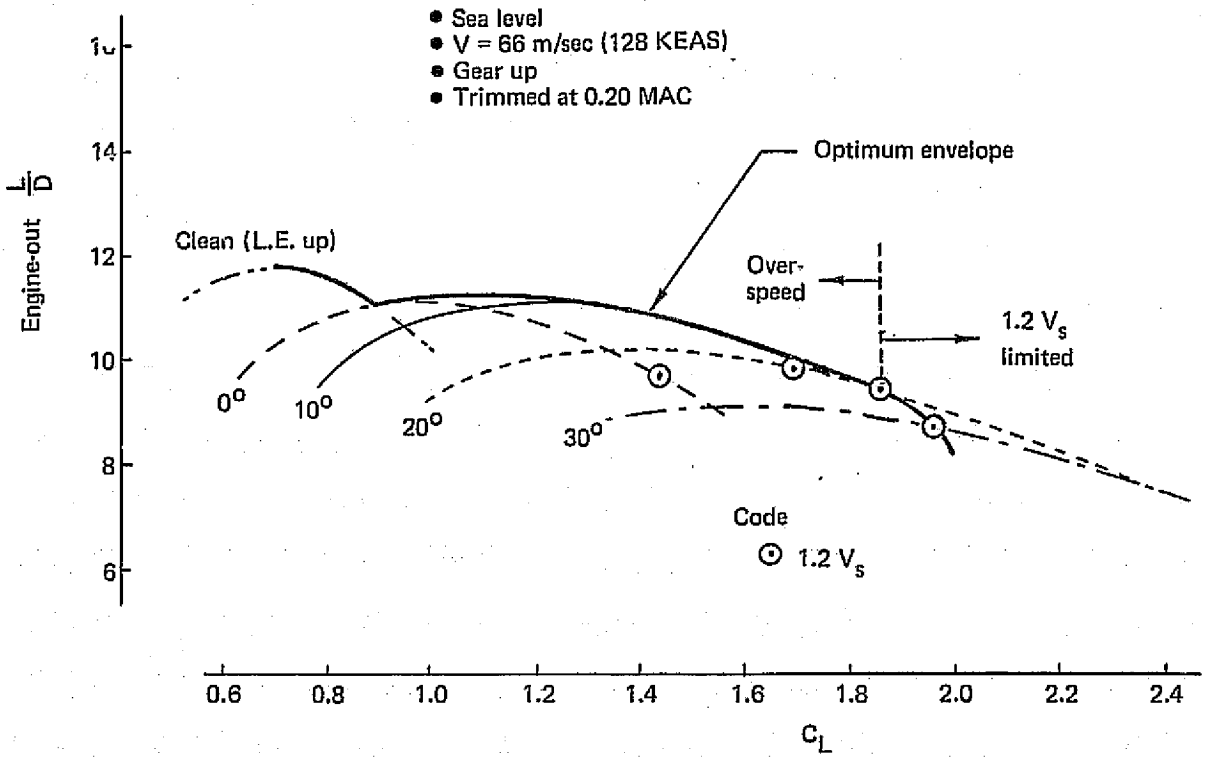

Figure 46 Sized Aft-Mounted Prop-Fan Engine-Out Climbout Lift-To-Drag Ratios

5.3.3 ENGINE/PROPELLER

The cruise power loading used for the wing-mounted prop-fan studies was also used for the tail-mounted arrangement. The required uninstalled power at sea level, zero speed, and standard day was 23 110 kW (30 990 shp) and the prop-fan diameter corresponding to the selected cruise power loading was 6.03 m (19.8 ft).

5.3.4 FLIGHT CONTROLS

The propeller effects on the aft-mounted prop-fan (767-764) airplane included in the analysis were a ΔC_{M_α} due to the propeller normal force and an increased dynamic pressure over the engine struts effecting pitch control. Due to the complex interactions, only a very rough estimate of the effects of the engine nacelles, struts and propellers have on the horizontal tail and longitudinal stability could be made. Powered model wind tunnel data on a similar configuration would be required for design. The overall effect is a 3% increase in longitudinal stability at approach. A summary of all the propeller effects is shown in figure 47.

Figure 48 is the horizontal tail sizing chart. Unlike the 767-761 and 767-762 the tail size ($\overline{V}_H = 1.2$) is determined by the airplane stability at dive speed. The aft c.g. limit (52% MAC) and the loading range (32% MAC) are set by the airplane balancing and loading limitations. This dictates the forward c.g. limit (20% MAC) and consequently the required pitch control for takeoff rotation. There also was an aft shift of wing position on the body, an aft landing gear shift on the wing (for airplane ground handling balance), and a raised thrust line relative to the wing-mounted 767-762 prop-fan. The result was that this airplane required increased pitch control power obtained by a 35% chord elevator and a 20% chord flap on the engine struts to meet the $\ddot{\Theta}_{TOR} = 1.5$ deg/sec^2 requirement. Again, rotation capability depends on a favorable contribution due to power. In the event of engine failure, the rotation speed would have to be increased, but the very large takeoff field length margin inherent in the design makes further increase in tail volume unnecessary.

(I) WING-MOUNTED PROP-FAN (767-762)
SLIPSTREAM EFFECTS

$\Delta C_{L\alpha_{WING}} = (\Delta q_s, \varepsilon\alpha_{P,W})$ — Destabilizing
— Increased rotation capability

$\varepsilon\alpha_{P,H} = f(C_{L\alpha_{WING}})$ — Destabilizing
— No effect on rotation

PROPELLER EFFECTS

$\Delta C_{m_\alpha} = f(C_{N\alpha_{PROP}})$ — Destabilizing
— No effect on rotation

(II) AFT BODY-MOUNTED PROP-FAN (767-764)
ENGINE STRUT EFFECTS

$\Delta\varepsilon_{\alpha_H} = f(C_{L\alpha_{ST}})$ — Destabilizing

$\Delta C_{m_{\alpha_{ST}}} = f(C_{L\alpha_{ST}})$ - Stabilizing

$\Delta C_{L_{STRUT}}$ T.E. FLAP $= f(FLAP, \Delta q_s)$ — Increased rotation capability

SLIPSTREAM EFFECTS

$\Delta C_{L\alpha_{ST}} = f(\Delta q_s, \varepsilon\alpha_{P,STRUT})$ — Stabilizing

$\Delta C_{L_{STRUT}}$ ELEV. $= f(\Delta q_s)$ — Increased rotational capability

PROPELLER EFFECTS

$\Delta C_{m_{\alpha_{PROP}}} = f(C_{N\alpha_{PROP}})$ — Stabilizing

NOTE: (SPEED STABILITY, LAT-DIR STABILITY EFFECTS DUE TO PROPELLERS NEGLECTED)

Figure 47 Summary of Propeller Effects on Pitch Stability and Control for the Prop-Fan Airplanes

NOTE:
- S_{ref} = 227.6 m^2 (2450 ft^2)
- Aft body-mounted engines
- SLST = 122.3 kN/engine (27 500 lb)
- 2/4 at BS 1034

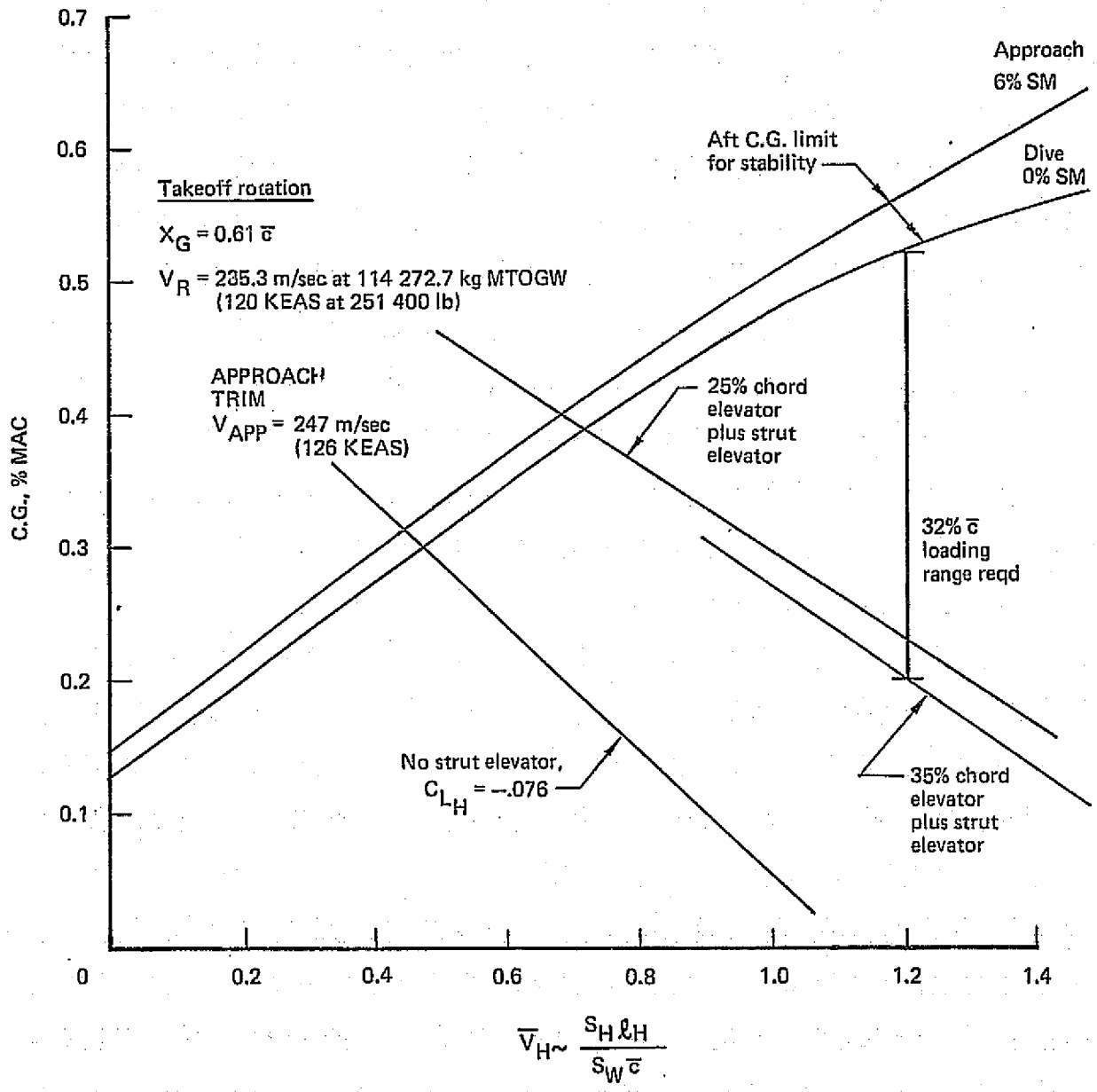

Figure 48 Horizontal Tail Sizing for Prop-Fan Airplane 767-764

The vertical tail size was set by directional stability (C_{n_β} = 0.002 deg^{-1}). Because of the long forebody, it grew to a point where the tail volume coefficient became as large ($\bar{V}_v$ = 0.08) as the wing-mounted configuration (table VI).

5.3.5 NOISE CONSIDERATIONS

The tail-mounted engine position of the 767-764 was intended to reduce the cabin noise exposure by placing the propeller disc plane behind the aft pressure bulkhead. The cabin noise environment noise reduction requirements are shown in figure 49.

These requirements are defined by the envelope of noise levels generated during takeoff and at cruise. The cabin noise reduction requirements are determined the requirements for takeoff noise reduction. The increase in noise for supersonic prop-tip speeds, whether the reference level or 10 dB lower does not affect the cabin noise requirements directly, but does affect the sonic fatigue design of the aft body.

Sound pressure levels predicted for the empennage of the aft-mounted fan installation are presented in figure 49. These sound pressure levels were used to estimate structural beef-up necessary to meet fatigue requirements for a 60 000 hr lifetime. Based on durability analysis and associated design data, the region data, the region having 163 dB requires increasing the skin thickness by 0.00325 m (0.128 in.). The region of 158 dB on the fin requires increasing the skin thickness by 0.00135 m (0.053 in.), and the body by 0.00211 m (0.083 in.). The region of 155 dB requires that the skin be increased by 0.00163 m (0.064 in.).

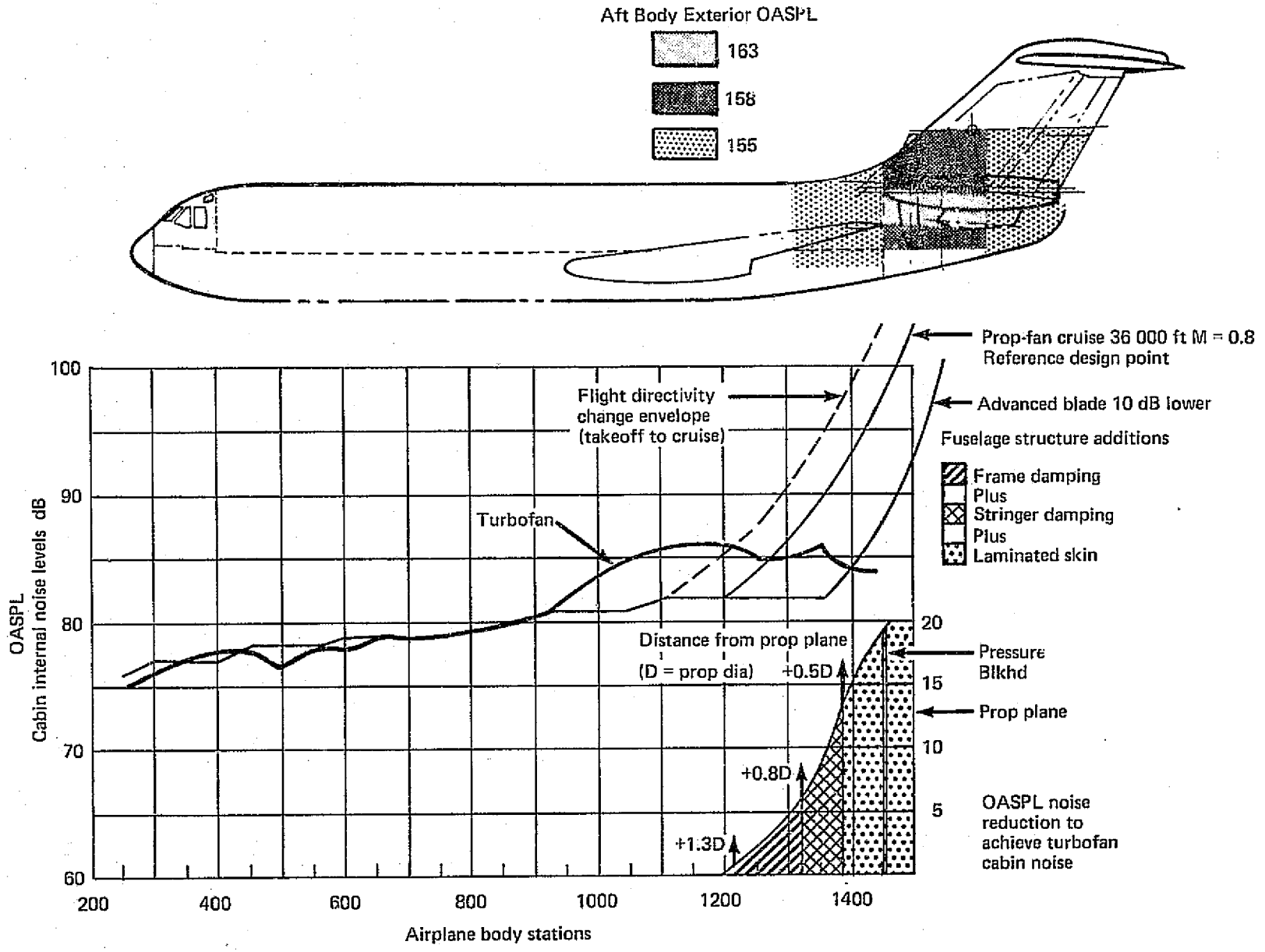

Figure 49 Prop-Fan 767-764 Fuselage Noise Reduction Requirements Aft-Mount, Tip Clearance 0.2D

5.3.6 WEIGHT AND BALANCE

Results of a complete weight analysis on the aft-mounted prop-fan Model 767-764 are shown in table XI.
Weight effects due to unique features of the aft-mounted prop-fan are:

Wing--This includes increment associated with loss of bending relief resulting from removal of engines. Wing weight also includes a flutter penalty due to the absence of the engine mass.

Empennage--Areas are increased over the wing-mounted airplane because of the short moment arm resulting from a more rearward c.g., and also because of the destabilizing influence of the longer forebody. In addition, portions of the fin are subject to very high sound pressure levels, and skin gages have been increased to prevent acoustic fatigue damage.

Body--This includes recognition of the following:

- Increase in body length to allow for aft-body engine mounting
- Provision of support structure for attaching the side-mounted struts
- Increase in aft body skin gages to account for increased loads due to the concentrated load imposed by the propulsion pod
- Cabin wall structure to maintain a cabin noise level comparable to the turbofan
- Aft body also includes increased skin gages to account for sonic fatigue

Landing gear--The landing gear is not affected by propeller-tip ground clearance as it is with the wing-mounted prop-fan model. Therefore, this landing gear is approximately 0.508 m (20 in.) shorter than that of the wing-mounted model.

Figure 50 shows loadability. The aft-engined configuration requires a greater c.g. range than the wing-mounted airplane because of the more forward location of the payload c.g. relative to the OEW c.g.

Table XI Weight Statement for the Aft-Mounted Prop-Fan (767-764)

MAXTAXI	kg	lb
Wing	18 570	40 930
Horizontal tail	2010	4430
Vertical tail	2520	5560
Body	15 840	34 930
Main landing gear	5840	12 870
Nose landing gear	690	1530
Nacelle and strut	2670	5880
Total structure	(48 140)	(106 130)
Engine	5770	12 730
Engine accessories	480	1070
Engine controls	50	110
Starting system	50	100
Fuel system	720	1590
Propeller	3250	7160
Gear box	3470	7650
Total propulsion system	(13 790)	(30 410)
Instruments	530	1170
Surface controls	1920	4240
Hydraulics	1310	2880
Pneumatics	410	900
Electrical	1140	2520
Electronics	960	2120
Flight provisions	310	690
Passenger accommodations	6950	15 310
Cargo handling	1230	2700
Emergency equipment	300	670
Air conditioning	1110	2450
Anti-icing	230	500
Auxiliary power unit	930	2060
Total fixed equipment	(17 330)	(38 210)
Exterior paint	70	150
Options	910	2000
Manufacturer's empty weight	(80 240)	(176 900)
Standard and operational items	4450	9800
Operational empty weight	(84 690)	(186 700)
Maximum taxi weight	124 860	275 270

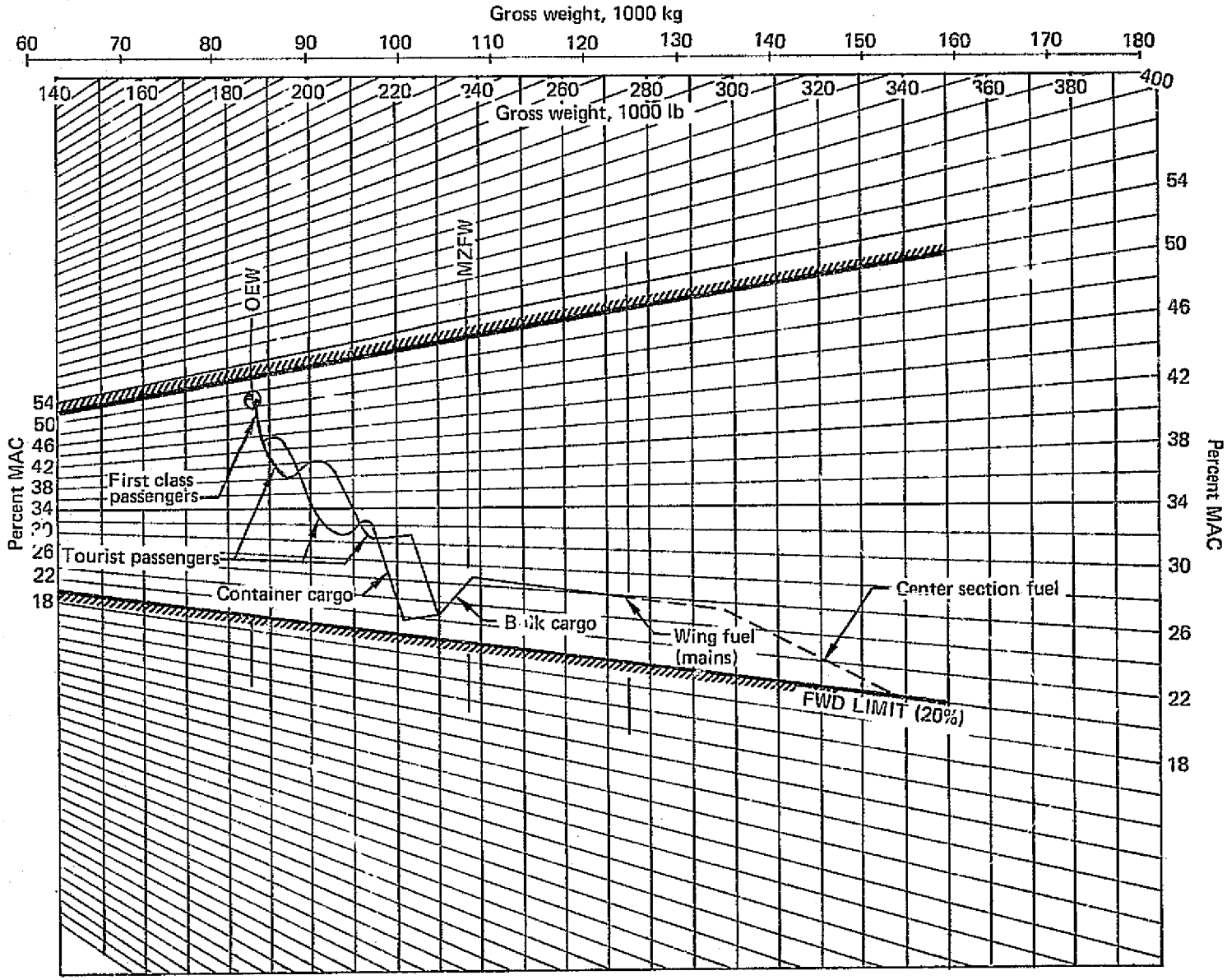

Figure 50 Loadability Diagram for the Aft-Mounted Prop-Fan (767-764)

5.4 COMPARATIVE DISCUSSION

Figure 51 summarizes the principal characteristics of the three airplanes. Both prop-fan designs offer substantial fuel savings over the reference turbofan, with the wing-mounted configuration superior to the aft-mounted prop-fan. However, the block fuel reductions fall far short of the 17.6% decrement that might have been expected on the basis of specific fuel consumption alone, as shown by figure 52. The reasons for the shortfall are the added drag and weight associated with these prop-fan installations.

5.4.1 DRAG

Table XII shows a breakdown of drag differences among the three airplanes. The -762 wing-mounted prop-fan design has about 7% more wing area than the others because of the $C_{L_{max}}$ penalty for locating the nacelles on the wing leading edge. The overall friction drag is 6.3% higher than the turbofan's as a result of the added wing area, added empennage area, and extra friction in the elevated q of the slipstream over the wing. The aft-mounted prop-fan has substantially larger tail surfaces and engine struts.

Figure 53 shows drag polars at Mach 0.8. Note the added drag due to lift of the wing-mounted prop-fan, another penalty for the over-under nacelle placement. Figure 54 compares the drag rises. The effect of the higher Mach number in the slipstream of the -762 was estimated by using a weighted average of the drag rise Mach numbers of the immersed and unimmersed portions of the wing. The ΔM of -0.012 results in a drag rise penalty of 10 counts at fixed C_L.

The combined effect of the two penalties is to make the wing-mounted prop-fan airplane fly best at a slightly reduced C_L, and correspondingly lower altitude than the others.

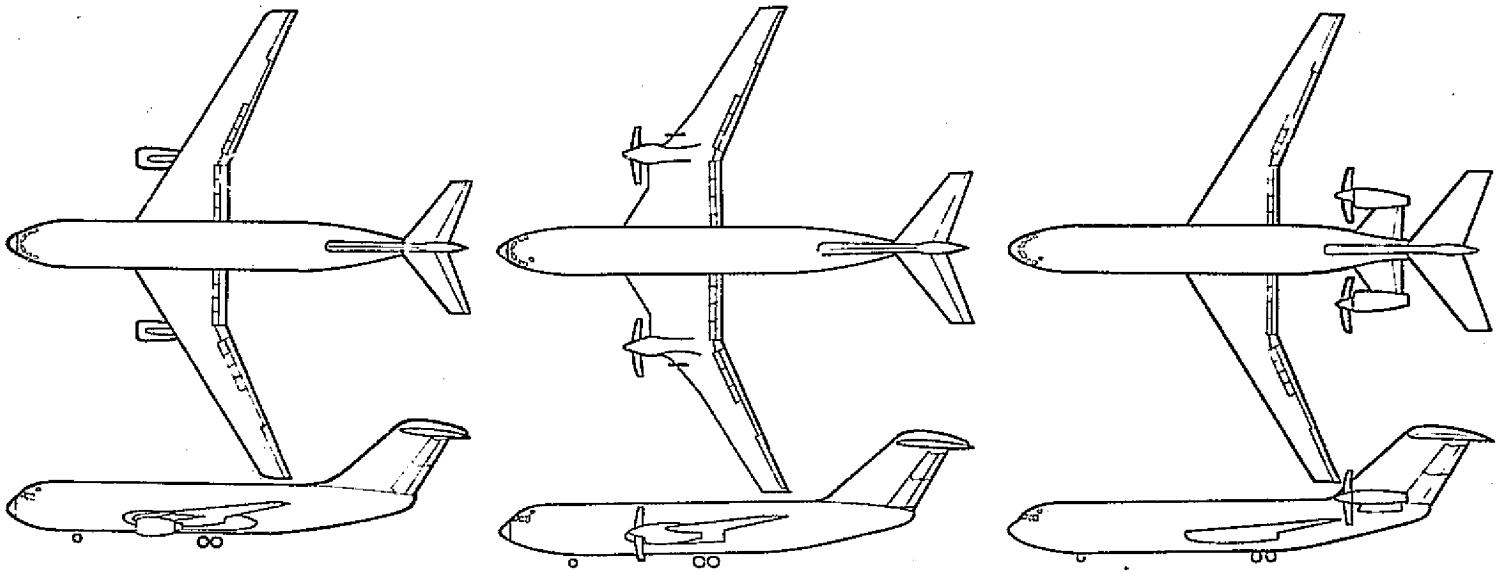

	Model 767-761 Reference Turbofan	Model 767-762 Wing-Mounted Prop-Fan	Model 767-764 Aft-Mounted Prop-Fan
Takeoff Weight (max)	115 350 kg (254 300 lb)	122 000 kg (269 100 lb)	123 970 kg (273 300 lb)
Operating Empty Weight	75 100 kg (165 570 lb)	83 000 kg (184 500 lb)	84 700 kg (186 700 lb)
Wing Area	243.2 m^2 (2618 ft^2)	260.8 m^2 (2807 ft^2)	242.8 m^2 (2613 ft^2)
Propulsion System	(2) 16 960 kg (37 400 lb) SLST BPR 6 turbofans	(2) 22 722 kw (30 470 hp) Engines * driving 5.98 m (19.6 ft) dia prop-fans	(2) 23 110 kw (30 990 hp) Engines * driving 6.03 m (19.8 ft) dia prop-fans
Block Fuel:			
3333.6 km (1800 nmi)	17 218 kg (37 960 lb)	15 549 kg (34 280 lb)	16 216 kg (35 750 lb)
1852 km (1000 nmi)	10 115 kg (22 300 lb)	9004 kg (19 850 lb)	9276 kg (20 450 lb)

*Scaled STS 476 turboshafts

Figure 51 Airplane Characteristics Comparison

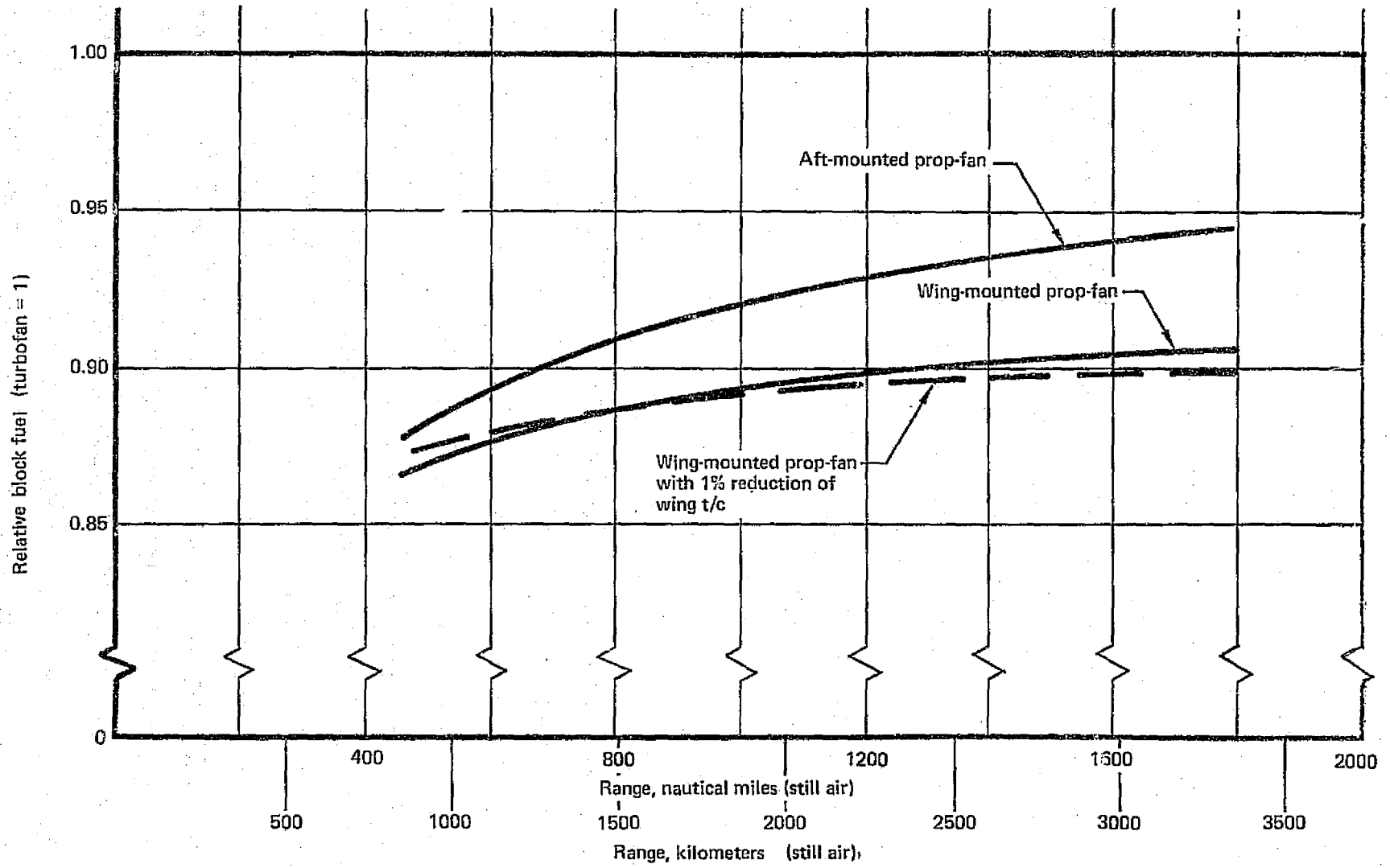

Figure 52 Fuel-Burned Comparison, 100% Load Factor

Table XII Drag Difference Summary

Item	Turbofan -761	Wing-mounted prop-fan -762	Aft-mounted prop-fan -764
Wing area, m^2 (ft^2)	243.20 (2618)	260.77 (2807)	242.75 (2613)
Parasite area, m^2 (ft^2)	4.062 (43.72)	4.318 (46.5)	4.503 (48.5)
At C_L = 0.5 and M = 0.8:			
$C_{D_{PARASITE}}$	0.0167	0.0166	0.0186
Total C_D	0.0275	0.0289	0.0294
ΔC_D (ref -761)	–	+0.0014	0.0019
ΔC_D BREAK-DOWN parasite	–	–0.0001	0.0019
ΔC_D BREAK-DOWN polar shape	–	+0.0005	0
ΔC_D BREAK-DOWN drag rise	–	+0.0010	0
L/D	18.18	17.3	17.01
$C_D \times S$ m^2 (ft^2)	6.69 (71.99)	7.54 (81.12)	7.14 (76.82)

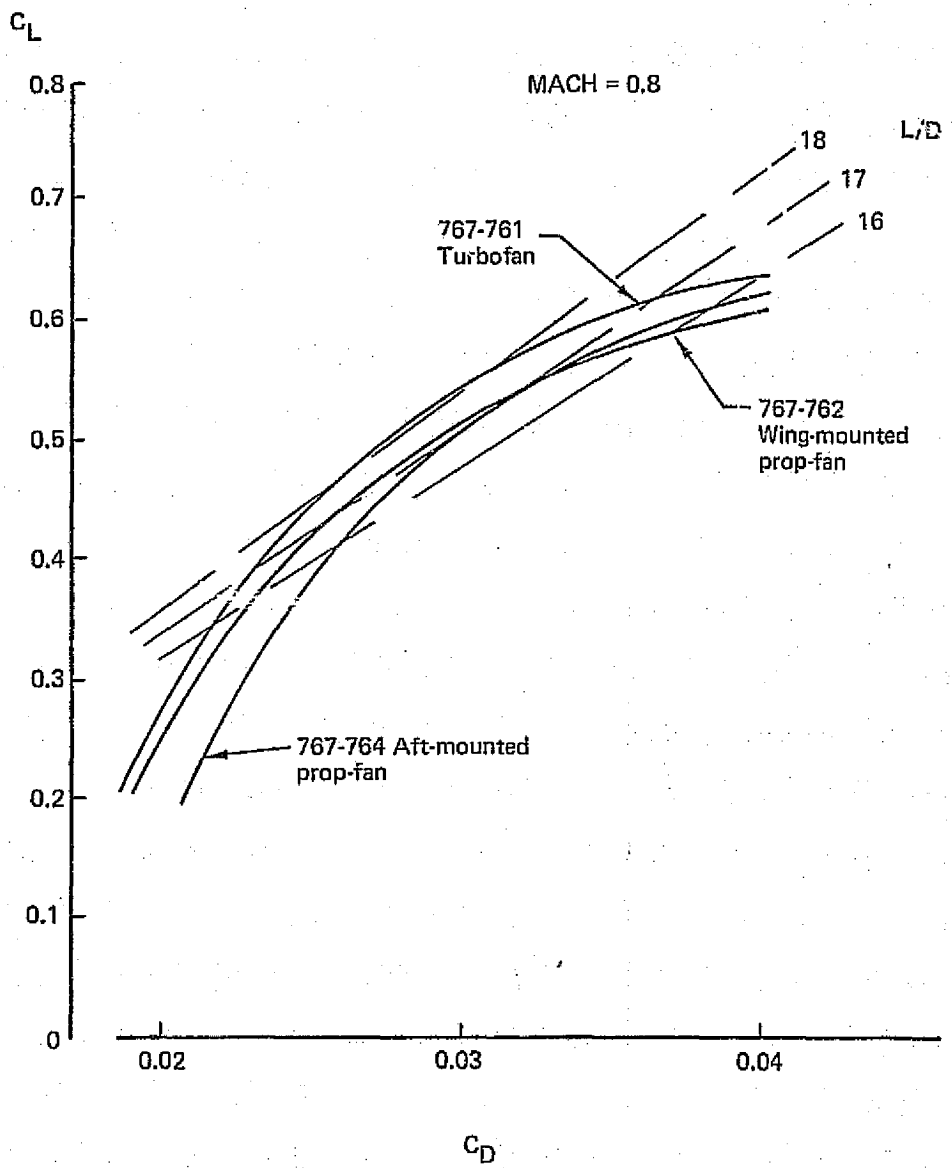

Figure 53 Drag Polar Comparison

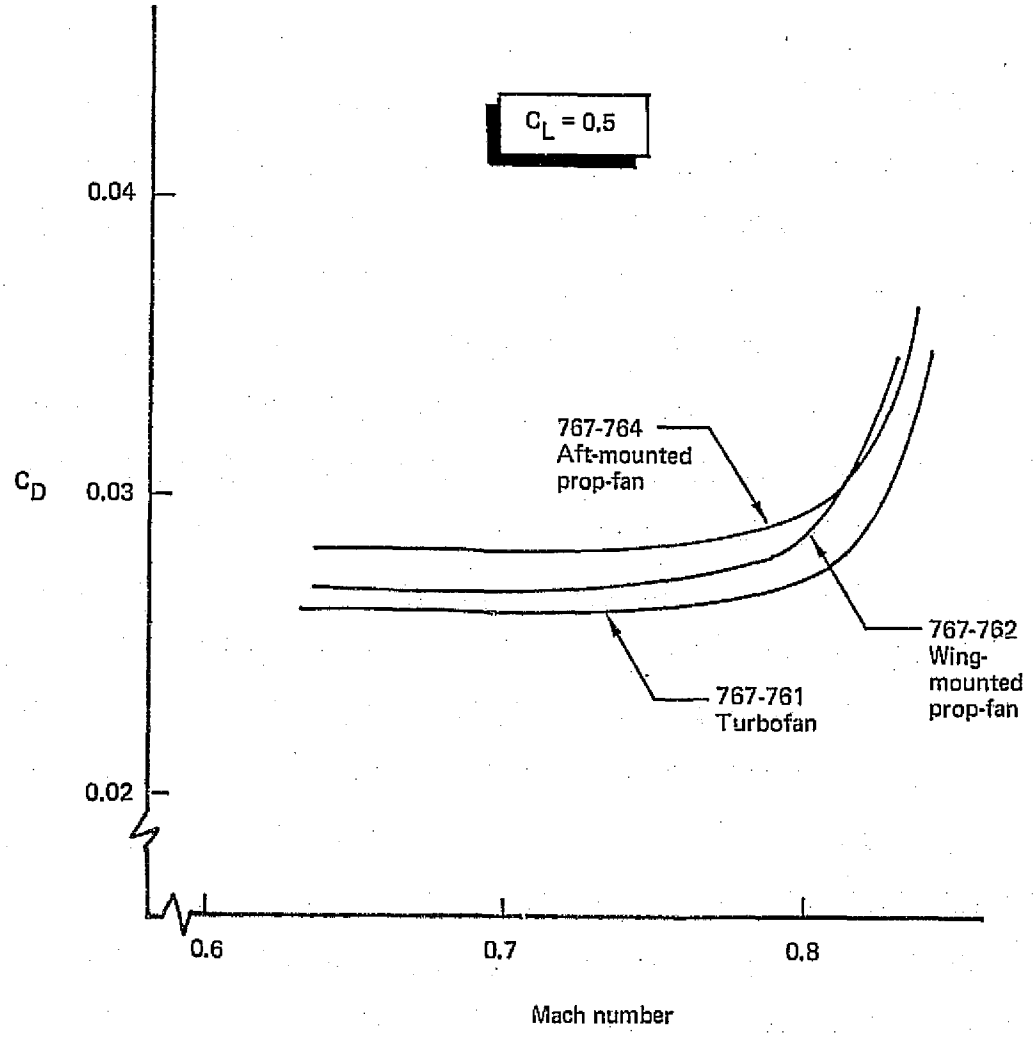

Figure 54 Drag Rise Comparison

The effect of reducing wing thickness ratio of the -762 airplane by 1% also was investigated.* This change is just sufficient to increase the drag rise Mach number by the 0.012 penalty assessed for the slipstream. The wing then would have become 1180 kg (2600 lb) heavier, including 454 kg (1000 lb) to maintain the original stiffness for flutter safety. The dashed line in figure 52 shows the fuel savings that would result. At the long-range end, the fuel saving is increased to 10.5%, but the added weight results in a small to unfavorable change at the shorter ranges. Because of the original uncertainty of the drag penalty, this result is not considered significant.

5.4.2 WEIGHTS

Table XIII is a comparative summary of weight differences. The most dramatic are due to effects of the high propeller noise. An extra 2670 kg (5880 lb) were added to the body structure of the wing-mounted prop-fan to reduce the cabin noise level to that of the turbofan, costing about 2% in block fuel at the design range. There were 808 kg (1780 lb) added to increase the skin thickness of the aft body and fin of the aft-mounted prop-fan to prevent sonic fatigue, costing 1% in block fuel.

Other major differences are increased empennage areas of the prop-fan and higher weight of the propulsion systems associated with the gearboxes and propellers.

*Using more sweep instead of reduced thickness would have resulted in a slightly higher weight penalty.

Table XIII Summary of Weight Differences

Item		-761 t/f	-762 t/p	-764 aft t/p
Wing	Area	243.2 m^2 (2618 ft^2)	260.8 m^2 (107.2%) (2807 ft^2)	242.8 m^2 (99.8%) (2613 ft^2)
	Weight	17 050 kg (37 580 lb)	18 470 kg (108.4%) (40 720 lb) — Flutter	18 570 kg (109.0%) (40 940 lb) — Loss of bending relief
Empennage	Area	100.3 m^2 (1080 ft^2)	119.4 m^2 (119.0%) (1285 ft^2)	149.5 m^2 (149.1%) (1610 ft^2)
	Weight	3030 kg (6690 lb)	3710 (122.4%) (8180 lb) — Destabilizing effect of propellers	4530 (149.5%) (9990 lb) — Short-coupled (aft engines = aft cg)
Body weight		13 720 kg (30 250 lb)	16 470 kg (120.0%) (36 310 lb) — Cabin noise reduction	15 840 kg (115.5%) (34 938 lb) — Engine strut support structure; acoustic fatigue
Propulsion system	Size	166 310 N (37 400 lb)	22 722 kw (30 460 shp)	23 110 kw (30 980 shp)
	Weight	8770 kg (19 340 lb)	13 450 kg (153.4%) (29 652 lb)	13 790 kg (157.2%) (30 400 lb)
Operating empty weight		75 050 kb (165 480 lb)	83 710 kg (111.5%) (184 550 lb)	84 690 kg (112.8%) (186 710 lb)
Maximum taxi weight		116 240 kg (256 300 lb)	122 960 kg (105.9%) (271 080 lb)	124 860 kg (107.5%) (275 269 lb)

6.0 SENSITIVITY ANALYSIS

This section presents the sensitivities of the airplanes' weight and block fuel to a number of parameters considered uncertain at this time. The sensitivities were computed using the THUMBPRINT computerized parametric analysis discussed in section 4, but the higher confidence weight data of the evaluated airplanes were used as a point of departure.

6.1 PROPULSION SYSTEM WEIGHT

The change in airplane characteristics due to possible changes in propulsion system weight are shown in table XIV. The changes in takeoff gross weight (TOGW), operating empty weight (OEW) and block fuel are the changes between sized airplanes with and without the propulsion system weight change (i.e., cycled differences). It was determined that for a 20% change in propulsion system weight the changes in TOGW, OEW and block fuel would be doubled, because the propulsion system weight represents a significant change to the airplane performance.

Table XIV Sensitivity to Propulsion System Weight

Change to prop system,		+10	
Airplane		Wing-mount prop-fan	Aft-mount prop-fan
Change to TOGW,	%	+2.5	+2.5
Change to OEW,	%	+3.2	+3.2
Change to block fuel,	%	+1.8	+1.8

6.2 PROPELLER EFFICIENCY

Incremental changes in propeller efficiency in cruise of -0.05 and -0.10 were assessed on the wing-mounted prop-fan. The results are summarized in table XV.

Table XV Sensitivity to Propeller Efficiency (Wing-Mounted Prop-Fan)

Change in prop efficiency, %	−5	−10
Change in TOGW, %	+3.9	+8.3
Change in OEW, %	+3.5	+7.6
Change in block fuel, %	+8.1	+16.9

A reduction in propeller efficiency has two major effects. First, the engine must increase in size to restore the cruise thrust and retain the optimum airplane size for minimum block fuel. Second, the overall specific fuel consumption is increased by the percentage change of propeller efficiency. This latter effect produces nearly 80% of the change in block fuel, the remainder being caused by resizing the airplanes to meet the mission performance. The table shows that the sensitivities of TOGW, OEW, and block fuel to changes in propeller efficiency are nearly linear. The aft-mounted version of the prop-fan showed similar results to the wing-mounted prop-fan.

A reduction of 5% in propeller efficiency would effectively eliminate all potential fuel savings of the prop-fan and emphasizes the importance of obtaining as high a propeller efficiency in cruise as possible.

6.3 PROPELLER SIZE (POWER LOADING)

The basic prop-fan airplane studies were made with a power loading of 345 kW/m^2 (43.2 shp/ft^2) at Mach 0.8 and a cruise altitude of 9144 m (30,000 ft) at maximum cruise power. The basis for this selection was described in section 5.2.3. The required rotor diameter at this loading for the wing-mounted prop-fan airplane is 5.98 m (19.6 ft).

An alternative power loading was evaluated to determine the effects on block fuel, operating empty weight, and airplane TOGW. After considering the effects of substantially larger rotor diameters on the airplane arrangement, an alternative loading equal to 7/8 of the basic loading was selected and the number of blades was reduced from 8 to 7. This permitted the original blade loading to be maintained without changing the blade aspect ratio. Prop-fan characteristics with 7 blades and the alternative power loading were determined from reference 9. These are compared with the characteristics of the basic loading on table XVI.

Table XVI Characteristics of the Basic and Alternate Power Loadings

SEA LEVEL, TAKEOFF POWER

	Basic loading 8 blades	Alternate loading 7 blades
M	$\frac{N}{kW}$ ($\frac{lb}{SHP}$)	$\frac{N}{kW}$ ($\frac{lb}{SHP}$)
0.1	7.58 (1.27)	8.05 (1.35)
0.2	6.62 (1.11)	7.40 (1.24)

MACH 0.8, MAXIMUM CRUISE POWER

	Prop-fan efficiency	
Altitude	Basic loading 8 blades	Alternate loading 7 blades
9144 m (30 000 ft)	0.808	0.818
10 670 m (35 000 ft)	0.802	0.812

The other aircraft characteristics that could be affected by these changes in power loading are the drag and weight. The drag change was assessed as negligible because the increased immersed area of the wing was offset by the reduced q of the slipstream.

The weight change is more significant because not only is there an increase in weight of the propeller/gearbox amounting to 277 kg (610 lb)/airplane but the propeller blades are closer to the fuselage, requiring increased cabin noise insulation. (The engine location was considered fixed in this study.)

The weight penalty for increased noise insulation was assessed at 662 kg (1460 lb)/airplane. Total effects of the change in power loading are given in table XVII, and show that the power loading change provides a small improvement in block fuel but increases the takeoff weight and operating empty weight by small amounts.

Table XVII Effect of Power Loading Change on Airplane Performance

Wing-mounted prop-fan	Percent change in:		
	TOGW	OEW	Block fuel
Change in OEW 939kg (+2070 lb)	+1.73	+2.21	+1.26
Change in efficiency ($\Delta\eta p = 1\%$)	−.77	−.71	−1.61
Total	+0.96	+1.5	−0.35

6.4 ENGINE LOCATION STUDY—WING-MOUNTED PROP-FAN

The two major effects of changing the spanwise engine position of the prop-fan are cabin noise and vertical tail size. There are other effects, but they are considered secondary and to some extent cancelling. Changes in cruise drag were investigated but were found to be insignificant. There would be some measurable effect on the low-speed drag, which also has been ignored because there is adequate margin on the takeoff performance; therefore, neither airplane sizing nor weights would be affected.

Wing bending moment relief that might be obtained by an outboard shift in the engine would be countered by a weight penalty for flutter considerations. The vertical tail size is altered with engine spanwise location to retain the same engine-out control capability. The drag effect of the change in vertical tail size has been neglected. The trade study therefore involved only the changes in weight of the vertical tail and noise insulation with engine spanwise movement. The noise insulation requirements, as engine location is varied for both a conventional and tuned structure, are shown in table XVIII. The combined effects of noise insulation (tuned structure) and vertical tail size are shown in table XIX. The present position of the engine was determined to be very close to optimum. Inboard movement of the engine from its baseline

Table XVIII Cabin Noise and Weight Tradeoff Estimates of a Wing-Mounted Prop-Fan

Prop-tip-to-fuselage clearance Y/D	Fuselage structural design change	Noise relative to reference 767-762B propfan	Δ Weight, Kg	Δ Weight, lb	Remarks
0.8	Conventional	Reference	3810	8400	
0.8	"	−10 dB	1470	3240	
0.8	"	+5 dB	6170	13 600	
0.8	Tuned structure	Reference	2607	5747	Design reference
0.8	"	−10 dB	850	1875	Noise level sensitivity
0.8	"	+5 dB	4863	10 721	
0.5	"	Reference	3549	7825	Wing position sensitivity
1.2	"	Reference	2207	4865	

Δ Weight penalty for Cabin Noise Comparable to Turbofan at Cruise

Table XIX Engine Location Study

Engine location	Move inboard to 0.5D	Baseline	Move outboard to 1.2D
ΔOEW noise insulation, kg (lb)	+943 +2078	0	−400 −882
ΔOEW vertical tail, kg (lb)	−318 −700	0	+417 +920
Total ΔOEW, kg (lb)	+625 +1378	0	+17 +38
Percent change TOGW	+1.2	0	+0.04
Percent change OEW	+1.5	0	+0.05
Percent change block fuel	+0.9	0	+0.03

D = Propeller diameter

position would produce rapid increases in noise insulation requirements that cannot be offset by the linear decrease in vertical tail size. Outboard movement of the engine produces a less rapid decrease in noise insulation but the linear increase in tail size rapidly offsets the noise reduction benefits.

7.0 ECONOMICS

7.1 DIRECT OPERATING COST ANALYSIS METHOD

Direct operating costs were calculated by the 1976 Boeing DOC Method, an updated version of the 1967 ATA formula. The components of DOC are crew pay, fuel, insurance, airframe maintenance, engine maintenance, maintenance burden, and depreciation.

Crew pay is a function of maximum takeoff weight and cruise speed. Insurance is based on 1%/year of the airplane flyaway price. Maintenance burden is a function of maintenance labor. Depreciation is based on straight-line depreciation over 15 years to a residual value of 10%.

To allocate depreciation and insurance as a trip cost they must be based on trips per year. The formulae for utilization and trips per year are:

$$U\ (\text{hr/yr}) = \frac{4000}{1 + \frac{1}{\text{Block time} + .5\ (\text{hours})}} + 630$$

$$\text{Trips/year} = \frac{U}{\text{Block time (hours)}}$$

7.2 FIRST COSTS

Sales price estimates were based upon a production quantity of 600 airplanes with a peak production rate of eight airplanes per month. Sales price calculations utilized cash receipts, cash expenditures, airplane rollout, and delivery schedule for a reasonable return on investment for the airplane manufacturer. Cash receipts were based upon a selected airline payment and ordering schedule while cost expenditures were based upon the airplane

manufacturer's cost expenditures. Airplane costs for nonrecurring and recurring production blocks were estimated by each cost element, such as engineering, tooling, production labor, and materials for major airframe components, such as wing, body, empennage, landing gear, propulsion nacelle, and systems. Differences due to the unique airframe weight distribution for each model can thus be recognized in the cost estimate and consequently reflected in the airplane price. Generally, an increase in airframe weight will result in lower dollars per pound depending on distribution of weight by airplane section.

Prop-fan propeller and gearbox prices were provided by Hamilton Standard. The turbofan engine price was obtained by using a dollars per pound of thrust trend line for engines currently in service. This was shifted to pass through a point for the Pratt & Whitney JT10-D2, which is considered representative of the price of 1985 technology engines. On the basis of an estimate by Pratt & Whitney (ref. 10), the prop-fan core engine prices were taken to be 86% of the values corresponding to "equivalent thrust" turbofans.* These relationships are shown in figure 55.

Figure 56 shows the propulsion system, airframe, and total airplane prices of both prop-fan airplanes relative to the reference turbofan. Prop-fan airframes, while slightly more expensive than the turbofan, show a smaller price differential than would be expected on the basis of the ratios of empty weights less engines and props. This reflects a smaller proportion of propulsion-related airframe structure (e.g., fan air ducts), which is relatively costly.

---

*"Equivalent SLST" for the turboshaft core engine is the cruise SHP divided by 1.46, times lapse factors for speed and altitude.

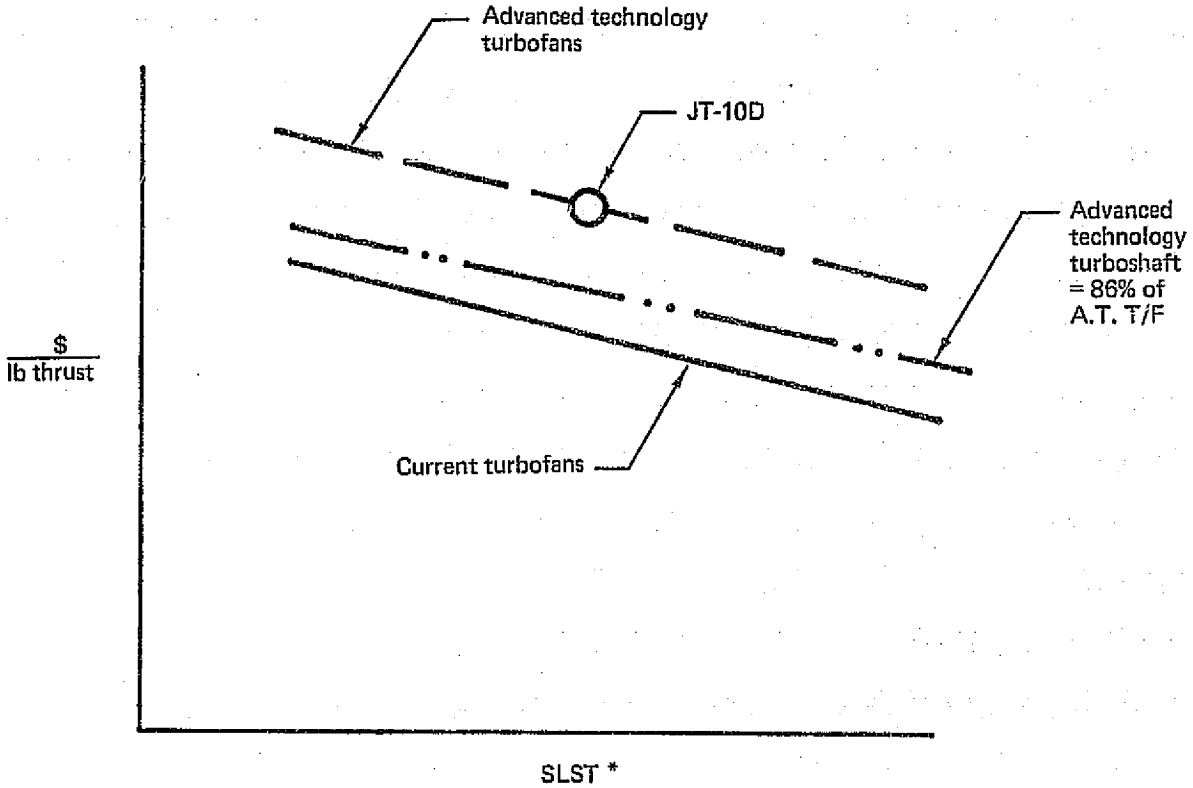

* SLST for turboshaft = $SHP_{CRUISE}/1.46$, times lapse factors for speed, altitude

Figure 55 Engine Price Calculation

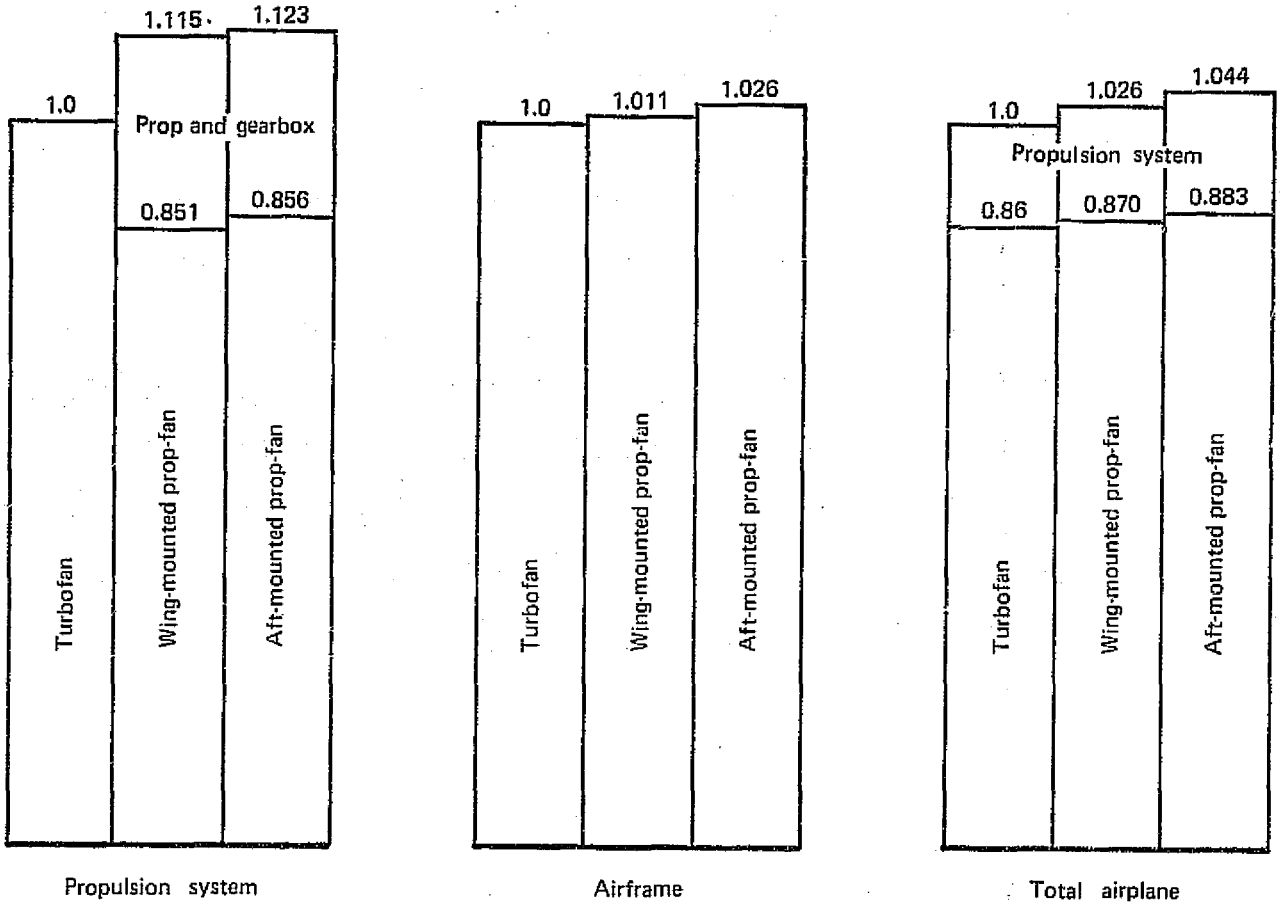

Figure 56 Price Comparison

7.3 PROPULSION SYSTEM MAINTENANCE COST

7.3.1 ENGINES

The engine maintenance material cost for the reference turbofan airplane equals the Boeing projection of JT10D-2 maintenance material cost multiplied by the price ratio of the turbofan to the JT10D-2. The maintenance labor equals th.. Boeing projection for the JT10D-2.

Maintenance costs for the prop-fan core engine were calculated using the JT10D-2 projection as a base and subtracting out the fan section, strut gear-box and thrust reverser, and adding to the remainder a portion for an added

low-pressure turbine stage. The result was then multiplied by the price ratio of the prop-fan engine to the JT10D-2.

The labor was calculated using the JT10D-2 projection as a base and subtracting out the fan section, strut gearbox and thrust reverser and adding a portion for the added low-pressure turbine. The line maintenance labor for the aft-mounted engines was increased to account for the requirement to use stands for access to the engines.

7.3.2 PROPELLER AND GEARBOX MAINTENANCE COST

Propeller and gearbox maintenance costs were provided by Hamilton Standard, as follows (1976 dollars):

Prop-Fan Diameter, m	(ft)	Man-hours, 1000 flight-hours	Parts Cost ($) 1000 flight-hours
4.9	(16)	62.7	1657
5.5	(18)	70.2	1962
6.1	(20)	77.7	2267

Maintenance costs for the prop-fan are independent of the average time per flight. These costs include the propeller controls, oil tank, and oil cooler.

Using $9.00 per hour as the labor rate, the maintenance cost (parts and labor) per engine flight-hour is $2.97 for a 6.1 m (20 ft) diameter prop-fan. Airline experience on the propeller/gearbox combination of the Lockheed Electra and Convair 540, extrapolated to the size and rating of the engine on the wing-mounted prop-fan, is about $19.22 per flight-hour. The 85% reduction anticipated by Hamilton Standard is attributed to design simplification, better modularity (permitting removal of individual blades instead of the complete rotor, for example) and increases in mean time between failures of major modules by factors of 4 to 15.

7.4 ESTIMATED DIRECT OPERATING COSTS

Figure 57 shows the DOC of the two prop-fan airplanes relative to the reference turbofan for ATA ranges of 966 and 1850 km (600 and 1150 statute miles), as functions of fuel price, using the Hamilton Standard projection of propeller and gearbox maintenance costs. Figure 58 shows the same data calculated with propeller and gearbox maintenance based on the current experience with old technology turboprop aircraft. The wing-mounted prop-fan has a modest cost advantage at today's fuel price--about 8.18¢/liter (31¢/gal.) for domestic trunk airlines, corresponding to 6.34¢/liter (24¢/gal) indexed to 1973, and a substantial one for fuel prices in the 13-16¢/liter (50-60¢/gal.) range, provided that the Hamilton Standard maintenance projection is realized.

Figure 59 shows a breakdown of the DOC for the reference turbofan and the wing-mounted prop-fan for 1850 km (1150 statute miles) ATA range at 7.92¢/liter (30¢/gal.) fuel cost (1973 money). Both the Hamilton Standard and the current experience levels of propeller and gearbox maintenance are shown. Note that the effect of this item appears in the maintenance burden cost element as well as directly.

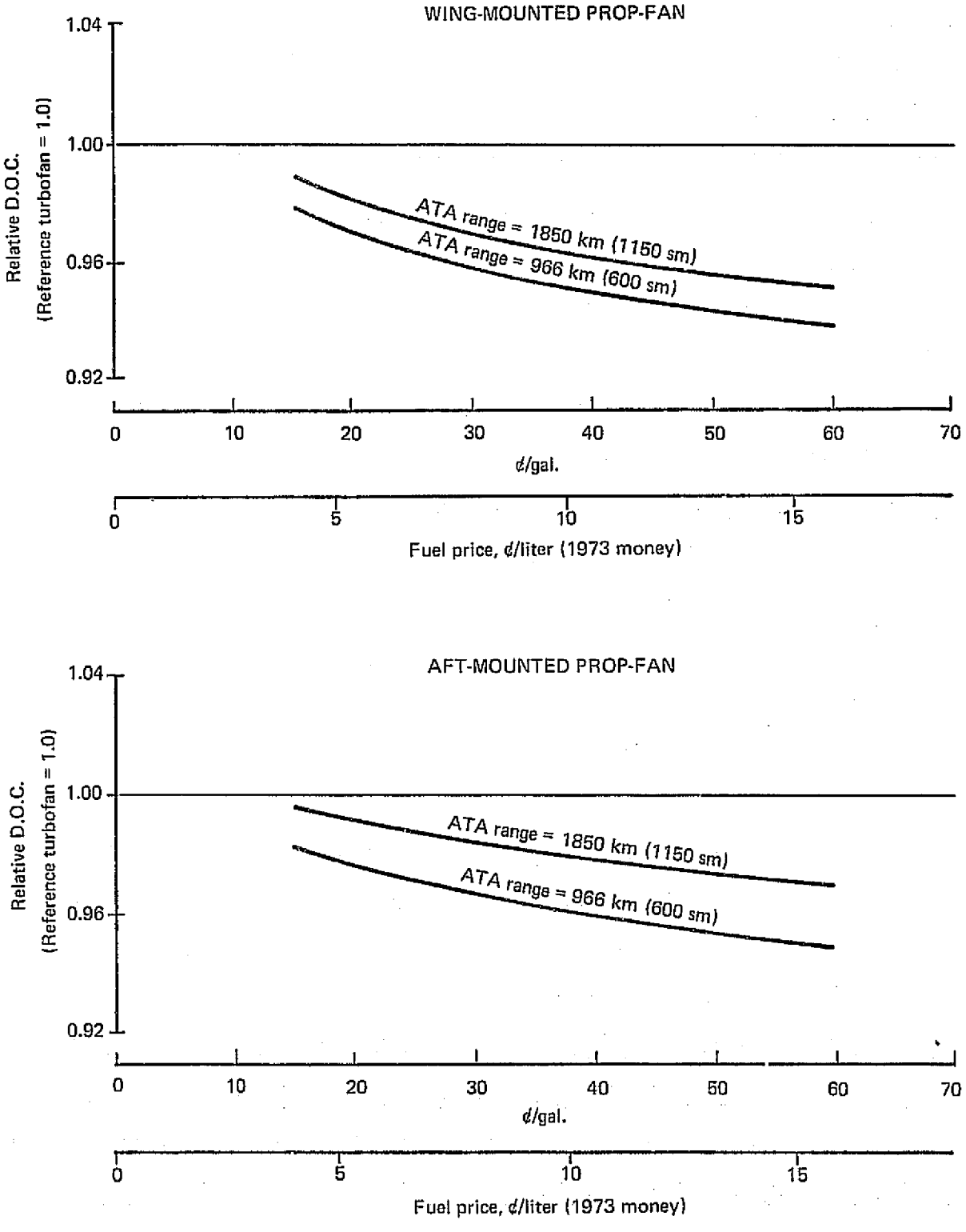

Figure 57 Direct Operating Cost, Hamilton Standard Projection Prop/Gearbox Maintenance

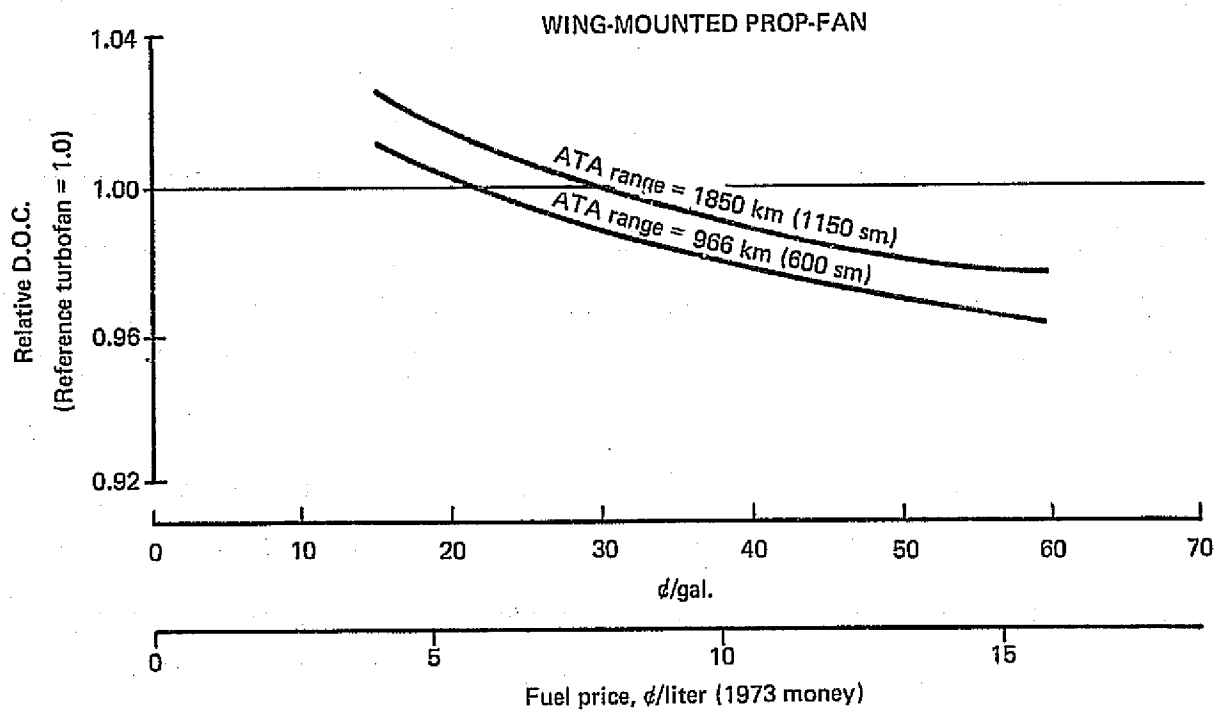

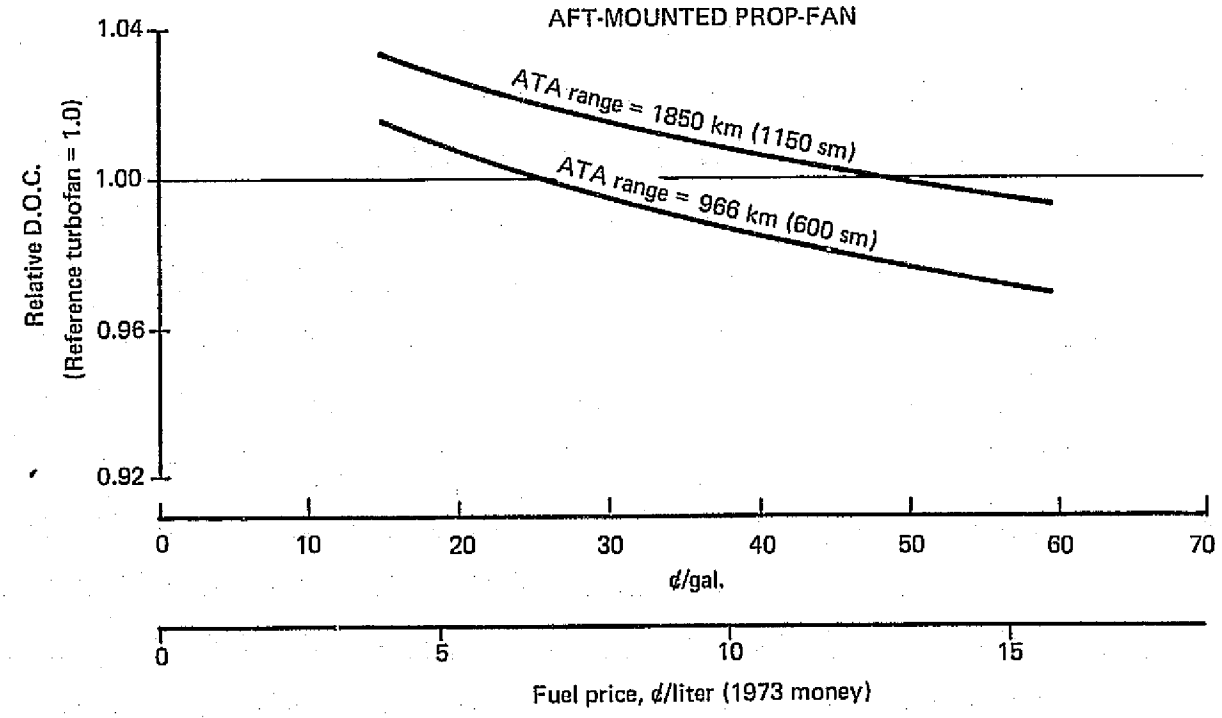

Figure 58 Direct Operating Cost, Current Experience Prop/Gearbox Maintenance

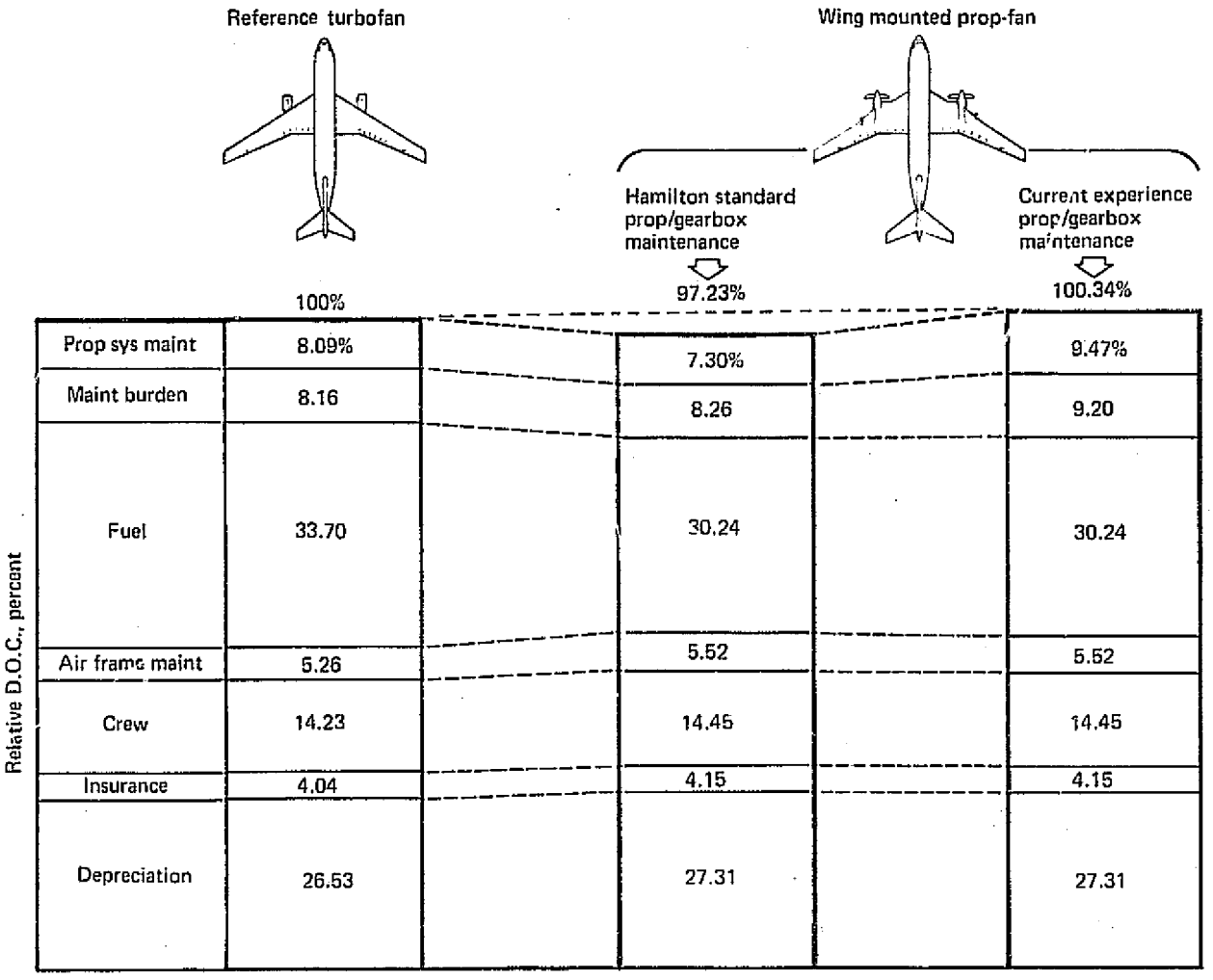

Figure 59 Direct Operating Cost Breakdowns—1850 Km (1150 sm) Trip, 30 Cents/Gallon (1973 Fuel)

APPENDIX

CABIN NOISE PROTECTION

A.1 BACKGROUND DISCUSSION

Passenger cabin interior noise has generally required conventional sidewall insulation, such as fiberglass blankets, lead vinyl septa, and interior trim panels. This insulation increases the noise transmission loss of the primary fuselage sidewall, and the noise actually perceived by the passenger is further decreased by the acoustic absorption of interior seats and furnishings. This noise reduction is most evident above 500 Hz, where the noise levels are most significant for minimum speech interference. The highest propulsion noise source from the jet exhaust decreases with flight speed, hence the excitation of the fuselage by the turbulent boundary layer (TBL) often determines the exterior noise level. These two noise sources are broad band in nature and are highest on the exterior in the 200 to 400 Hz frequency range.

Current practices of reducing fuselage noise transmission, such as reducing stringer pitch and adding mass to interior walls, usually achieve only modest noise reduction at low frequencies because of structure vibration as a whole. The concepts in development to resolve this problem include structural tuning and damping. A structure is designed to couple in preferred modes of vibration that can then be effectively reduced by damping material. When only discrete tones are the source of excitation, the structure can be tuned to have much reduced response at those frequencies. These concepts are currently in a state of analytical development, although some encouraging experimental results have been obtained. For this reason only very general trends of noise reduction and attendant weights of fuselage structure change are available now.

The prop-fan generates discrete tones with a fundamental near 100 Hz. As flight speed increases, the helical Mach number of the outer portion of the blade section becomes supersonic and the noise generation mechanism becomes more efficient, especially in the harmonics, so that similar sound levels are predicted for as high as the first 10 harmonics. In a turbofan engine, shock noises associated with the supersonic fan-tip speed are found at frequencies below the blade passage frequency, both statically and in flight.

It is not known whether such subharmonics of the prop-fan blade passage frequency will be found.

A.2 INTERIOR NOISE CALCULATIONS

Interior noise for the study configurations was calculated using a Boeing computer program that was developed for typical jet transport interior noise predictions. Inputs included engine exterior noise, turbulent boundary layer noise, and sidewall noise reduction.

The calculation of prop-fan exterior noise presented some difficulty because there is no standard procedure available for supersonic propellers in flight. After comparisons with several methods, a proposed SAE procedure for subsonic propellers was used with corrections recommended by Hamilton Standard, representing an "advanced design" estimate.

The "advanced design" took credit for (1) increasing blade critical Mach number, (2) decreased thickness ratio, and (3) beneficial effects of blade-tip sweep. Whereas these three effects are documented as beneficial at subsonic tip speeds, the same benefit at supersonic conditions is questionable. In particular, use of shock wave relationships

applied to supersonic airfoils indicated benefits might be due only to blade sweep and would be small (2 dB) for the prop-fan designs. For these reasons a level 10 dB higher than the Hamilton Standard estimate was considered most appropriate by Boeing as the baseline design point for this study. This SAE modified procedure was further adjusted and expanded so that by appropriate parameters input to the Boeing computer program, a propeller noise spectrum with appropriate directivity could be calculated. In this way, a fair computer prediction comparison could be made between the prop-fan configurations and the turbofan. A comparison of prop-fan and turbofan interior noise estimates is shown in figure 41 of this report. The aft convection of noise radiation in forward flight was considered in the calculations.

Interior noise levels were predicted for the range of exterior OASPLs indicated in figure A-1. Here various free-field measurements were scaled to the cruise conditions of the wing-mounted prop-fan by Hamilton Standard and an anticipated prop-fan characteristic curve also was shown. The two levels used for this study are labeled "Advanced Design Point" as recommended by Hamilton Standard and "Reference Design Point" considered the appropriate realistic level by Boeing calculations. Calculations supporting the Boeing "Reference Design Point" are given in section A.4 below.

The level indicated by "Allowance for shock wave" is 5 dB above the Boeing design point. This higher level indicates a probable upper limit on near-field noise to account for unforeseen P/F noise generation problems in the same way that the Hamilton Standard point represents optimistic noise reduction results.

The interior noise spectra predicted using the turbofan cabin sidewall noise reduction are shown in figure A-2, and compared with measurements inside other aircraft. The commercial jet transport composite values

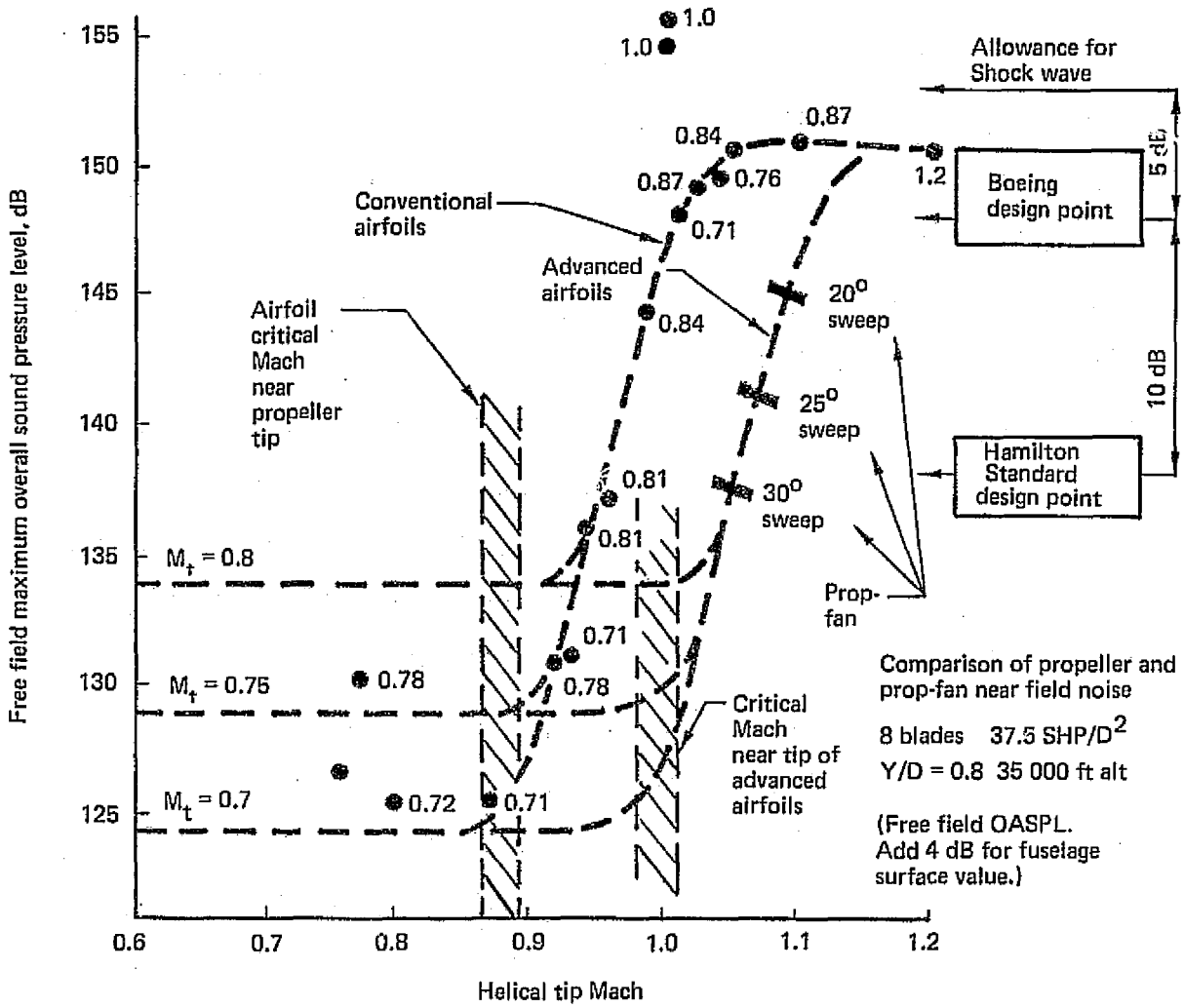

Figure A-1 Hamilton Standard Exterior Noise Comparison and Boeing Design Point

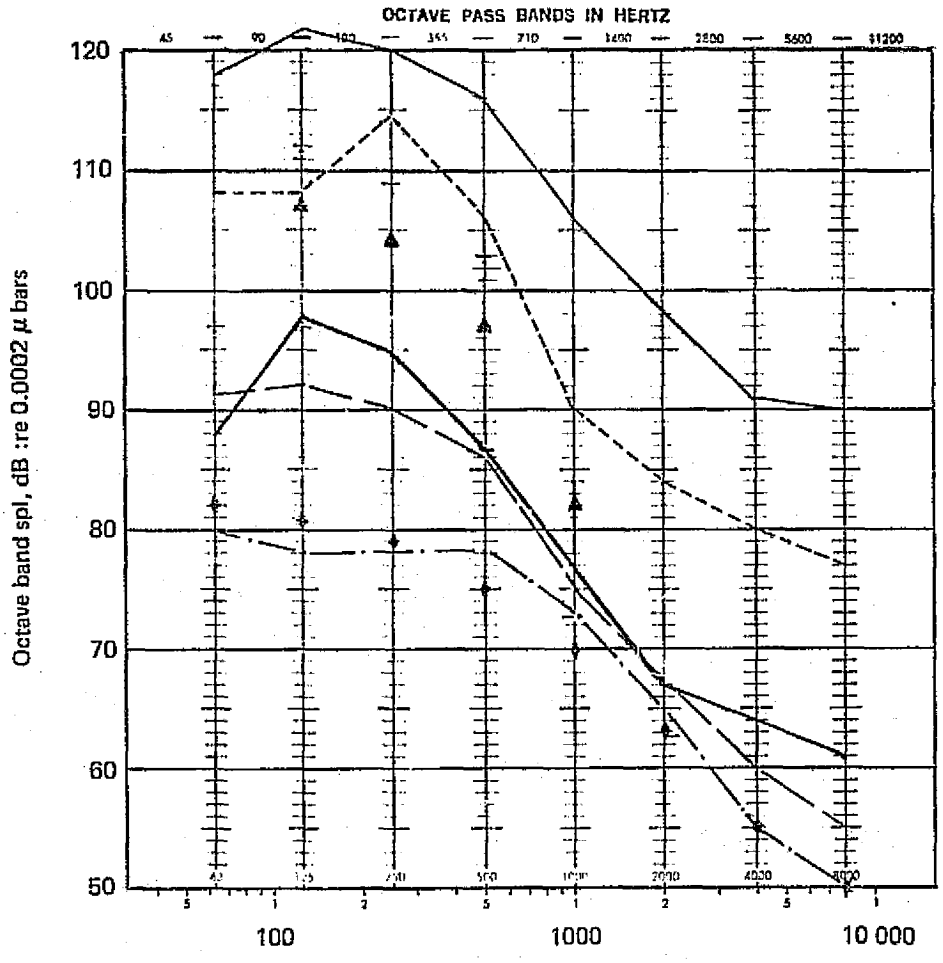

		OASPL	PSIL
Measured	Military turboprops high-noise region		
———	4—engine noisy airplane	124	107
- - - -	2—engine noisy airplane	116	93
———	4- and 2-engine quiet airplane	103	76
—— ——	Commercial jet transport high-noise region (aft)	96	77
—— · ——	Commercial jet transport quietest region (forward)	85	72
Estimated ♦	Turbofan 767-761 (aft noisiest)	86	70
▲	Prop-fan (midcabin noisiest) 767-762 (with same treatment as 767-761)	111	73

Figure A-2 Cabin Noise in High-Noise Locations

shown represent a typical higher level area behind the engines, as well as a quieter area forward of the wing, with turbulent boundary layer being the primary source. The predicted 767-761 turbofan level at its noisiest location is as quiet as has been measured for current commercial jet aircraft. A range of noise levels measured in turboprop military aircraft also is shown. All measurements are for the noisiest region, forward of the wing. The maximum and minimum values for several aircraft were used to compose the data. About the same noise levels occur for the quietest type of two-and four-engine turboprops. A 25 dB reduction is required for the prop-fan to match the turbofan noise levels.

The initial excess in P/F over T/F interior noise is highest below 1000 Hz, where some basis for propeller noise prediction is available, but there is less basis for accurate structural transmission loss prediction. There is not a good basis for P/F noise prediction above 1000 Hz, but there is plenty of data for sidewall treatment transmission loss. In fact, should the prop-fan actually be higher at frequencies above 1000 Hz, the additions of fiberglass treatment is small compared to other additions required for frequencies below 1000 Hz.

A.3 FUSELAGE STRUCTURE ADDITIONS

The requirements for additional fuselage structure to reduce prop-fan cabin noise were defined by dividing the fuselage into regions with different noise reduction requirements, as shown in figure 41 of the report.

First, the interior noise of the P/F at cruise was estimated on the basis of the exterior noise. To account for any changes in noise directivity between low (takeoff) and high (cruise) airspeeds, the estimate at takeoff was faired into the cruise estimate to make a "flight directivity change envelope." For a realistic comparison with turbofan noise levels,

the T/F maximum noise region was shifted for peak-to-peak comparisons. The difference between the envelope of P/F cabin noise and T/F cabin noise represents the required additional fuselage attenuation.

Cabin noise is influenced not only by the local exterior source, but by transmission of sound from one region to another within the fuselage, and by local vibrations of fuselage structure. Similarly, for the desired noise reduction of a localized source, such as the prop-fan, local sidewall reinforcement is needed, but in addition, adjacent structure must minimize or prevent transmission of fuselage excitation that would be characteristic of low-frequency noise. In table A-I, five types of fuselage treatments are listed. They are added cumulatively in each fuselage section as the required noise reduction increases. A design employing efficient frame damping is used throughout. The next additive treatment, where more than 6 dB additional attenuation is needed, is stringer damping. The succeeding additions also are assumed to be high-efficiency designs. The incremental weight of the overall treatment for a range of required attenuation levels from 5 to 30 dB is shown in figure A-3.

The damping requirements used in the prop-fan wing position trade are given in table A-II.

A.4 SONIC BOOM THEORY APPLIED TO SUPERSONIC PROPELLER NOISE

As a check on the OASPL numbers of figure A-1 and the proposed decreases in levels according to the Hamilton Standard blade design, a sonic boom equation from reference 11 was used. It is shown in table A-III and includes both lift (loading) and volume (thickness) effects. It has been verified in the far field by supersonic projectile measurements (reference 12).

Table A-1 Prop-Fan Fuselage Structure Additions to Achieve Turbofan Cabin Interior Noise at Cruise **

Extent of structure additions (range is number of diameters forward or aft of prop disc plane) *				
Structure addition (% of existing weights)	Wing-mounted prop Y/D = 0.8, BS 672 disc plane			Aft-mounted prop Y/D = 0.2 BS 1504 disc plane 767-764
	Boeing design point 767-762	Hamilton Standard design point (10 dB lower) 767-762	Shock wave allowance 5 dB higher	Reference design point 767-764
Damping applied to frames (30% of frame weight)	1.8 D. fwd to 3.5 D. aft	1.0 D. fwd to 3.0 D. aft	1.8 D. fwd to 3.5 D. aft	1.3 D. fwd to prop plane
PLUS				
Damping applied to stringers (30% of stringer weight)	1.8 fwd to 3.5 aft	1.0 D. fwd to 2.2 D. aft	1.8 D. fwd to 3.5 D. aft	0.8 D. fwd to prop plane
PLUS				
Laminated skin (30% of skin weight)	0.8 D. fwd to 2.4 D. aft	0.5 D. fwd to 1.3 D. aft	1.8 D. fwd to 3.5 D. aft	0.5 fwd to prop plane
PLUS				
Doubled frames and stringers with damping (130% of frame and stringer weight)	Prop plane to 1.7 D. aft	—	0.7 D. fwd to 2.3 D. aft	—
PLUS				
Double advanced structure (100% of skin, frame, stringer weight)	—	—	0.3 D. aft to 1.1 D. aft	—

* Structure additions extend around 75% of fuselage circumference, tip-fuselage clearance = Y/D; D = prop diameter

** Peak prop-fan cabin noise region comparable to peak turbofan cabin noise region

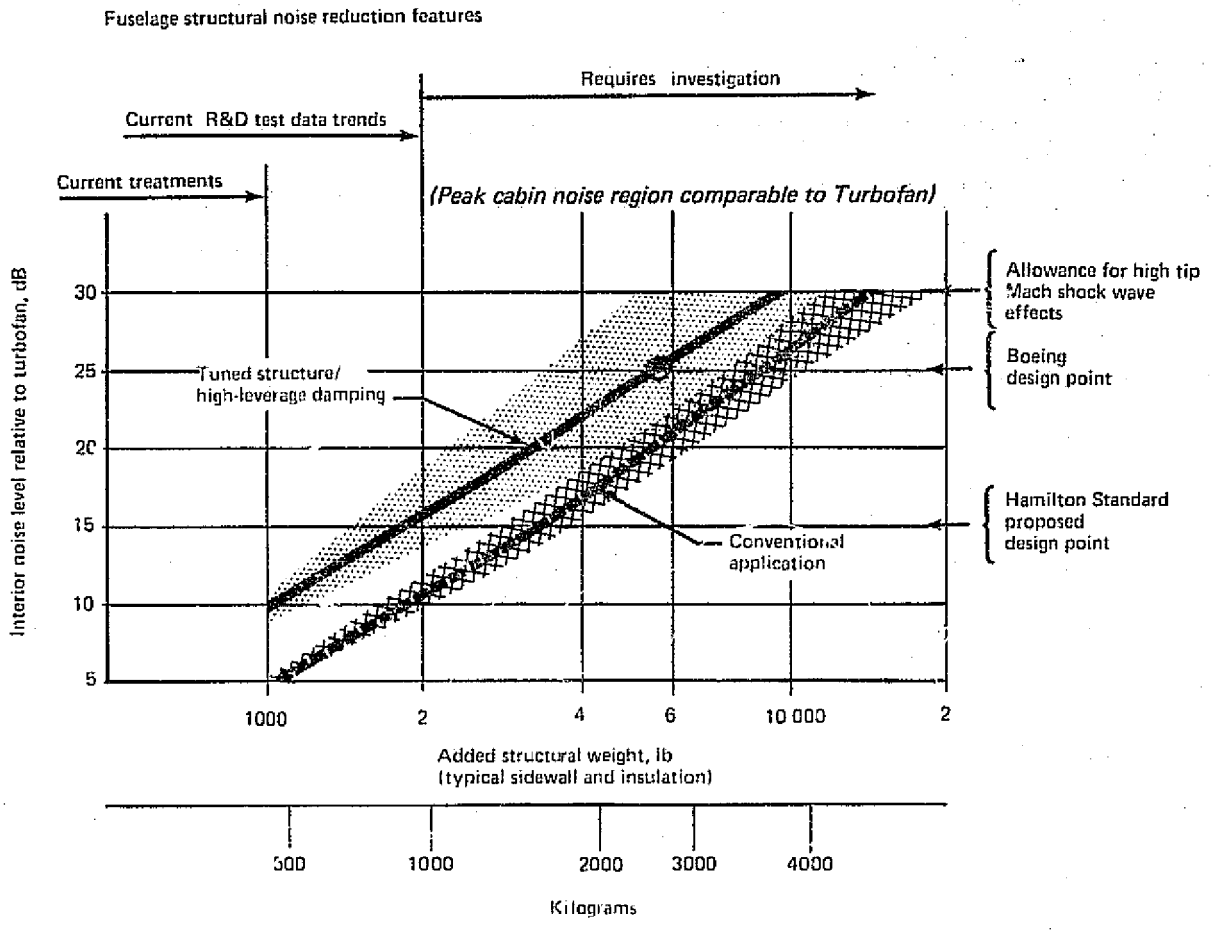

Figure A-3 Weight Trends of Wing-Mounted Propeller for Cruise Interior Noise Requirements

Table A-II 767-762 Prop-Fan Fuselage Structure Additions to Achieve Turbofan Cabin Noise at Cruise for Different Wing Positions*

Wing-mounted prop; tip-fuselage clearance Y/D; D= prop diameter			
Structure addition (% of existing weights)	Extent of structure additions** (range is number of diameters forward or aft of prop disc plane)		
	Y/D = 0.5	Y/D = 0.8	Y/D = 1.2
Damping applied to frames and stringers (30% of frame and stringer weight)	1.8 D. fwd to 3.5 D. aft	1.8 D. fwd to 3.5 D. aft	1.8 D. fwd to 3.5 D. aft
PLUS			
Laminated skin (30% of skin weight)	0.8 D. fwd to 2.4 D. aft	0.8 D. fwd to 2.4 D. aft	0.8 D. fwd to 2.4 D. aft
PLUS			
Doubled frames and stringers with damping (130% of frame and stringer weight)	1.1 D. aft to 1.7 D. aft	Prop plane to 1.7 D. aft	0.6 D. aft to 1.7 D. aft
PLUS			
Double advanced structure (100% of skin, frame, stringer weight)	0.3 D. fwd to 1.1 D. aft	---	---

* Assumes cabin noise peak region (middle) comparable to turbofan peak region (aft)

** Structure additions extend around 75% of fuselage circumference

Table A-III Sonic Boom Equations

Boom intensity		Flight altitude	Surface effectivity	Airplane speed	Airplane weight	Airplane design parameters
ΔP_V (volume)	=	$\frac{\sqrt{P_a P_g}}{h^{3/4}}$	K_R	$(M^2-1)^{1/8}$	–	$\frac{d}{\ell_B^{1/4}} K_V$
ΔP_L (lift)	=	$\frac{\sqrt{P_a P_g}}{P_a^{1/2} h^{3/4}}$	K_R	$\frac{(M^2-1)^{3/8}}{M}$	$W^{1/2}$	$\frac{d}{\ell_W^{1/4}} K_L$

Pa – pressure at altitude
Pg – pressure at surface
h – altitude
K_R – reflection coefficient
M – Mach number
d – diameter of equivalent body of revolution

K_V – volume shape factor 0.54 to 0.81
K_L – lift shape factor 0.5 to 0.6
ℓ_B – body length
ℓ_W – effective wing length
W – weight (wing loading)

Total overpressure $\Delta P^* = (\Delta P_V^2 + \Delta P_L^2)^{1/2}$

The method used to calculate the shock wave strength acting on the body of the prop-fan airplane due to the supersonic-tip propeller is strictly applicable only to the calculation of the sonic boom overpressure directly under the flightpath of a SST in steady, level flight. The method assumes a homogeneous atmosphere and that the point of measurement is in the far field. A reflection factor of 2.0 was assumed, which results in an overpressure equal to twice that of a single shock wave.

The volume factor, K_V, in the equation for the boom intensity due to volume was assumed to be 0.8, which is on the high side of the normal SST range of 0.54 to 0.81. This is because the equation was derived for a body of revolution rather than the 2-D type body being analyzed in this cas-

The lift shape factor, K_L was assumed to be 0.7, which is higher than the normal SST range of 0.5 to 0.6. This is because the longitudinal lift distribution on an SST is likely to be more gradual than that on the propeller.

The prop-fan fuselage wall is only 10 propeller chord lengths from the tip of the propeller, which means that it is still in the near field. To account for this, a factor of 0.75 was applied to the volume and lift overpressures. This factor is based upon the experimental data of reference 12.

The total overpressure was computed from:

$$\Delta P_{TOT} = \sqrt{(\Delta P_{VOL})^2 + (\Delta P_{LIFT})^2}$$

in accordance with reference 13.

The applicability of the sonic boom equation to propeller noise was tested using the propeller parameters and noise measurements of ref. 14. Three factors were found to be important and are associated with the numbers computed for table A-IV. First, the peak overpressure value p* calculated for the sonic boom type of N-wave should be expressed as an rms value, Prms, which would be read in terms of sound pressure level on an SPL analyzer and which would be the effective pressure for cyclic excitation of fuselage structure. As shown in table A-IV, this N-wave correction for p* to Prms gives the correct far-field OASPL using the volume effects, P_V alone.

The second factor is the importance of both volume and lift overpressure values in the near field for closest agreement. In Table A-IV, the sonic boom equation underpredicts the OASPL even when the conservative factor of 0.75 applied for a near-field overpressure is left out. It may also be the importance of body shape on nearfield noise as indicated in reference 11.

The third factor may be the additional oscillating pressures generated by other blades. When an additional "shock pulse" of duration T* is added within the blade passage period, T, the agreement shown in table A-IV is closest although the physical interpretation may not be complete.

The conclusion of this type of comparison is that far-field OASPL may be represented by the volume effects calculation of a single blade sonic boom corrected to an rms pulse, but near-field effects may be influenced by both volume (thickness) and lift effects as well as the number of blades.

To choose a reasonable design OASPL reference for the prop-fan, several calculated numbers are shown in table A-V. If effects of only a single blade occur in the near field in flight, a number (136) close to the

Table A-IV *Free Field Supersonic Propeller Noise Comparison of Sonic Boom Formula and NACA TN 1079 (Ref. 14)*

	Far Field y/D = 7 Assume Thickness Noise Only (ΔP_V)	Near Field y/D = 0.5 (Conservative Factor of 0.75) Assume Thickness Noise Only (ΔP_V)	Assume (ΔP_V and ΔP_L) No Conservative Factor 0.75	Assume No Conservative Factor, and 2 Blade Effect or T*
OASPL* sonic boom calculation	150	164	169	169
OASPL (rms) sonic boom calculation	131	145	150	153
OASPL NACA data	131	154	154	154

For N-wave, $\frac{Prms}{\Delta P^*} = \frac{T^*}{3T}^{\frac{1}{2}}$ $\underset{(rms)}{OASPL} - \underset{(peak\text{-}peak)}{OASPL^*} = 20 \log \frac{T^*}{T}^{\frac{1}{2}}$

$T = \frac{\tau D}{BV_T}$ $T^* = \frac{c}{M_h a_o}$

T^* = blade chord passage time

T = cyclical time between each blade passage

Table A-V *Free Field Estimates of Prop-Fan Noise at Distance Y/D = 0.8 at Cruise M 0.8, 10668 m (35,000 ft.)*

	OASPL—dB
Hamilton Standard design estimate	137
Boeing sonic boom calculation—rms averaged (one blade, 0.75 factor)	136
Boeing sonic boom calculation—adjusted on basis of Ref 1 comparison (2 blades)	141.5
Boeing sonic boom calculation—possible effect of 8 blades	147.5
Empirical data scaled according to sonic boom equation	149
Boeing design poont	148

Hamilton Standard proposed level (137) occurs. However, if eight blades have equal reinforcing contributions, an OASPL of 147.5 results. If the empirical data (151) is scaled according to the change in blade parameters given by the sonic boom equation (effectively chord length, $\ell^{-\frac{1}{4}}$) a decrease of 2 dB to 149 dB results. The average of these last two values, 148 dB, then represents the Boeing position on a reasonable estimate based on current knowledge. The potential for lower noise levels than these depends on the oscillating pressures from advanced propeller blade designs with swept tips and their superposition on a fuselage in flight.

REFERENCES

1. Study of Unconventional Aircraft Engines for Low Energy Consumption. NASA CR-135065, March 16, 1976.

2. Fuel Conservation Possibilities for Terminal Area Compatible Aircraft. Boeing Commercial Airplane Company, NASA CR-132608, 1975.

3. Edwards, George G., et al, The Results of Wind Tunnel Tests to a Mach Number of 0.9 of a Four-Engine Propeller-Driven Airplane Configuration Having a Wing with 40^{o} of Sweep-Back and an Aspect Ratio of 10. NACA TN 3789, 1956.

4. Lippert, J., A Method for Estimating the Power On Drag of Multi-Engine Propeller-Driven Aircraft. ADR-01-03-63.1, Grumman Aircraft Corp., 1963.

5. Grainger, M., Low-Speed Aerodynamic Prediction Method. Boeing Document D6-26011TN, 1970.

6. Preliminary Data Pack for the STS 476 Turboshaft Engine. Pratt & Whitney Aircraft, 1975.

7. Prop-Fan Performance Estimation for the Eight(8) Blade Prop-Fan Configuration. SPO2A76, Hamilton Standard Division of United Technologies, 1976.

8. Glauert, H., Airplane Propellers. Volume 4, Division L, Aerodynamic Theory, W. F. Durand, editor-in-chief, Dover Publications, Inc., 1963.

9. Generalized Prop-Fan Performance and Weight. SPO5A75, Hamilton Standard Division of United Technologies, 1976.

10. Bergquist, A. H., Memorandum. Pratt & Whitney Aircraft, June 21, 1976.

11. Lifting Effects in Sonic Boom. Boeing Document D6-5845, 1960.

12. Kane, E. J., Determination of the Far-Field from Ballistic Range Sonic Boom Test Data. Boeing Document D6-7165, 1961.

13. Carlson, H. W., An Investigation of the Influence of Lift on Sonic-Boom Intensity by Means of Wind-Tunnel Measurements of the Pressure Fields of Several Wing-Body Combinations. Boeing Document D6-7165 and NASA TN D-881, 1961.

14. Hubbard, H. H., and Lassiter, L. W., Sound from a Two-Bladed Propeller at Supersonic Tip Speeds. NACA Rep. 1079, 1952.